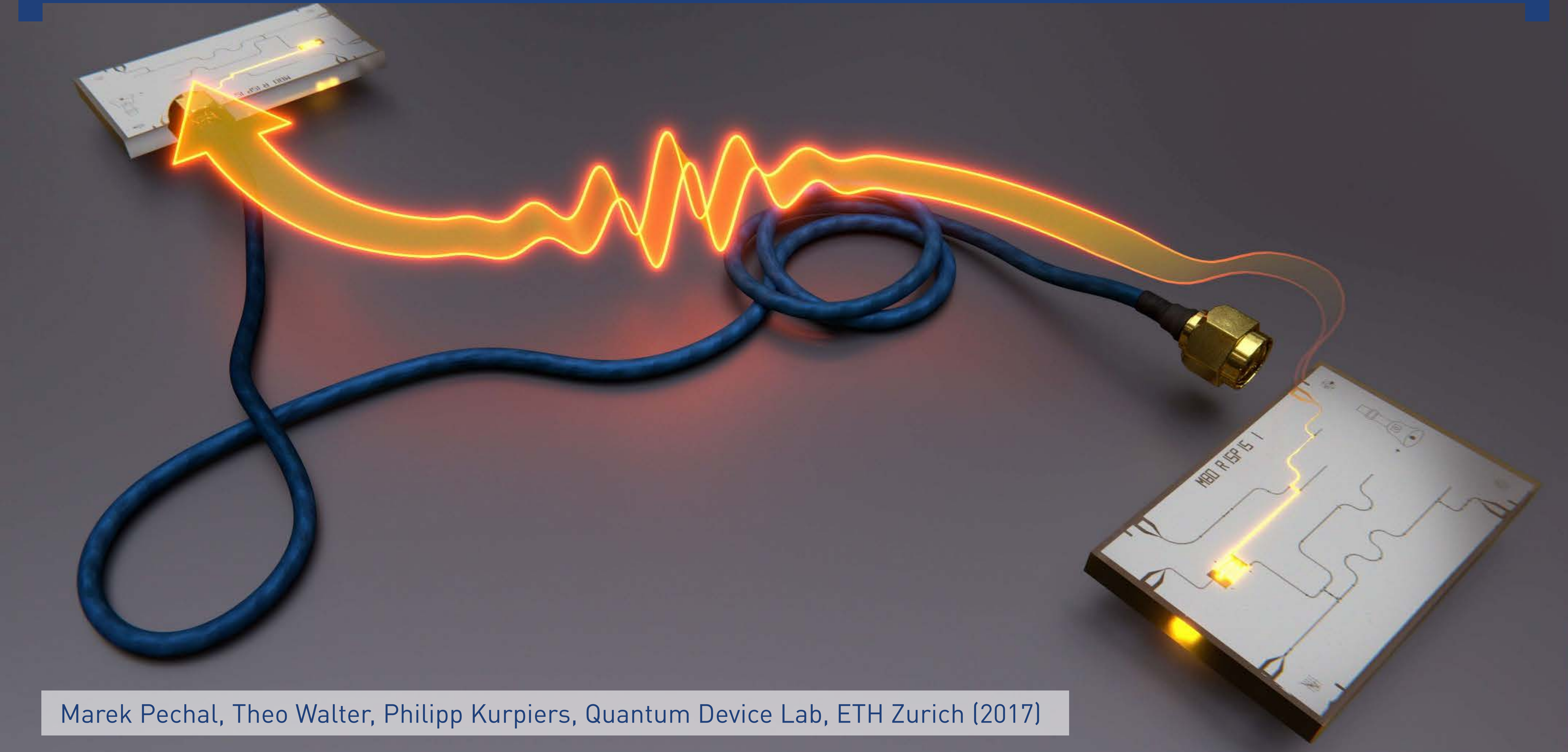

Marek Pechal, Theo Walter, Philipp Kurpiers, Quantum Device Lab, ETH Zurich (2017)

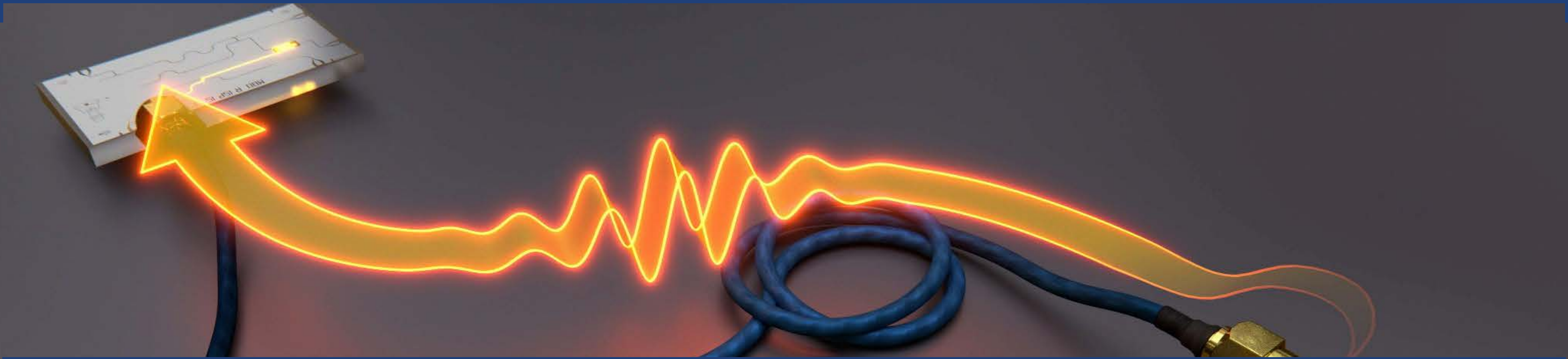

Quantum Networks with Superconducting Circuits: Creating, Transmitting and Detecting Microwave Photons

Science Team: C. Andersen, J.-C. Besse, M. Collodo, J. Heinsoo, J. Herrmann, S. Krinner, P. Kurpiers, S. Lazar, P. Magnard, G. Norris, A. Remm, C. Eichler, A. Wallraff *(ETH Zurich)*
B. Royer, and A. Blais *(Université de Sherbrooke)*
Technical Team: A. Akin, M. Frey, M. Gabureac, J. Luetolf

FNSNF Swiss National Science Foundation
QSIT Quantum Science and Technology National Centre of Competence in Research
erc
IARPA BE THE FUTURE
QuSurf

Acknowledgements

www.qudev.ethz.ch

Former group members now
Faculty/PostDoc/PhD/Industry

A. Abdumalikov (Gorba AG)
M. Allan (Leiden)
M. Baur (ABB)
J. Basset (U. Paris Sud)
S. Berger (AWK Group)
R. Bianchetti (ABB)
D. Bozyigit (MIT)
A. Fedorov (UQ Brisbane)
A. Fragner (Yale)
S. Filipp (IBM Zurich)
J. Fink (IST Austria)
T. Frey (Bosch)
S. Garcia (College de France)
S. Gasparinetti (Chalmers)
M. Goppl (Sensirion)
J. Govenius (Aalto)
L. Huthmacher (Cambridge)
D.-D. Jarausch (Cambridge)
K. Juliusson (CEA Saclay)
C. Lang (Radionor)
P. Leek (Oxford)
P. Maurer (Chicago)
J. Mlynek (Siemens)
M. Mondal (IACS Kolkata)
M. Oppliger
M. Pechal (Stanford)
A. Potocnik (imec),
G. Puebla (IBM Zurich)
A. Safavi-Naeini (Stanford)
Y. Salathe (Zurich Inst.)
P. Scarlino (Microsoft)
M. Stammeier (Huba Control)
L. Steffen (AWK Group)
A. Stockklauser (Rigetti)
T. Thiele (UC Boulder, JILA)
A. van Loo (Oxford)
D. van Woerkom (Microsoft)
T. Walter (deceased)
S. Zeytinoğlu (ETH Zurich)

Collaborations (last 5 years) with groups of

A. Bachtold (ICFO Barcelona)
A. Blais (Sherbrooke)
A. Chin (Cambridge)
M. Delgado (UC Madrid)
L. DiCarlo (TU Delft)
P. Domokos (WRC Budapest)
K. Ensslin (ETH Zurich)
J. Faist (ETH Zurich)
A. Fedorov (Brisbane)
K. Hammerer (Hannover)
M. Hartmann (Hariot Watt)
T. Ihn (ETH Zurich)
F. Merkt (ETH Zurich)
L. Novotny (ETH Zurich)
M. A. Martin-Delgado (Madrid)
T. J. Osborne (Hannover)
S. Schmidt (ETH Zurich)
C. Schoenenberger (Basel)
E. Solano (UPV/EHU)
H. Tureci (Princeton)
W. Wegscheider (ETH Zurich)

SEVENTH FRAMEWORK PROGRAMME
SOLID
GEOMDISS
aqute
scaleQIT

ETH
Eidgenössische Technische Hochschule Zürich
Swiss Federal Institute of Technology Zurich
FNSNF
Swiss National Science Foundation
QSIT Quantum Science and Technology
National Centre of Competence in Research
(-)QED
CIRCUIT AND CAVITY QUANTUM ELECTRODYNAMICS
erc

Constructing Linear Quantum Electronic Circuits

electronic photon

basic circuit elements:

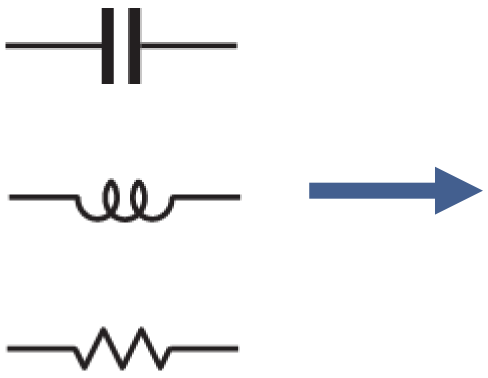

harmonic LC oscillator:

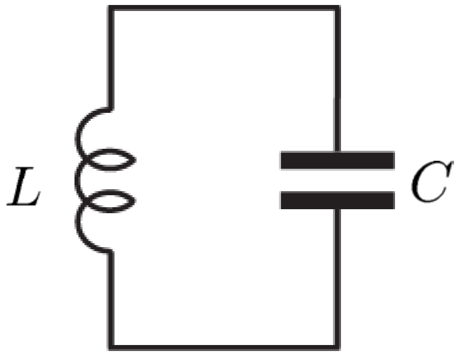

$$\omega = \frac{1}{\sqrt{LC}} \sim 5\,\mathrm{GHz}$$

typical inductor: L = 1 nH
wire in vacuum L ~ 1 nH/mm

typical capacitor: C = 1 pF
size 10 x 10 μm² and
dielectric AlOx (ε = 10) of
10 nm thickness: C ~ 1 pF

energy:

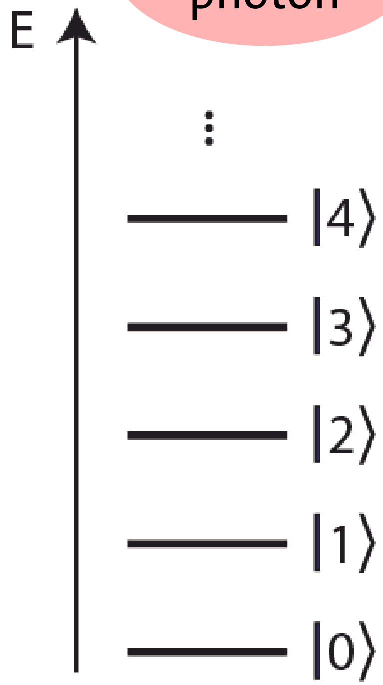

classical physics:

$$H = \frac{\phi^2}{2L} + \frac{Q^2}{2C}$$

quantum mechanics:

$$\hat{H} = \frac{\hat{\phi}^2}{2L} + \frac{\hat{Q}^2}{2C} = \hbar\omega(\hat{a}^\dagger \hat{a} + \frac{1}{2}) \qquad \left[\hat{\phi}, \hat{Q}\right] = i\hbar$$

Review: M. H. Devoret, A. Wallraff and J. M. Martinis, condmat/0411172 (2004)

Quantization of an Electronic Harmonic LC Oscillator

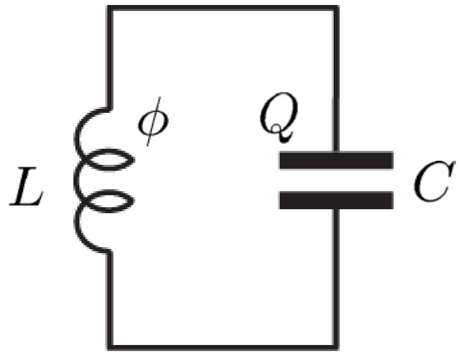

$$\begin{aligned} Q &= CV \\ \phi &= LI \\ V &= -L\dot{I} = -\dot{\phi} \end{aligned}$$

Charge on capacitor

Flux in inductor

Voltage across inductor

Classical Hamiltonian:

$$H = \frac{CV^2}{2} + \frac{LI^2}{2} = \frac{Q^2}{2C} + \frac{\phi^2}{2L}$$

Conjugate variables:

$$\frac{\partial H}{\partial \phi} = \frac{\phi}{L} = I = \dot{Q}\,, \quad \frac{\partial H}{\partial Q} = \frac{Q}{C} = V = -L\dot{I} = -\dot{\phi}$$

Hamilton operator:

$$\hat{H} = \frac{\hat{\phi}^2}{2L} + \frac{\hat{Q}^2}{2C}$$

Flux and charge operator:

$$\begin{aligned} \hat{\phi} &= \phi \\ \hat{Q} &= -i\hbar\frac{\partial}{\partial \phi} \end{aligned}$$

Commutation relation:

$$\left[\hat{\phi}, \hat{Q}\right] = i\hbar$$

Voltages and Currents as Creation and Annihilation Operators

Hamilton operator of harmonic oscillator in second quantization:

$$\hat{H} = \frac{\hat{\phi}^2}{2L} + \frac{\hat{Q}^2}{2C} = \hbar\omega(\hat{a}^\dagger\hat{a} + 1/2)$$

Compare with mechanical harmonic oscillator

$$\hat{a}^\dagger |n\rangle = \sqrt{n+1}\,|n+1\rangle$$ Creation operator

$$\hat{a} |n\rangle = \sqrt{n}\,|n-1\rangle$$ Annihilation operator

$$\hat{a}^\dagger\hat{a} |n\rangle = n\,|n\rangle$$ Number operator

$$\hat{Q} = \sqrt{\frac{\hbar}{2Z_C}}(\hat{a}^\dagger + \hat{a})$$ Charge/voltage operator $\hat{V} = \frac{\hat{Q}}{C}$

$$\hat{\phi} = i\sqrt{\frac{\hbar Z_C}{2}}(\hat{a}^\dagger - \hat{a})$$ Flux/current operator $\hat{I} = \frac{\hat{\phi}}{L}$

With characteristic impedance:

$$Z_C = \sqrt{\frac{L}{C}}$$

Flavors of Superconducting Resonators

lumped element resonator:

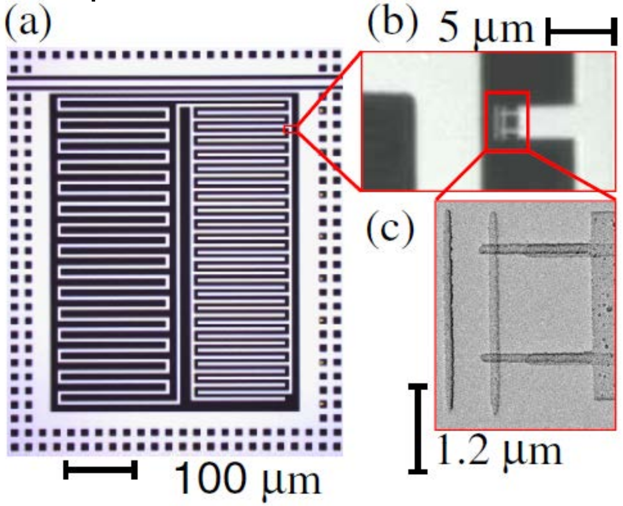

Kim *et al.*, *PRL* **106**, 120501 (2011)

3D cavity:

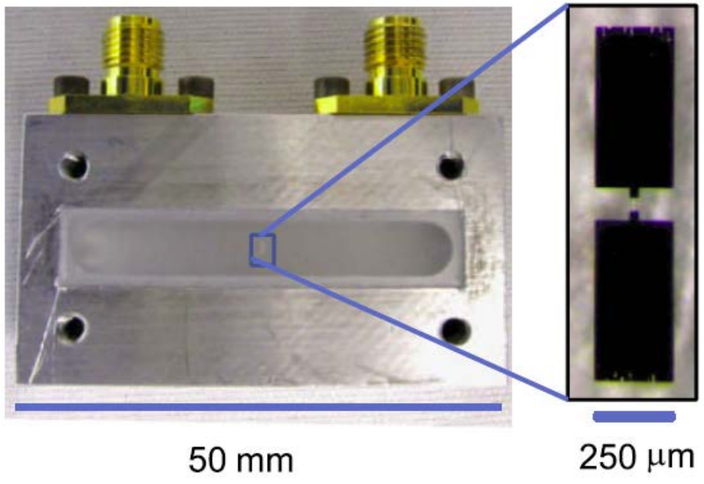

Paik *et al.*, *PRL* **107**, 240501 (2011)

planar transmission line:

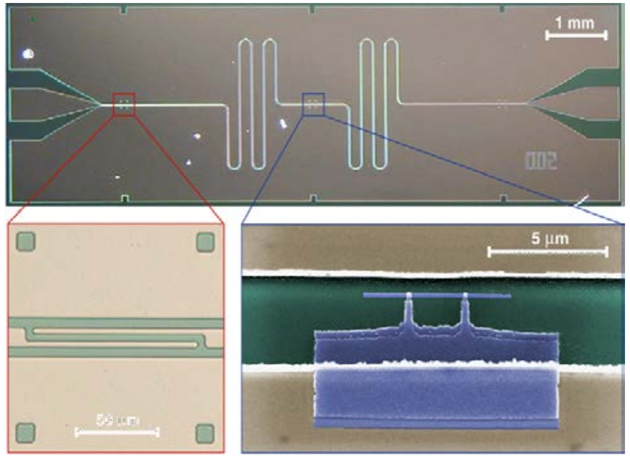

Wallraff *et al.*, *Nature* **431**, 162 (2004)

weakly nonlinear junction:

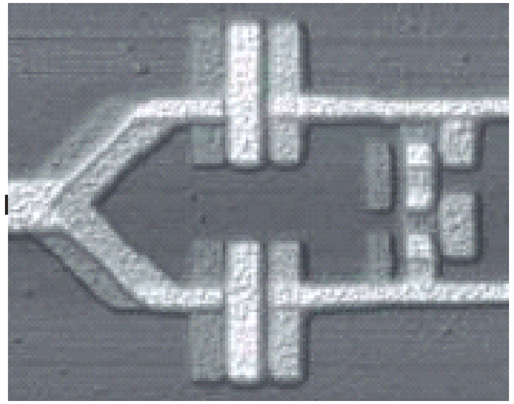

Chiorescu *et al.*, *Nature* **431**, 159 (2004)

The Josephson Junction as an Ideal Non-Linear Inductor

a nonlinear inductor without dissipation

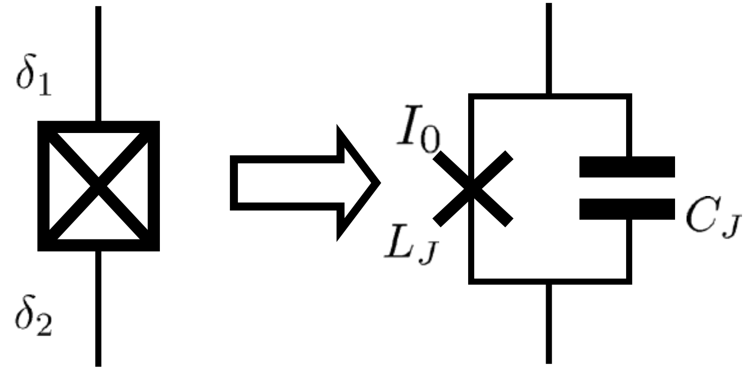

DC/AC Josephson relations: $I = I_0 \sin\delta = I_0 \sin\left[2\pi\phi(t)/\phi_0\right]$ $\qquad V = \frac{\phi_0}{2\pi}\dot{\delta} = \dot{\phi}$

nonlinear current/phase relation

gauge inv. phase difference: $\delta = \delta_2 - \delta_1 = 2\pi\phi(t)/\phi_0$

Josephson inductance: $V = -L_J \dot{I} = \frac{\phi_0}{2\pi I_0}\frac{1}{\cos\delta}\dot{I}$

specific Josephson inductance: $L_{J0} = \frac{\phi_0}{2\pi I_0}$

I_0 = 100 nA corresponds to L_{J0} ~ 3 nH

Josephson energy:

$$E_J = \int V I dt = \frac{I_0\phi_0}{2\pi}\cos\delta$$

specific Josephson energy: $E_{J0} = \frac{I_0\phi_0}{2\pi} = \frac{h\Delta}{8e^2 R_J}$

I_0 = 100 nA corresponds to E_{J0}/h ~ 50 GHz

M. Tinkham, Introduction to Superconductivity, McGraw-Hill

Linear vs. Nonlinear Superconducting Electronic Oscillators

LC resonator:

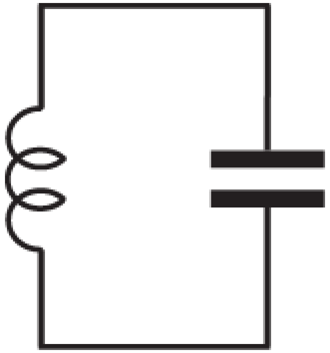

Josephson junction resonator:
Josephson junction = nonlinear inductor

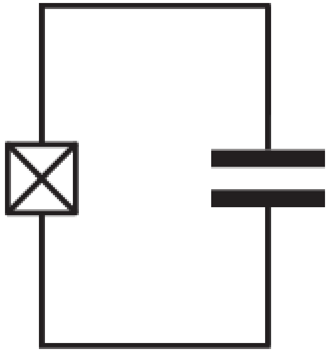

anharmonicity defines effective two-level system

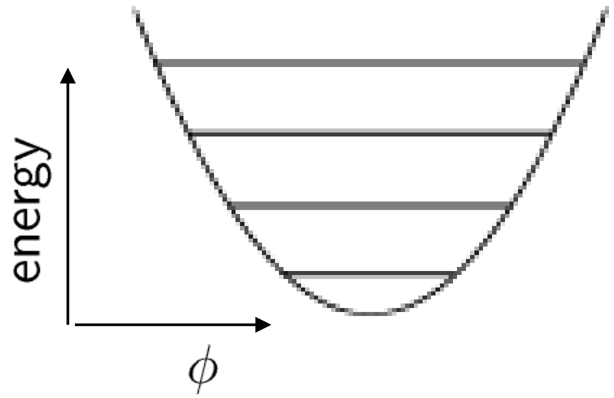

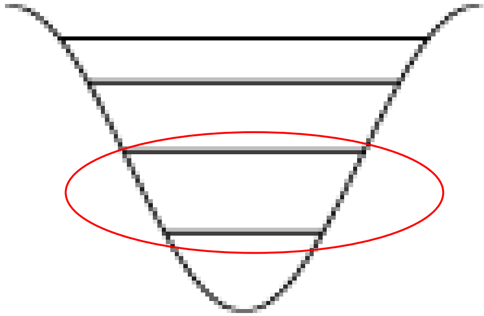

A Low-Loss Nonlinear Element: The Josephson Tunnel Junction

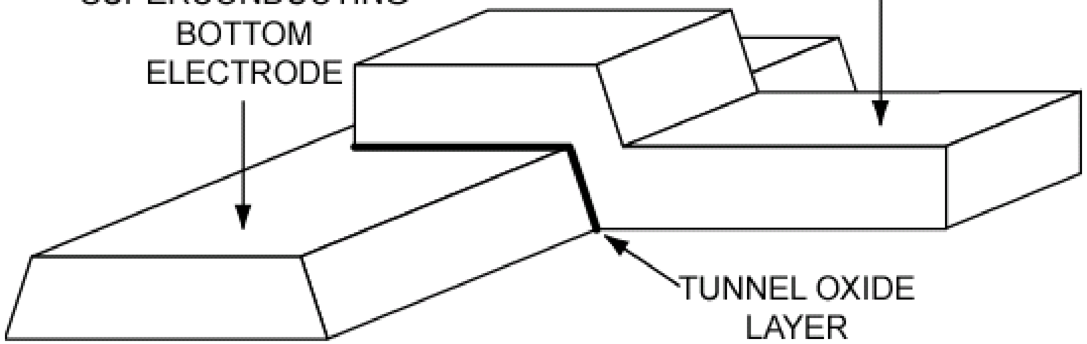

superconductors: Nb, Al
tunnel barrier: AlO_x

Josephson junction fabricated by shadow evaporation:

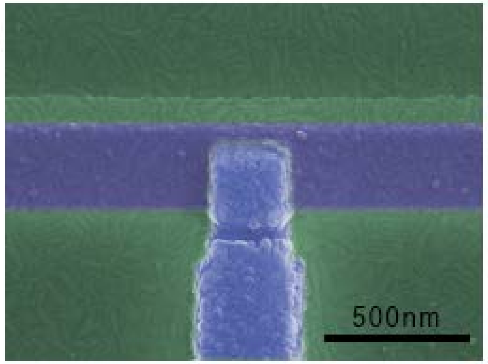

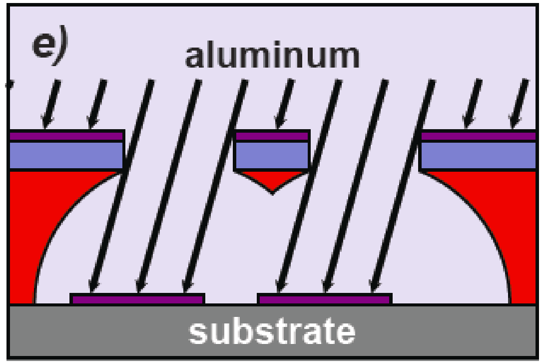

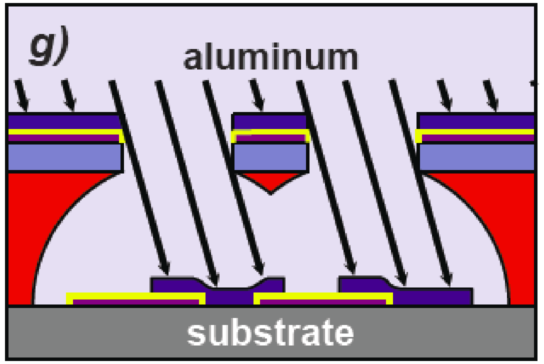

M. Tinkham, Introduction to Superconductivity, McGraw-Hill

Flavors of Superconducting Quantum Bits

Cooper pair box:

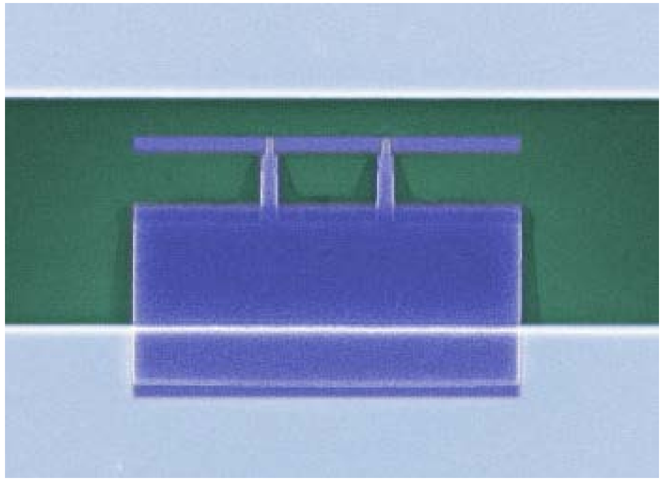

Bouchiat et al., *Physica Scripta* T76, 165 (1998).

Transmon:

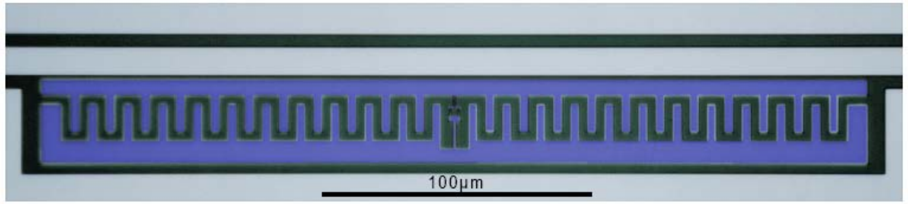

J. Koch *et al.*, PRA 76, 042319 (2007)

(Jellymon):

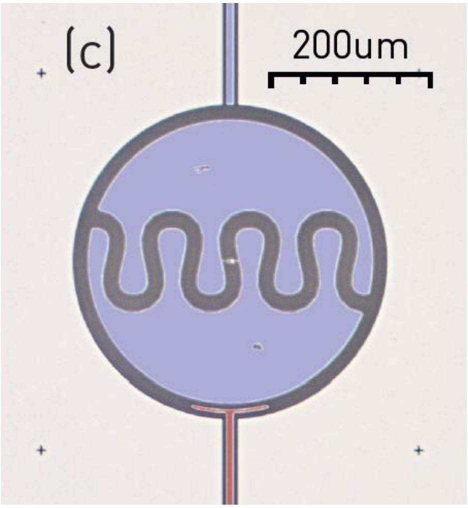

M. Pechal et al., *Phys. Rev. Applied* 6, 024009 (2016)

Xmons:

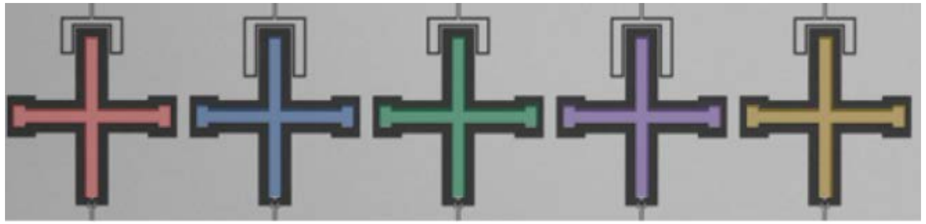

Barends *et al.*, *Phys. Rev. Lett.* 111, 080502 (2013)

Superconducting Circuits as Components for a Quantum Computer

constructing quantum electronic circuits from basic circuit elements:

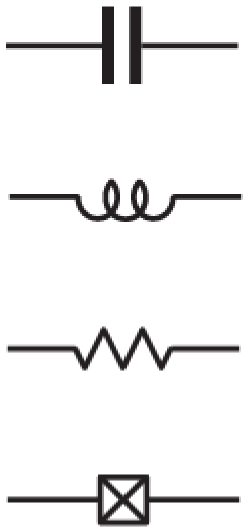

Josephson junction: a non-dissipative nonlinear element (inductor)

harmonic LC oscillator:

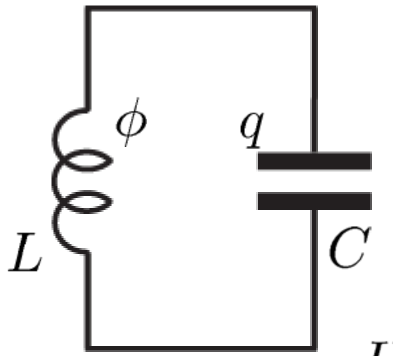

$$H = \hbar\omega(\hat{a}^\dagger \hat{a} + \frac{1}{2})$$

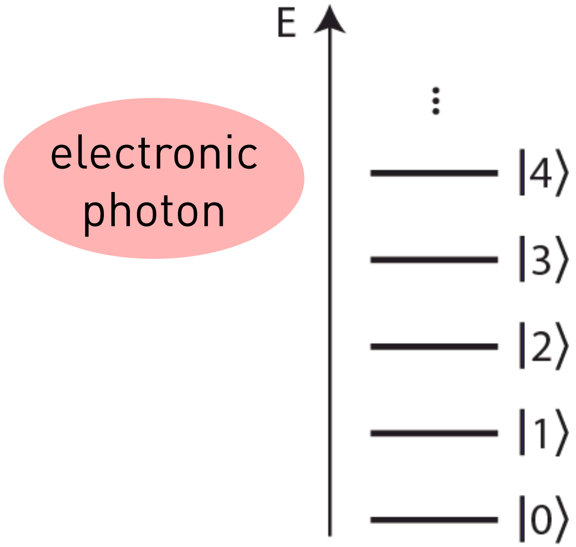

anharmonic oscillator:

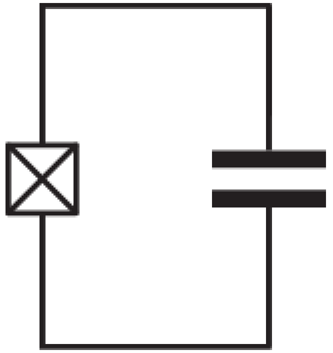

$$H \approx \hbar(\omega_{ge}\,\hat{b}^\dagger \hat{b} - \frac{\alpha}{2}\,\hat{b}^{\dagger 2}\hat{b}^2)$$

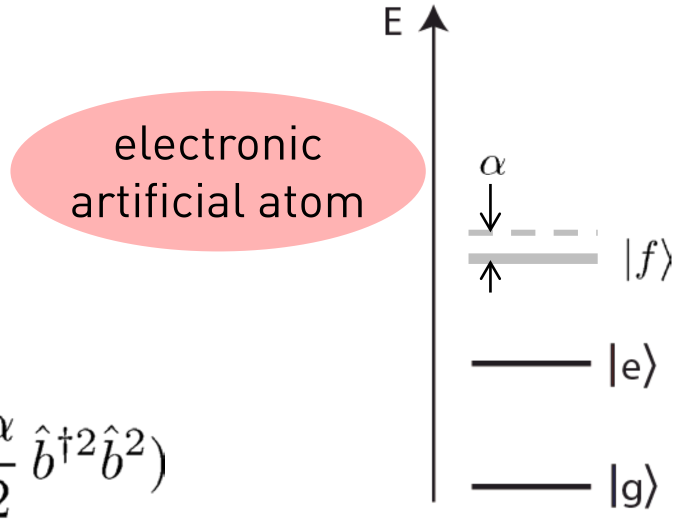

Review: M. H. Devoret, A. Wallraff and J. M. Martinis, *condmat/0411172* (2004)

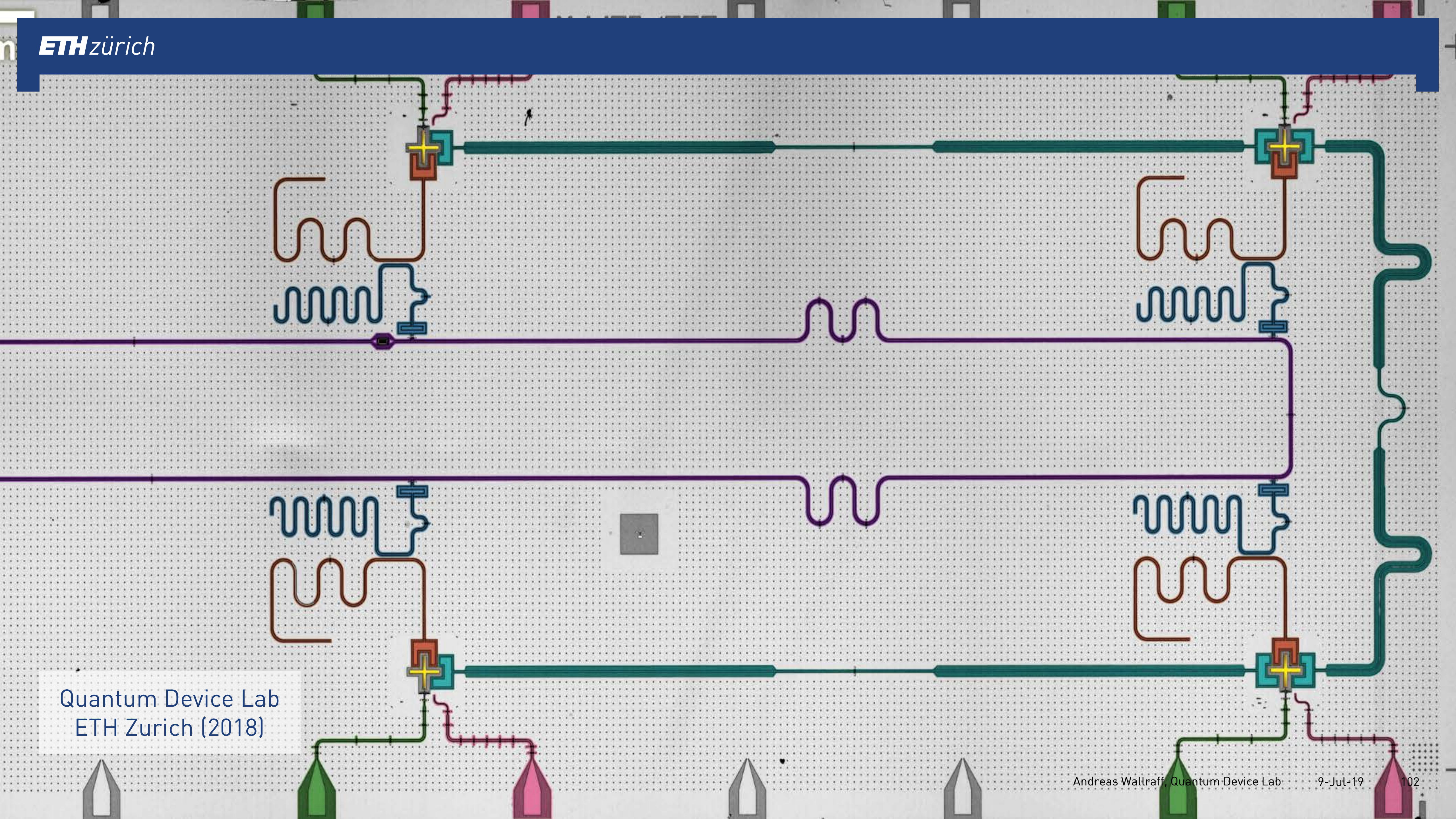

Quantum Device Lab
ETH Zurich (2018)

4 Qubit Device with Multiplexed Readout

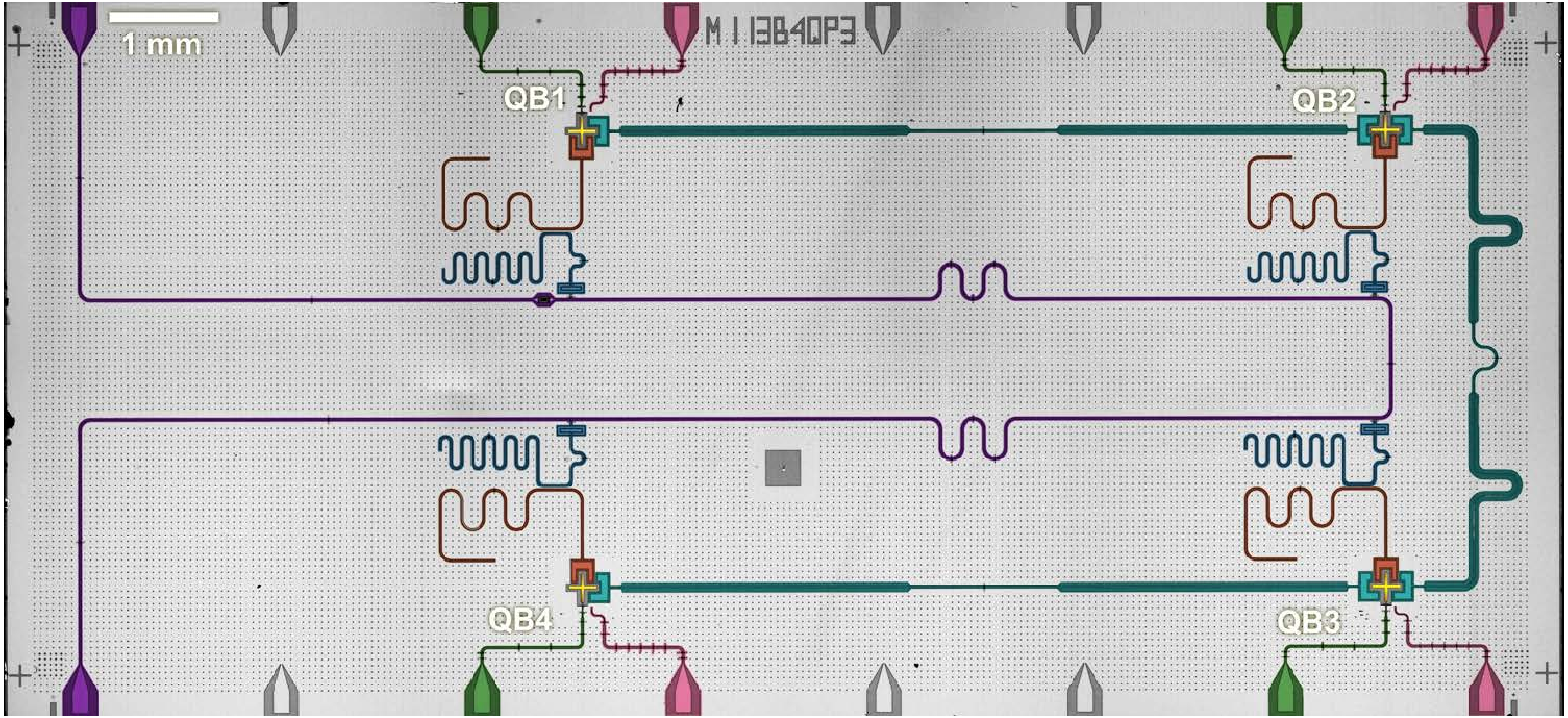

Qubits
Readout resonators
Purcell filters
Coupling Bus resonators
Charge lines
Flux lines
Feed line

C. Andersen, A. Remm, S. Balasiu *et al., arXiv:*1902.06946 (2019)

Features of 4 Qubit Device

Coupler from feedline to **Purcell filter:**

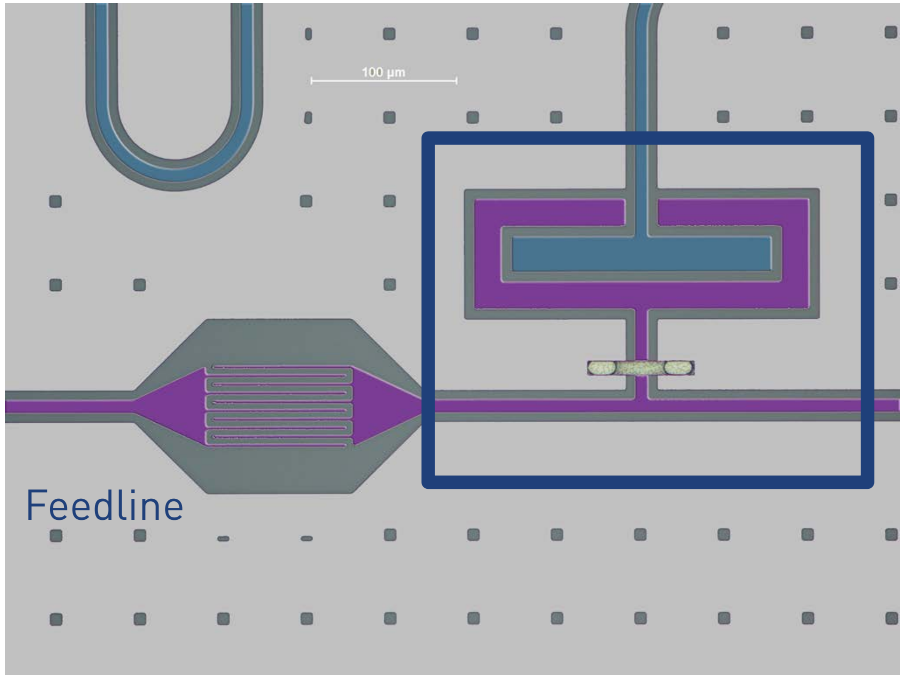

- Designed for improved reproducibility of linewidths.
- Achieved using larger feature size compared to interdigitated finger capacitor.

Qubit Design:

- Nb ground plane
- Nb qubit pad
- Al junction
- Al bandage for good contact to Nb without milling Si

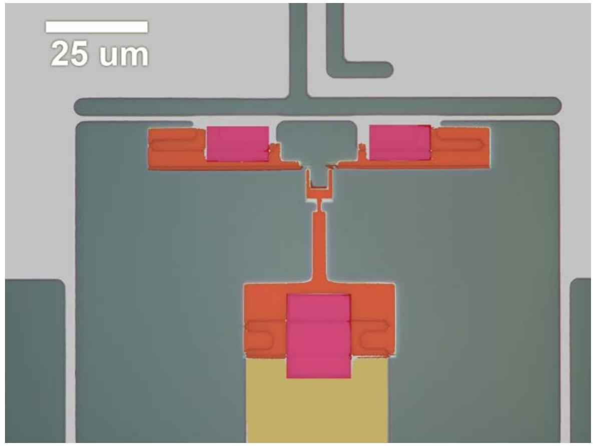

Coupling resonator:

- Increased impedance for larger exchange interaction $J \propto Z_0$
- Increased gap between center conductor and ground

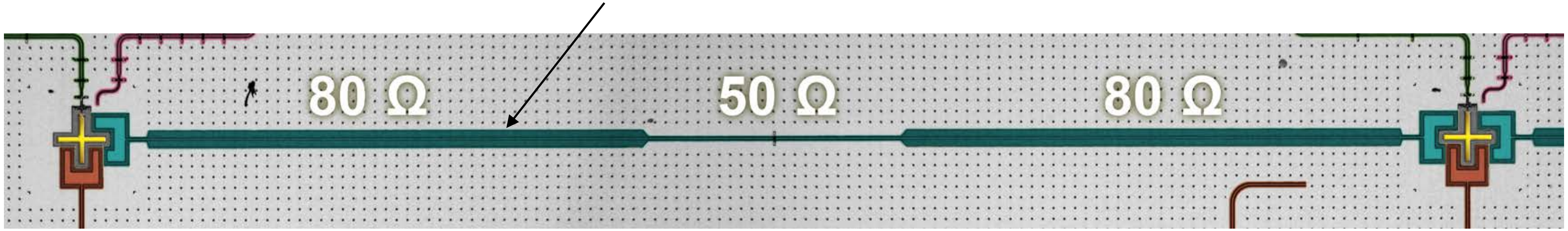

C. Andersen, A. Remm, S. Balasiu et al., *arXiv*:1902.06946 (2019)

Qubit Design and Performance

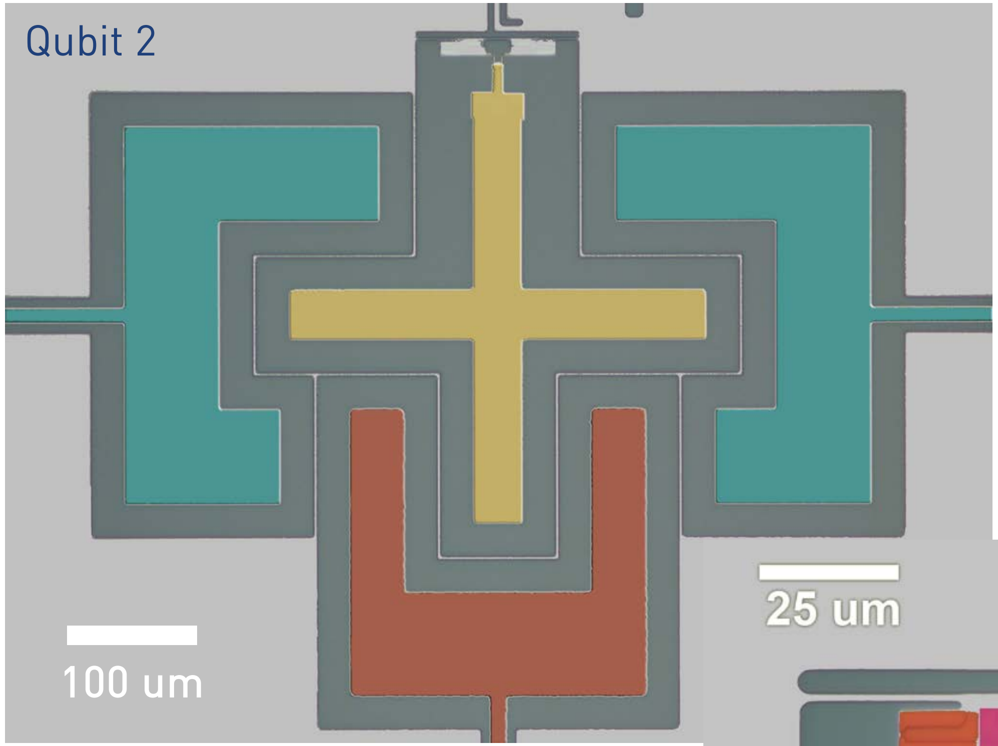

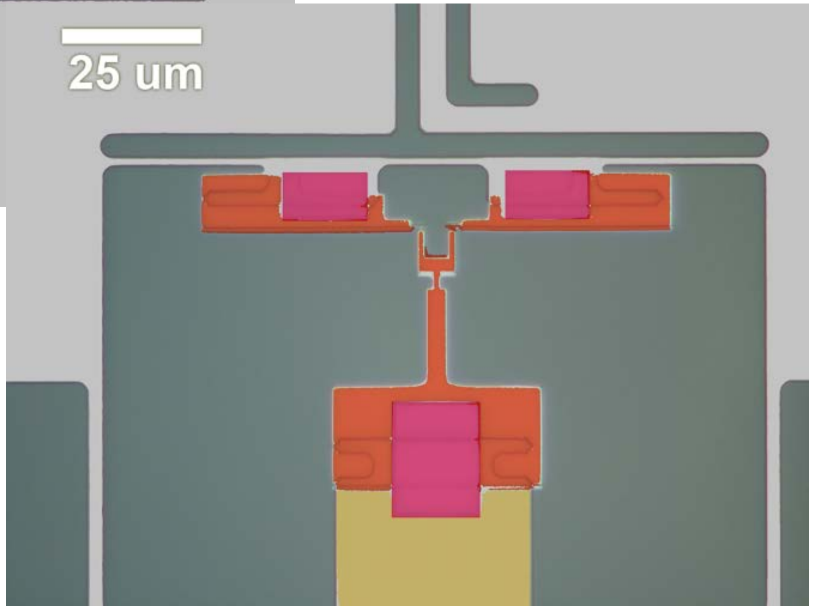

		QB1	QB2	QB3	QB4
Maximum qubit frequency,	$\omega_{Q,\mathrm{max}}/2\pi$ (GHz)	**5.721**	**5.210**	5.530	5.160
Minimum qubit frequency,	$\omega_{Q,\mathrm{min}}/2\pi$ (GHz)	5.083		**4.880**	**4.386**
Qubit lifetime,	T_1 (µs)	19.7	10.3	23.6	43.1
Ramsey coherence time,	T_2^* (µs)	14.3	11.3	14.2	10.7
Echo coherence time,	T_2^{e} (µs)	19.3	12.1	19.5	20.2

- Coherence times are measured at the boldfaced frequencies
- Qubits have asymmetric SQUIDs (ratio 1:8) for decreased flux noise sensitivity

C. Andersen, A. Remm, S. Balasiu et al., *arXiv:*1902.06946 (2019)

How to Operate Electronic Circuits Quantum Mechanically?

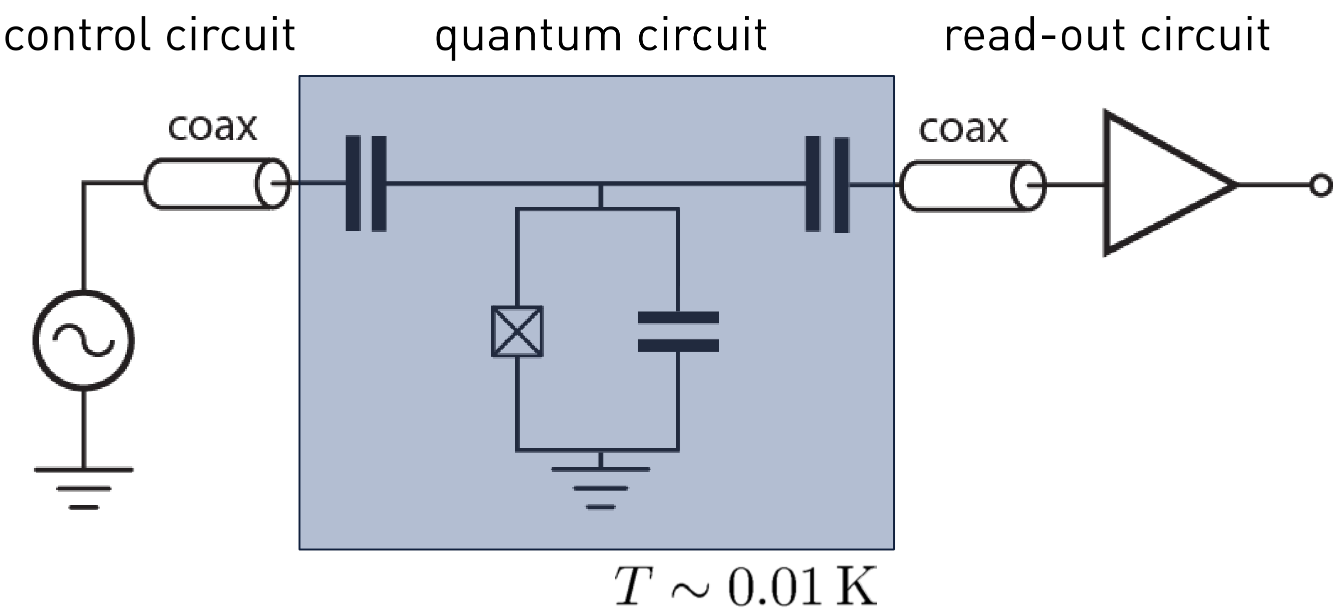

Recipe for preserving coherence:

- avoid dissipation
- work at low temperatures
- isolate quantum circuit from environment

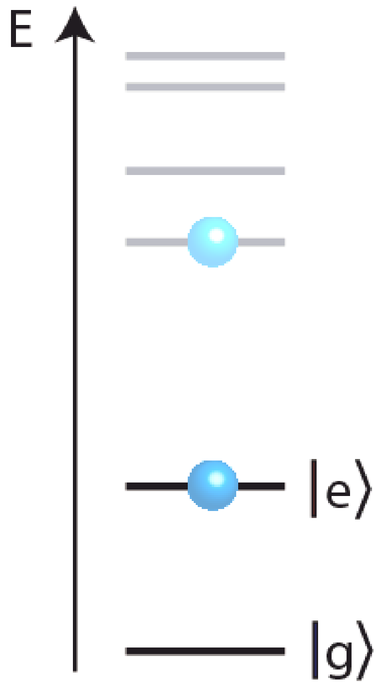

Review: M. H. Devoret, A. Wallraff and J. M. Martinis, *arXiv:condmat/0411172* (2004)

Sample Mount for Superconducting Quantum Circuit

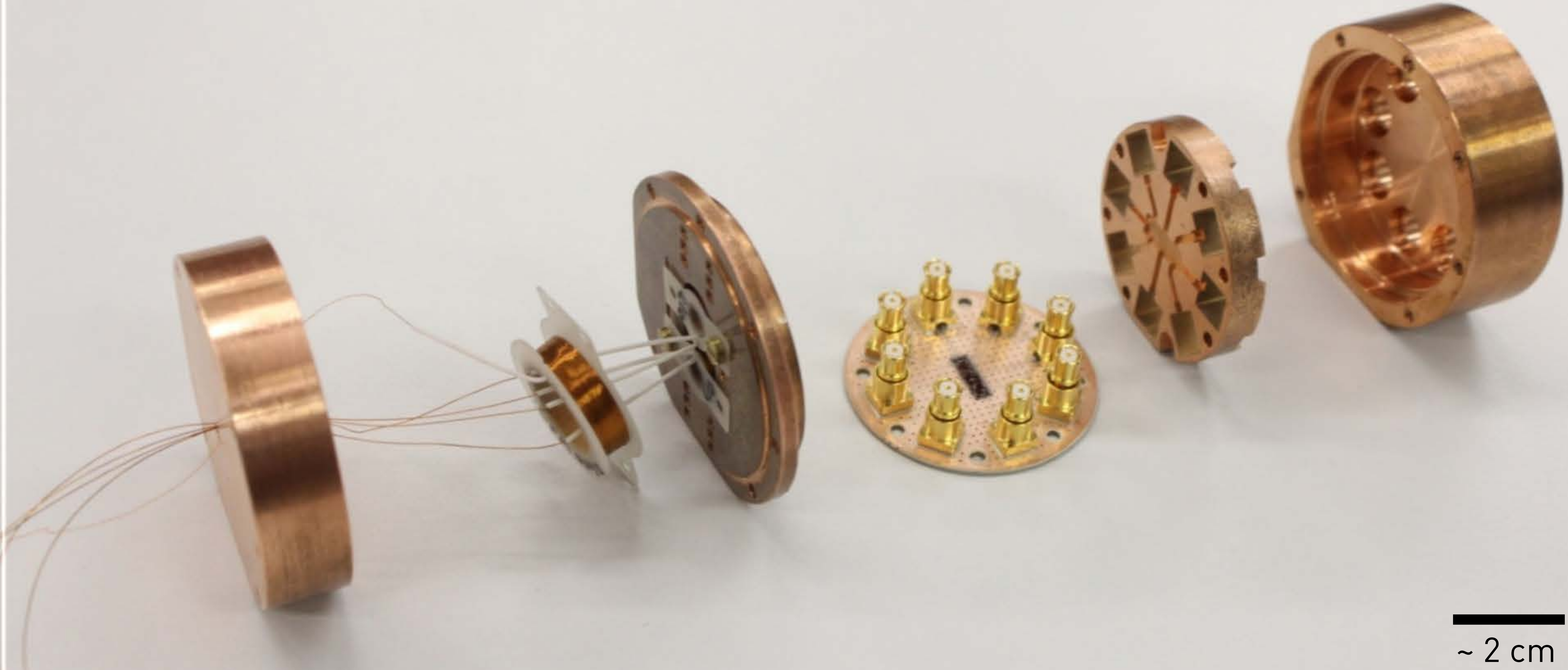

M. Peterer *et al.*, Quantum Device Lab, ETH Zurich (2012)

Ultra-low Temperatures

S. Krinner *et al.*,
EPJ Quantum Technology **6**, 2 (2019)

~ 20 cm

Microwave Control Electronics

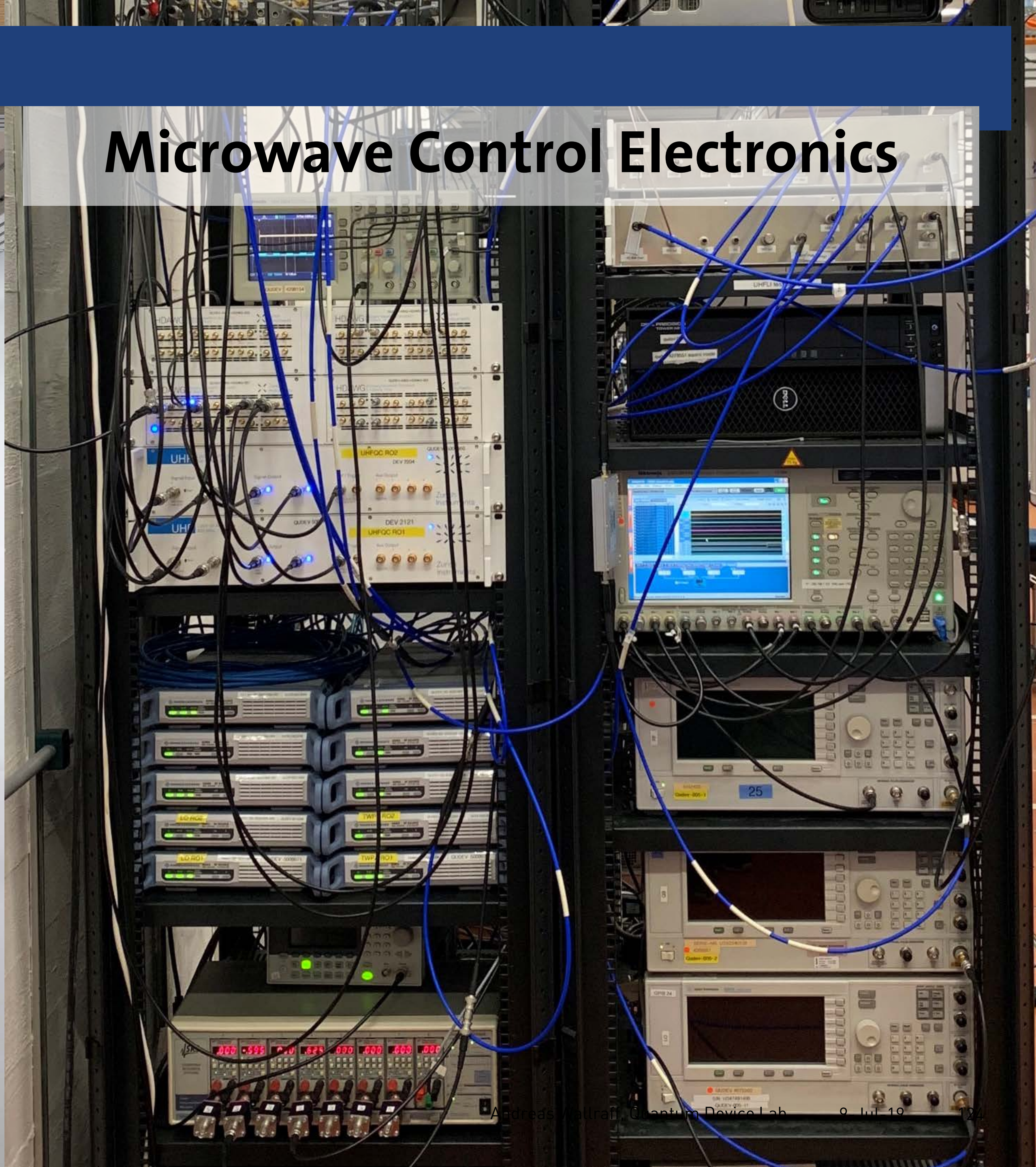

Quantum Device Lab, ETH Zurich

A Single Architecture ...

... for fast, high fidelity single shot readout

F ~ 98.25 (99.2) % at 48 (88) ns integration time and resonator population n ~ 2.2 with

- Optimized sample design
- Low-noise phase-sensitive Josephson parametric amplifier

T. Walter, P. Kurpiers *et al.*, *Phys. Rev. Applied* **7**, 054020 (2017)

... for unconditional reset

- 99% reset fidelity in < 300 ns

P. Magnard *et al.*, *Phys. Rev. Lett.* ***121***, 060502 (2018)

... that is multiplexable

- Single feedline for 8 qubits (nodes)
- Reduced cross-talk using Purcell filters

J. Heinsoo *et al.*, *Phys. Rev. Applied* **10**, 034040 (2018)

... for remote entanglement and state transfer, with time-bin encoding against photon loss

- Deterministic, 50 kHz rate
- ~ 80% transfer and entanglement fidelity

P. Kurpiers, P. Magnard *et al.*, *Nature* **558**, 264 (2018)
P. Kurpiers, M. Pechal *et al.*, *arXiv:*1811.07604 (2018)

... for single-shot parity and single photon detection

- 13% dark count probability, 16% detection inefficiency
- Wigner tomography, propagating cat states

J.-C. Besse *et al.*, *Phys. Rev. X* **8**, 021003 (2018)

J.-C. Besse *et al.*, *Quamtum Device Lab* (2019)

... for parity check with feedback and reset

C. Andersen, A. Remm, S. Balasiu *et al.*, *arXiv:*1902.06946 (2019)

Fast, High-Fidelity Single Shot Readout

Ingredient for

- Fast qubit initialization
  - at start of computation
    Riste *et al.*, *PRL* **109**, 050507 (2012)
  - for resetting ancilla qubits
- For feedback or feed forward
  - in error correction
    Reed *et al.*, *Nature* **482**, 382 (2012)
    Kelly *et al.*, *Nature* **519**, 66 (2015)
    Corcoles *et al.*, *Nat. Com.* **6**, 6979 (2015)
    Ristè *et al.*, *Nat. Com.* **6**, 6983 (2015)
  - in measurement based entanglement generation
    Riste *et al.*, *Nature* **502**, 350 (2013)
  - in teleportation protocols
    Steffen *et al.*, *Nature* **500**, 319 (2013)
  - and more …

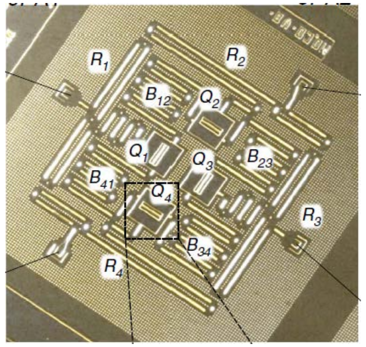

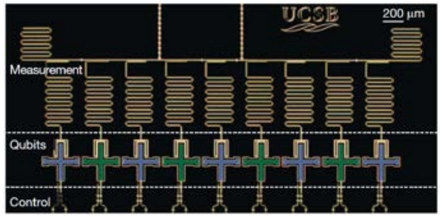

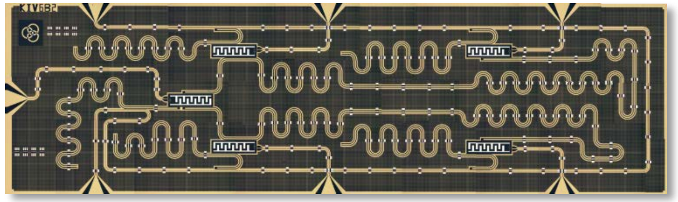

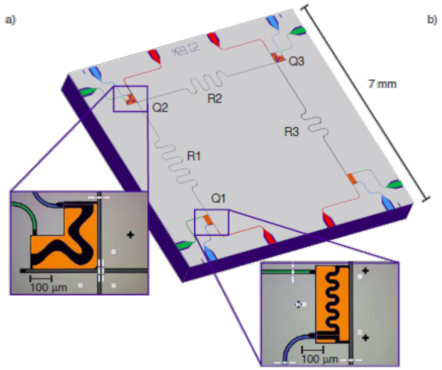

How to achieve fast, high-fidelity single shot readout?

Prior Work

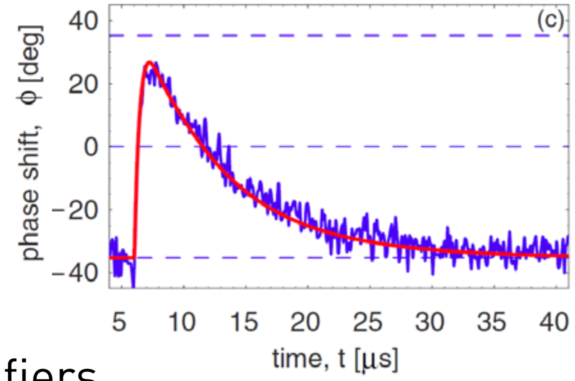

- Dispersive readout using HEMT amplifiers
  B. Johnson *et al.*, *Nat. Phys.* **6**, 663 (2010)
  A. Wallraff *et al.*, *PRL* **95**, 060501 (2005)
- Heralded preparation using parametric amplifiers
  J. E. Johnson *et al.*, *PRL* **109**, 050506 (2012)
  D. Riste *et al.*, *PRL* **109**, 050507 (2012)
- Purcell filters and multiplexing for high fidelity
  E. Jeffrey *et al.*, *PRL* **112**, 190504 (2014)
- Resonator depletion
  C. C. Bultink *et al.*, *Phys. Rev. Applied* **6**, 034008 (2016)
- and more …

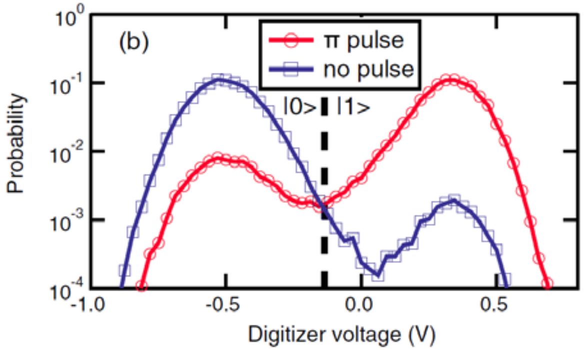

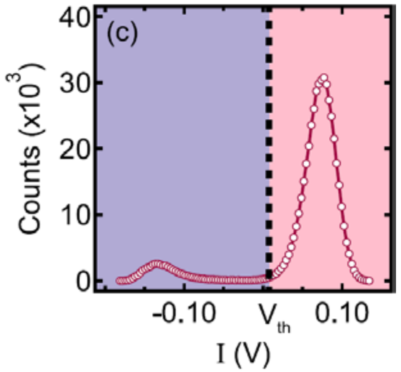

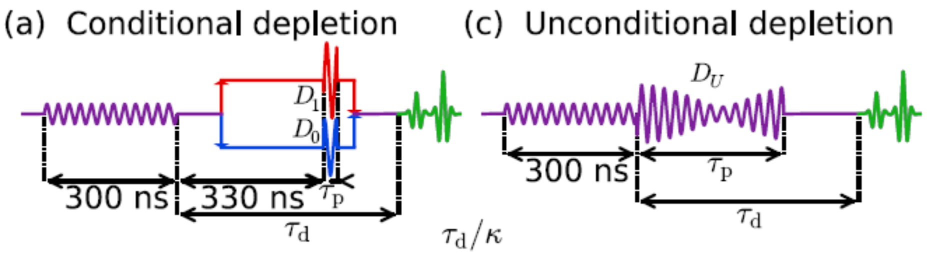

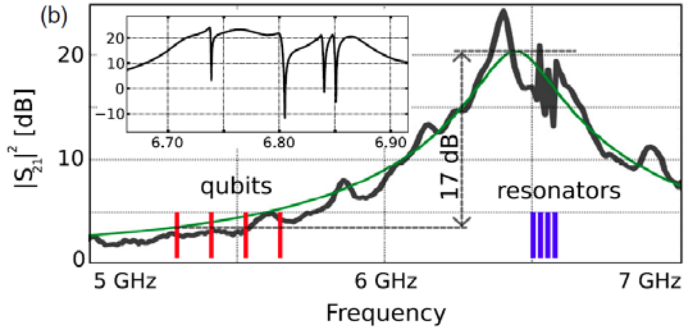

Improvements in speed and fidelity presented in this work
T. Walter, P. Kurpiers *et al.*, *Phys. Rev. Applied* **7**, 054020 (2017)

Chip Design

Quantum bit:
- Transmon
- Drive line

Readout (bottom):
- $\lambda/4$ readout resonator
- $\lambda/4$ Purcell filter

Transfer (top):
- $\lambda/4$ Transfer resonator
- $\lambda/4$ Purcell filter

Features:
- large dispersive shift χ
- large resonator BW κ
- Purcell protection
- 2 channels

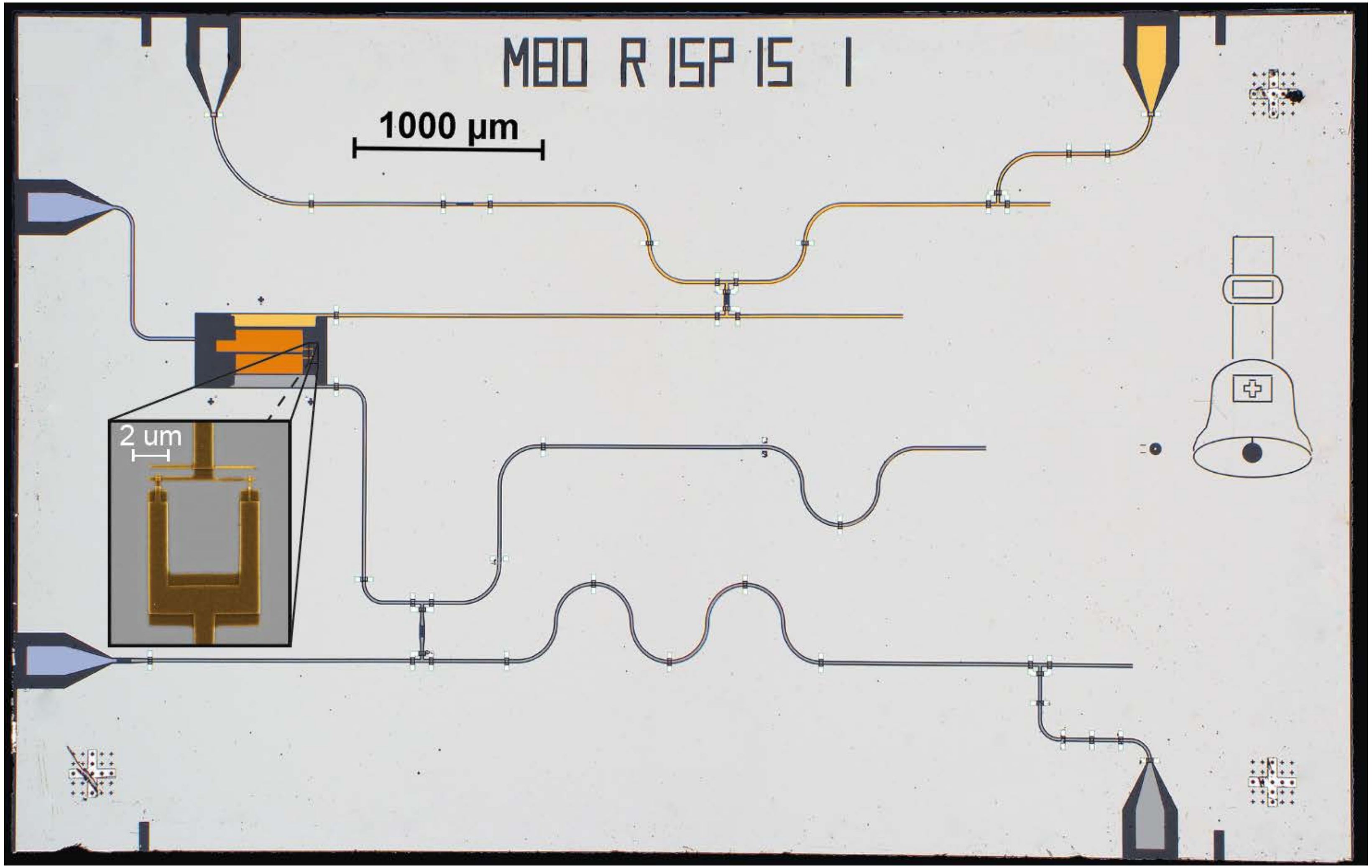

T. Walter, P. Kurpiers *et al., Phys. Rev. Applied* **7**, 054020 (2017)
P. Kurpiers , P. Magnard *et al., Nature* **558**, 264 (2018)

Characterizing Qubit and Resonator in Spectroscopy

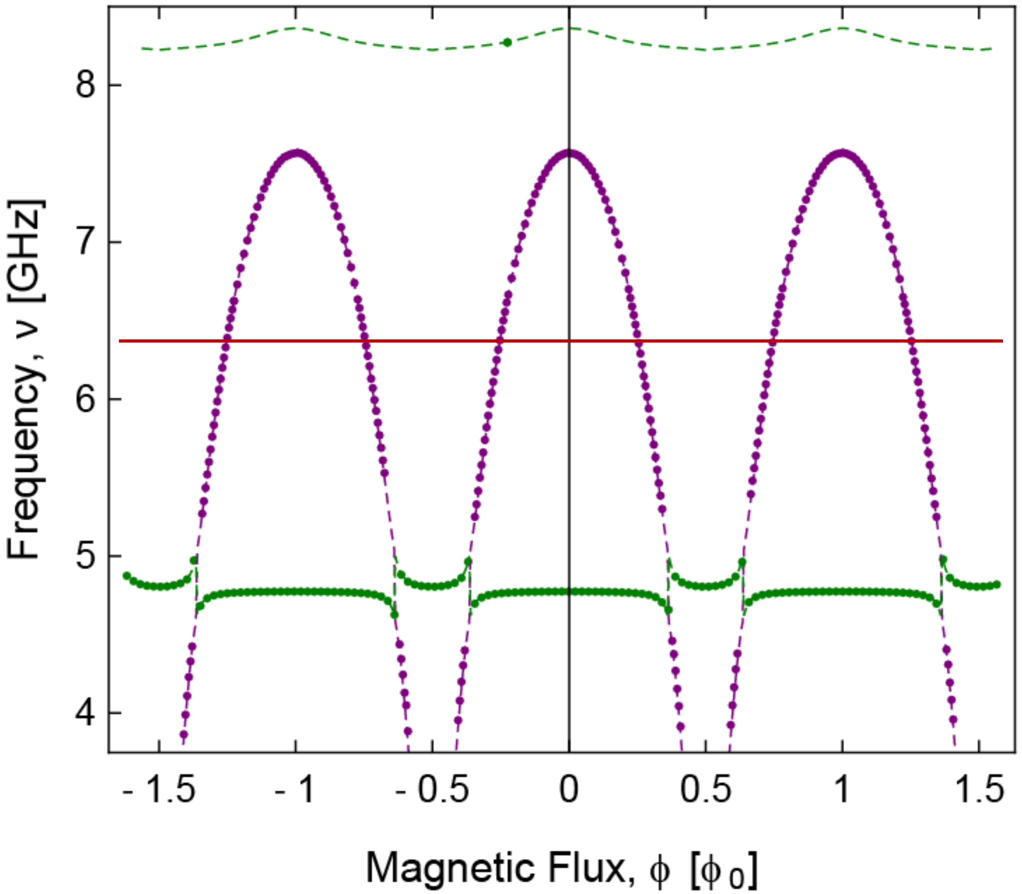

Qubit Parameters @ ν_{ge} = 6.316 GHz

- Energy relaxation time, T_1 ~ 8 μs
- Est. Purcell limit, T_{1p} > 500 μs
- Ramsey dephasing time, T_2 = 1.8 μs
- Anharmonicity, α = 340 MHz
- Cryostat temperature, T = 9 mK
- Equilibrium thermal population, P_e < 0.003

- Measured qubit/resonator freq. (*,*)
- Fit to full Hamiltonian (-,-)
- Operating Frequency (-)

Readout Resonator Response

Transmission amplitude of readout resonator extracted through Purcell filter for qubit prepared in ground (g) or excited (e) state :

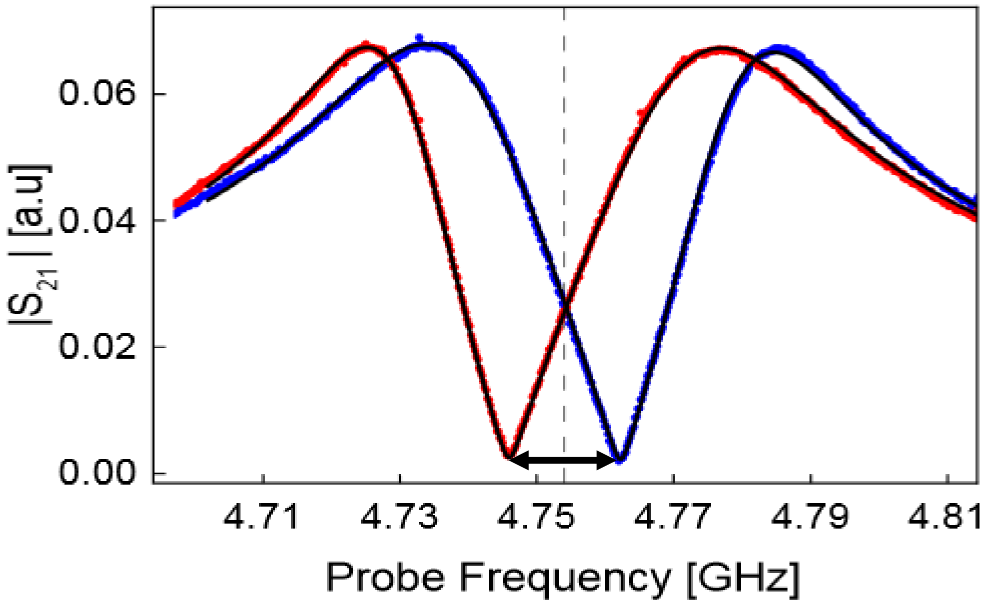

Parameter fit (model):

- Purcell filter $\kappa_p/2\pi$ = 64 MHz
- Readout resonator $\kappa_r/2\pi$ = 37.5 MHz
- State dependent resonator shift $2\chi/2\pi \simeq$ -16 MHz

In ground/excited state:

- Data measured after state prep. (*,*)
- Fit to resonator response model (-)

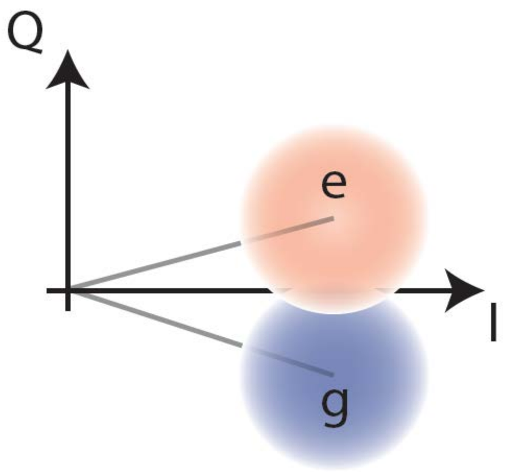

T. Walter, P. Kurpiers *et al., Phys. Rev. Applied* **7**, 054020 (2017)

Time Dependence of Measured Quadrature

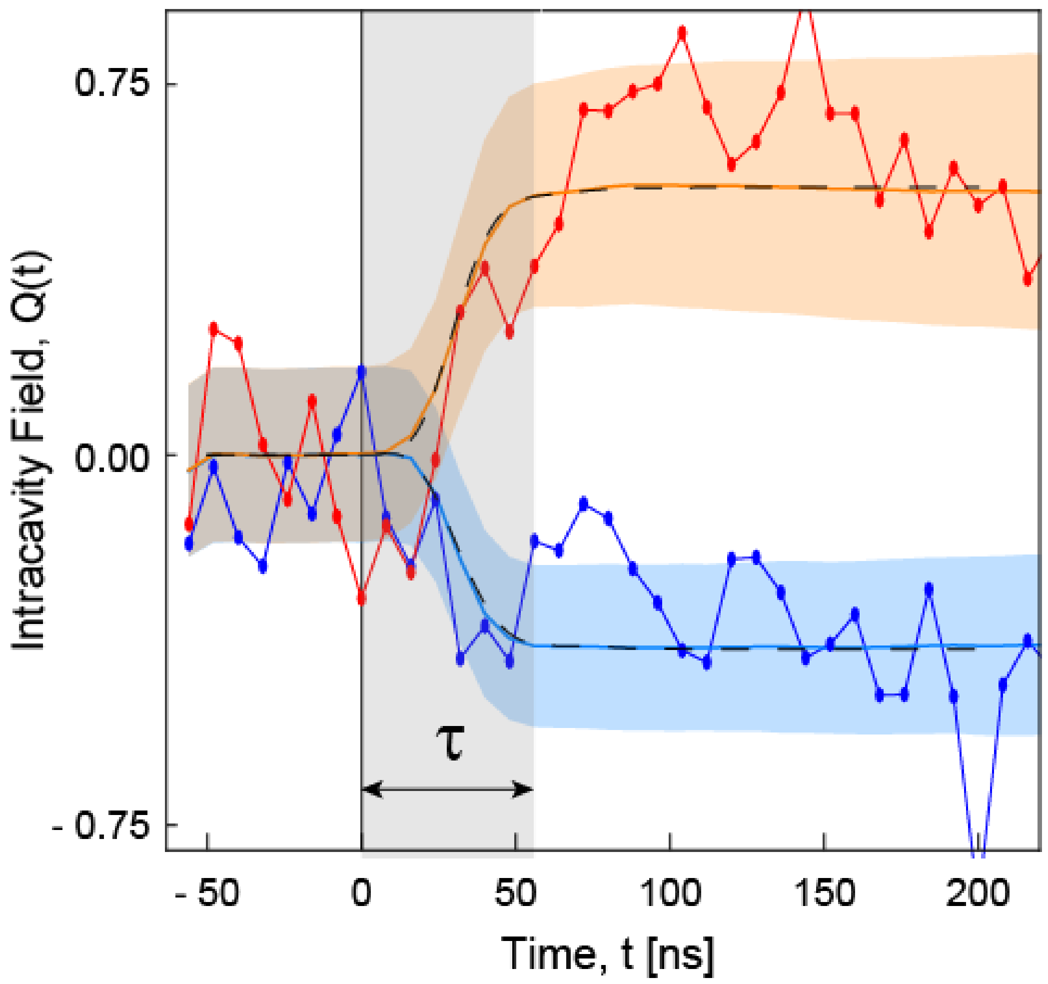

Quantities:

- Single ground state (g) trace
- Average and Stdv of g traces
- Simulated dynamics (-)
- Single excited state (e) trace
- Average and Stdv of e traces
- Simulated dynamics (-)
- Integration time τ

Observations:

- Fast rise of measurement signal (< 50 ns) due large χ (and κ)
- Small decay of average excited state trace due to Purcell protected T_1
- Little increase of average ground state trace due to measurement induced mixing

T. Walter, P. Kurpiers *et al., Phys. Rev. Applied* **7**, 054020 (2017)

Histograms of Integrated Quadrature Signals

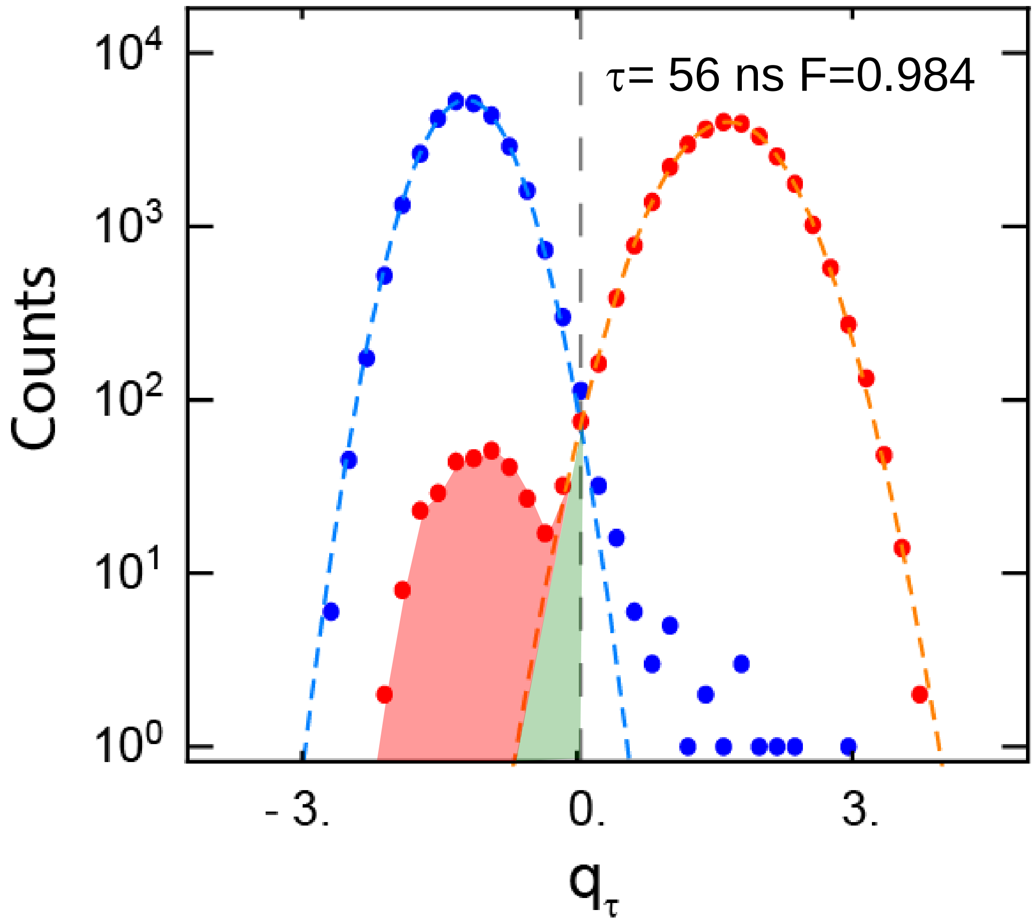

Transmission quadrature integrated with opt. filter in ground/excited state:

- Data of 30k preparations each (*,*)
- Fitted Gaussian distribution (-,-)
- Constant threshold (---)

Definition of errors and fidelities in ground/excited state:

- Overlap error: $\varepsilon_{o,g/e}$
- Transition, preparation (and other) errors: $\tilde{\varepsilon}_{g/e}$
- Total error $\varepsilon_{g/e} = \varepsilon_{o,g/e} + \tilde{\varepsilon}_{g/e}$

For measurement of unknown state:

- Total error $\varepsilon = \varepsilon_g + \varepsilon_e$
- Total fidelity $F = 1 - \varepsilon$

Note:

- Threshold is either kept fixed at midpoint or adjusted for highest fidelity

T. Walter, P. Kurpiers *et al., Phys. Rev. Applied* **7**, 054020 (2017)

Fast, High-Fidelity Readout

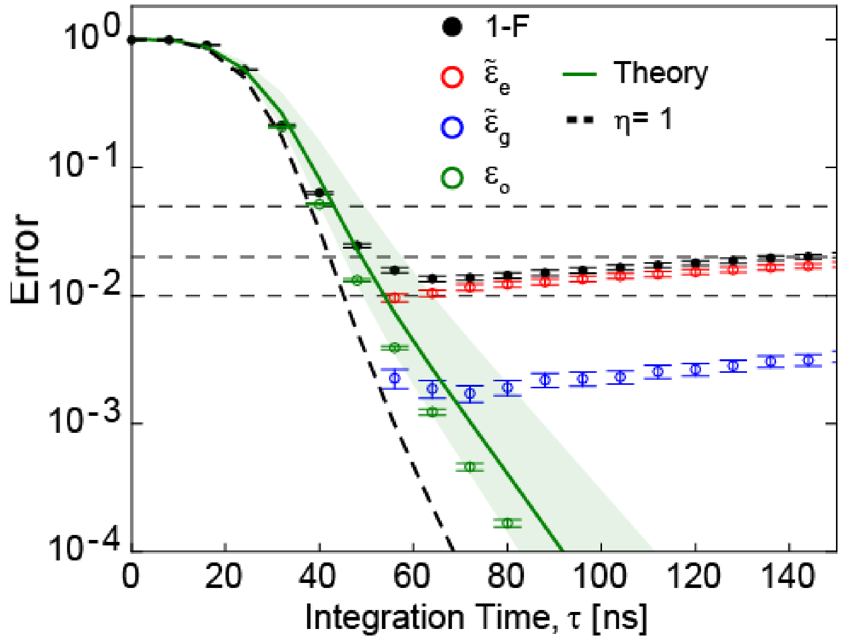

Measurement Error *vs.* Integration Time:

- Fast state discrimination with overlap error dropping to below 1 % in only < 50 ns
- Excited state error < 0.96 %
- Ground state error < 0.23 %
- Max. total fidelity > 98 % limited (in this data) by qubit T_1

Readout power dependence

- Tradeoff between reduction of overlap error and measurement induced mixing errors

Improvements

- Two-step readout pulse
- Higher measurement efficiency at 36 dB paramp gain
- 99.2% total fidelity reached

T. Walter, P. Kurpiers *et al., Phys. Rev. Applied* **7**, 054020 (2017)

A Comparison of Quality Measures of Readout

Reference	[1]	[2]	[3]	[4]	[5]	[6]
Integration time τ [ns]	48	140	300	300	50	750
Total fidelity F [%]	98.4	98.7	97.6	91.1	94.7	97.8
Readout $\kappa/2\pi$ [MHz]	37	4.3	0.6	9	10	1.6
Dispersive shift $2\chi/2\pi$ [MHz]	-16	~	-5.2	7.4	'~60'	'1.3'
Resonator population n,	2.5	~	3300	37.8	-	2.6
Number of qubits on chip	1	4	10	1	1	1
Qubit T_1 [μs]	8	12	25	1.8	3.3	90

[1] T. Walter, P. Kurpiers et al., *Phys. Rev. Applied* 7, 054020 (2017)
[2] E. Jeffrey et al., *PRL* 112, 190504 (2014)
[3] C. C. Bultink et al., *Phys. Rev. Applied* 6, 034008 (2016)
[4] J. E. Johnson et al., *PRL* 109, 050506 (2012)
[5] R. Dassonnevilleet al., *arXiv*:1905.00271 (2019)
[6] S. Touzard et al., *PRL* 109, 080502 (2019)

A Single Architecture …

… for fast, high fidelity single shot readout

F ~ 98.25 (99.2) % at 48 (88) ns integration time and resonator population n ~ 2.2 with

- Optimized sample design
- Low-noise phase-sensitive Josephson parametric amplifier

T. Walter, P. Kurpiers *et al., Phys. Rev. Applied* **7**, 054020 (2017)

… for unconditional reset

- 99% reset fidelity in < 300 ns

P. Magnard *et al., Phys. Rev. Lett.* ***121***, 060502 (2018)

Reset Concept

cQED

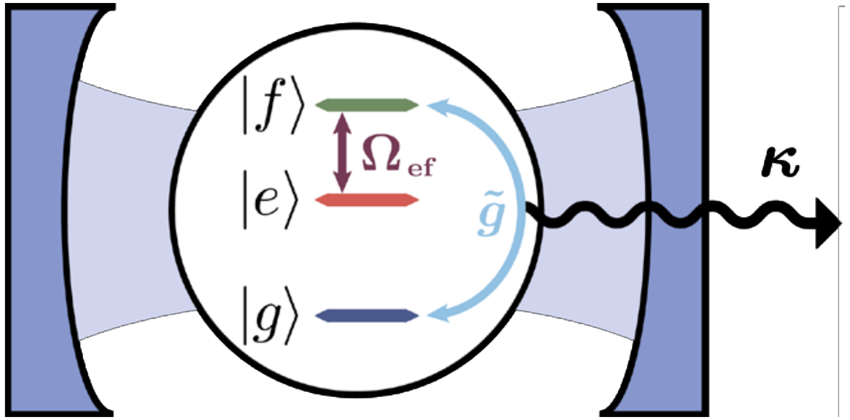

Jaynes-Cumming ladder

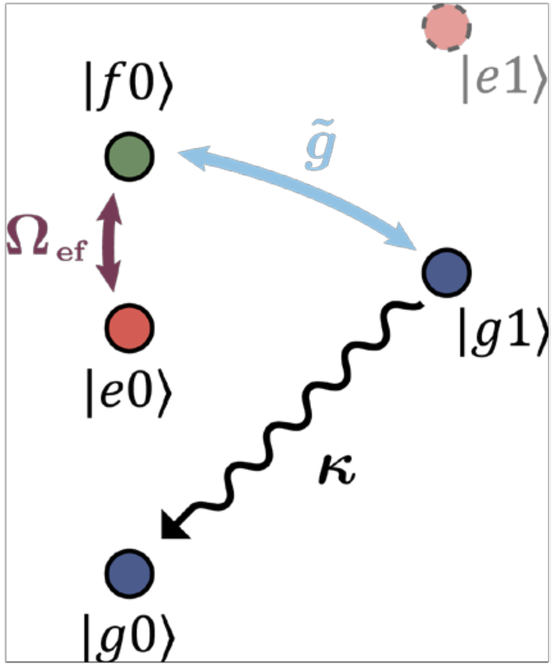

Ingredients

- Strong coupling, dispersive regime
- Cavity dissipation κ
- Raman transition $|f,0\rangle \leftrightarrow |g,1\rangle$[1]
- $|e\rangle \leftrightarrow |f\rangle$ drive

Both $|e\rangle$ and $|f\rangle$ level are reset.

[1] M. Pechal et al. *Phys. Rev. X* 4, 041010 (2014)
[2] P. Magnard et al. *Phys. Rev. Lett.* **121**, 060502 (2018)

State of the Art Reset of Superconducting Qubits

Measurement-based reset[1-4]

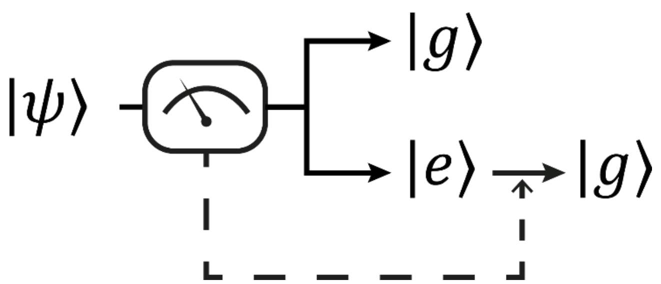

- $P_{\mathrm{exc}} < 2 - 5\%$
- Reset time $\sim 0.3 - 2\mu s$
- Feedback hardware

Frequency tuning reset[5]

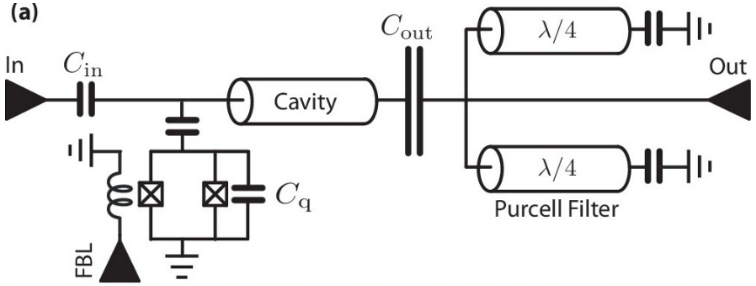

- $P_{\mathrm{exc}} < 1\%$
- Reset time $\sim$ 80ns
- Fast flux line

All-microwave driven reset[6-7]

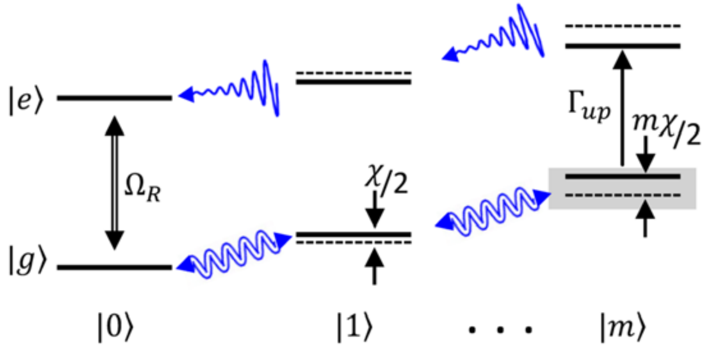

- $P_{\mathrm{exc}} < 1\%$
- Reset time $\sim 2\ \mu s$
- Minimal hardware
- Constraint on parameters ($\kappa < \chi$)

Here: All-microwave - Low P_{exc} - Fast - Minimal hardware - No constraints on parameters

[1] D. Ristè et *al.*, PRL **109**, 240502 (2012)
[2] J. E. Johnson et *al.*, PRL **109**, 050506 (2012)
[3] P. Campagne-Ibarcq et *al.*, PRX **3**, 021008 (2013)
[4] Y. Salathé et *al.*, *Phys. Rev. Appl.* **9**, 034011 (2018)
[5] M. D. Reed et *al.*, APL **96**, 203110 (2010)
[6] K. Geerlings et *al.*, PRL **110**, 120501 (2013)
[7] D. Egger et *al.*, Phys. Rev. Appl. 10, 044030 (2018)

Concept: Unconditional All-Microwave Reset

Large BW Cavity QED System

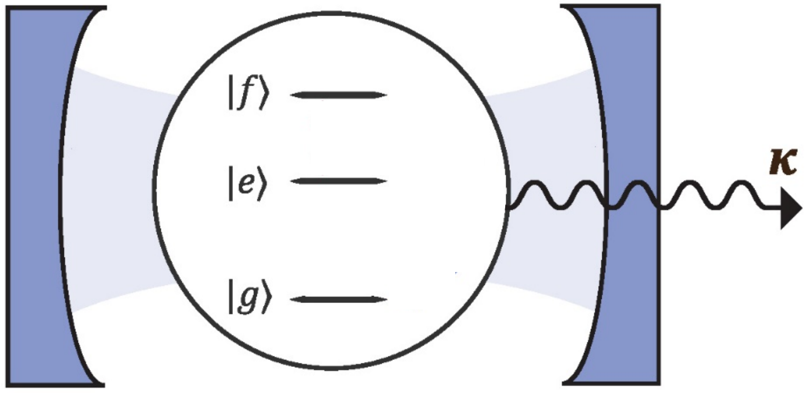

Jaynes-Cumming Ladder

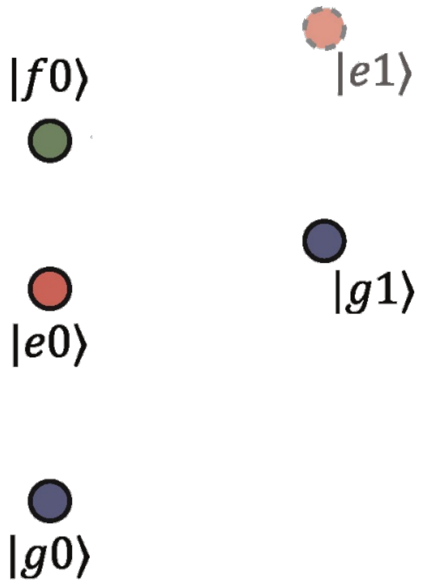

P. Magnard et al. *Phys. Rev. Lett.* **121**, 060502 (2018)
M. Pechal et al. Phys. Rev. X 4, 041010 (2014)
P. Kurpiers et al., *Nature* **558**, 264-267 (2018)

Ingredients:

- Cavity with large decay rate κ
- Continuous drives
  - $|f,0\rangle \leftrightarrow |g,1\rangle$ Raman transition
  - $|e\rangle \leftrightarrow |f\rangle$ transition

Advantages:

- Measurement-free, unconditional (no feedback)
- Fast, high reset rate
- Resets both $|e\rangle$ and $|f\rangle$ level
- All-microwave (no frequency tuning no additional constraints on parameters)
- Small induced excitation relative to dispersive readout

Physical Implementation

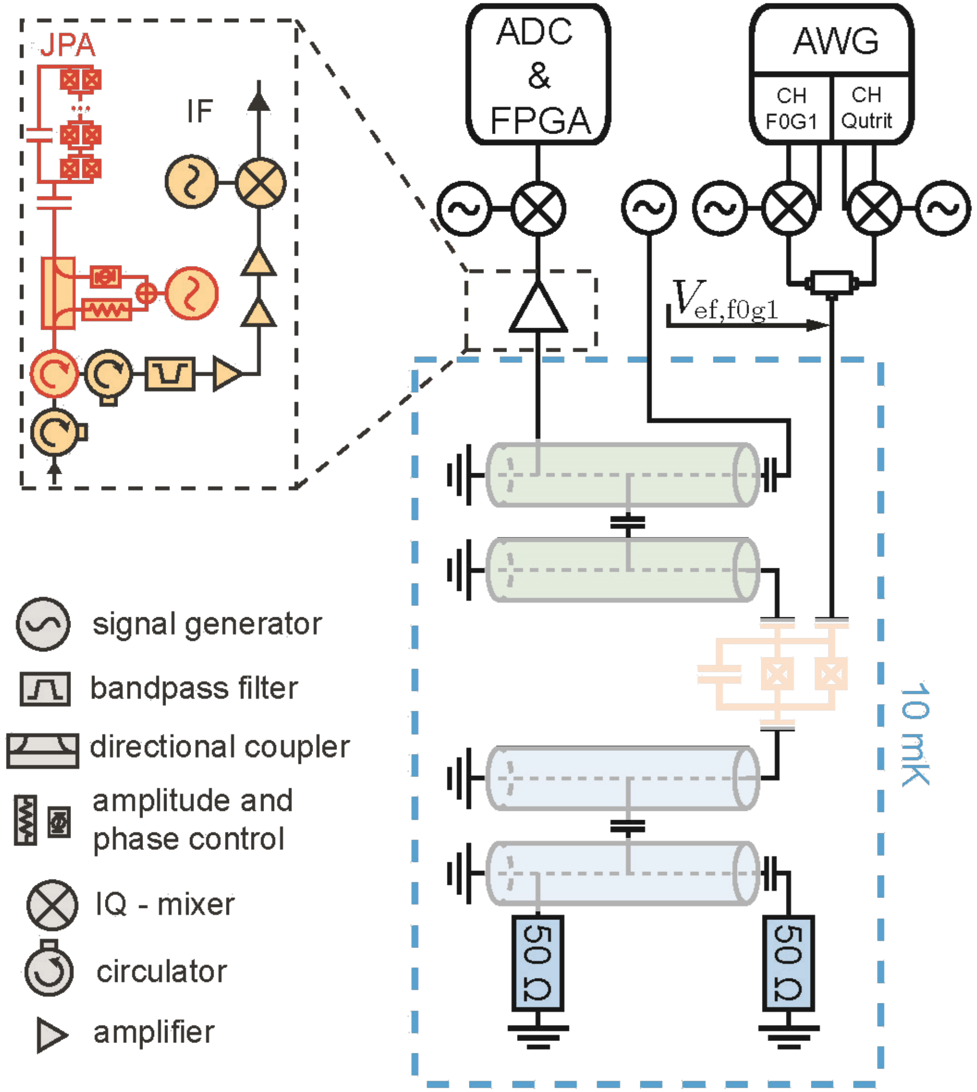

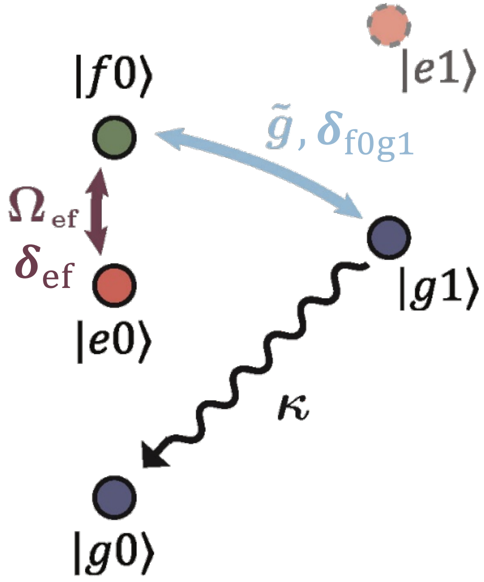

- Parametrized by: $\Omega_{ef}, \delta_{ef}, \tilde{g}$ and δ_{f0g1}
- Purcell filter and resonator with higher effective κ provides faster reset (see conclusion)

Transmon	
$\omega_q/2\pi$	6.343 GHz
$\alpha/2\pi$	-265 MHz
T_1	5.5 μs
T_2	7.6 μs

Reset resonator	
$\omega_r/2\pi$	8.400 GHz
$\chi_r/2\pi$	-6.3 MHz
$\kappa/2\pi$	9 MHz

Readout resonator	
$\omega_m/2\pi$	4.787 GHz
$\chi_m/2\pi$	-5.8 MHz
$\kappa_m/2\pi$	12.6 MHz

P. Magnard et al. *Phys. Rev. Lett.* **121**, 060502 (2018)

Tune-Up of Unconditional All-Microwave Reset Protocol

Protocol requires careful calibration of

- AC-Stark shifts δ_{ef} and δ_{f0g1}
- Rabi rates Ω_{ef} and $\tilde{g}$

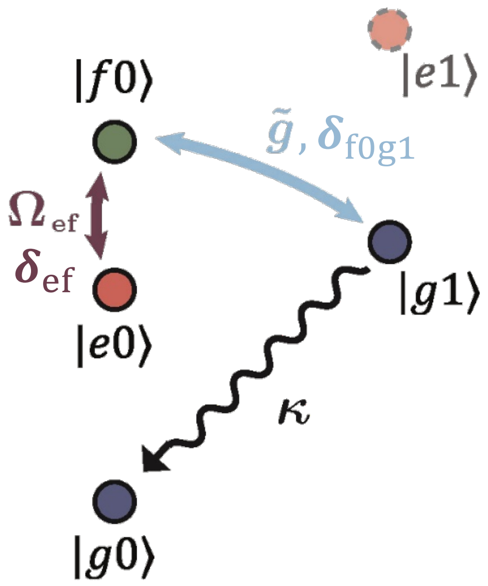

P. Magnard et al. *Phys. Rev. Lett.* **121**, 060502 (2018)

Calibration steps: (1) AC-Stark Shift Calibration for δ_{f0g1}

- Determine frequency shift of the transition as a function of drive strength
- Pulsed for better accuracy of δ_{f0g1}

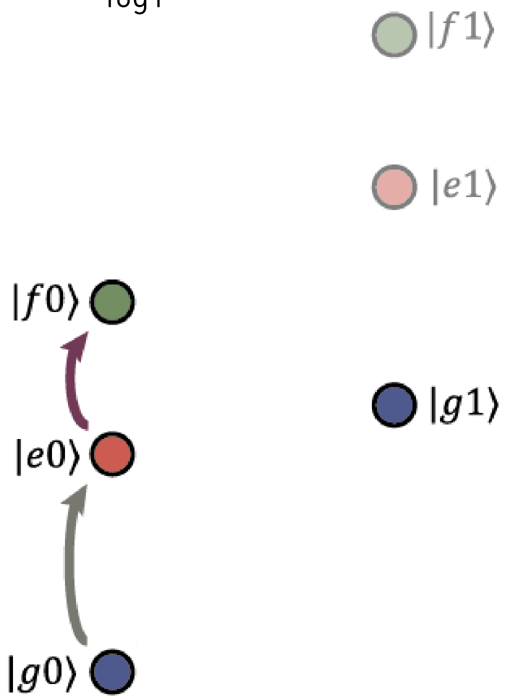

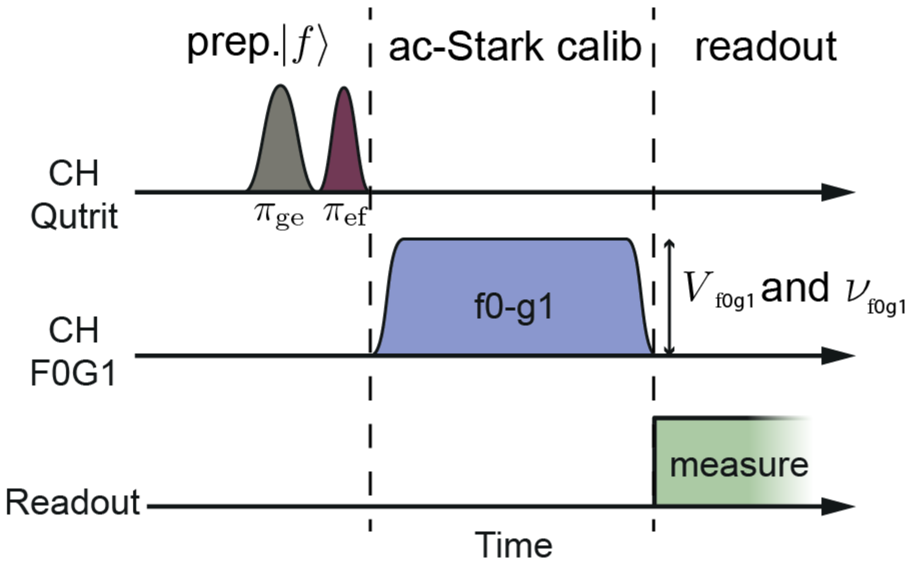

- Prepare qutrit in $|f\rangle$ state
- Sweep **frequency** ν_{f0g1} of $|f,0\rangle \leftrightarrow |g,1\rangle$ drive for fixed Rabi angle ($V_{f0g1} \bullet t_r$)
- Determine resonant frequency by maximum of ground state population Pg
- Repeat for different **amplitudes** V_{f0g1}, keeping Rabi angle fixed.

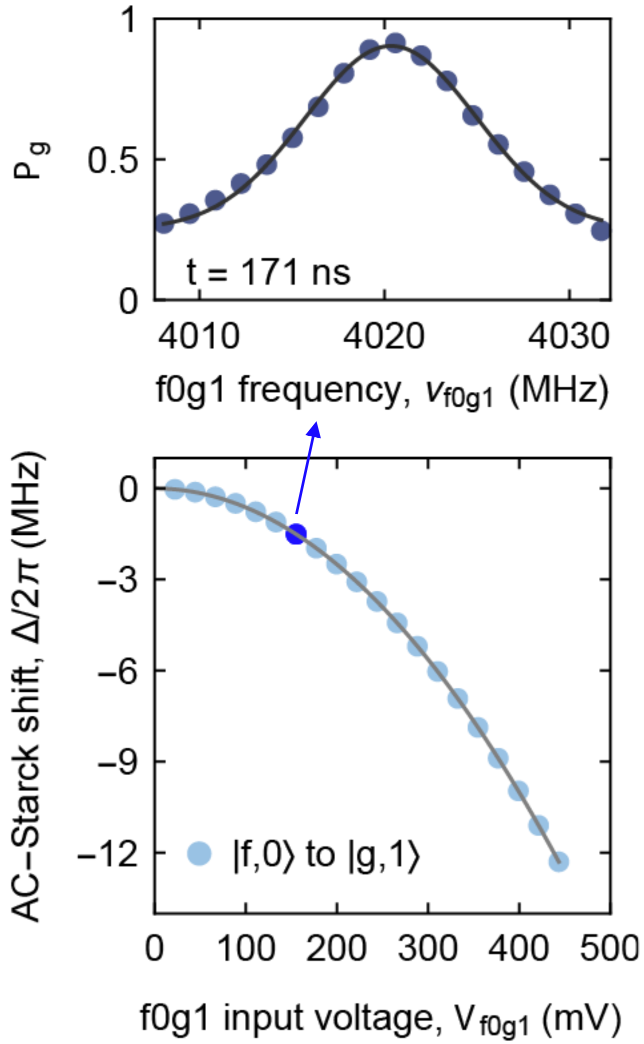

P. Magnard et al. *Phys. Rev. Lett.* **121**, 060502 (2018)

Calibration steps: (2) Calibrate Rabi rate Ω_{ef}

- Determine Rabi rate as a function of drive strength V_{ef}
- Prepare qutrit in state $|e\rangle$

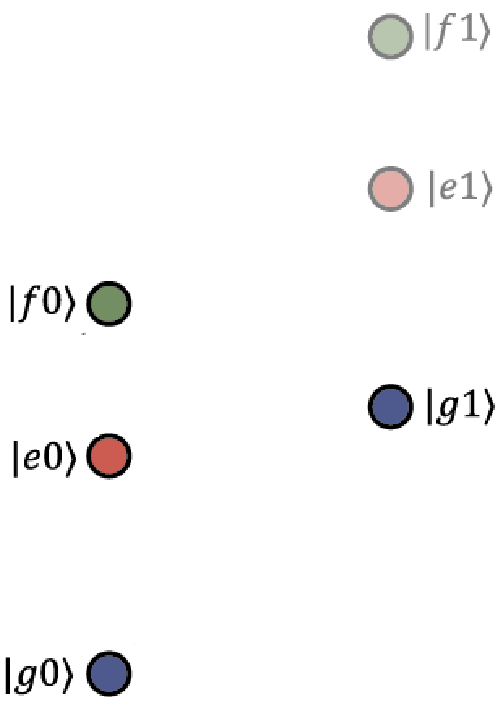

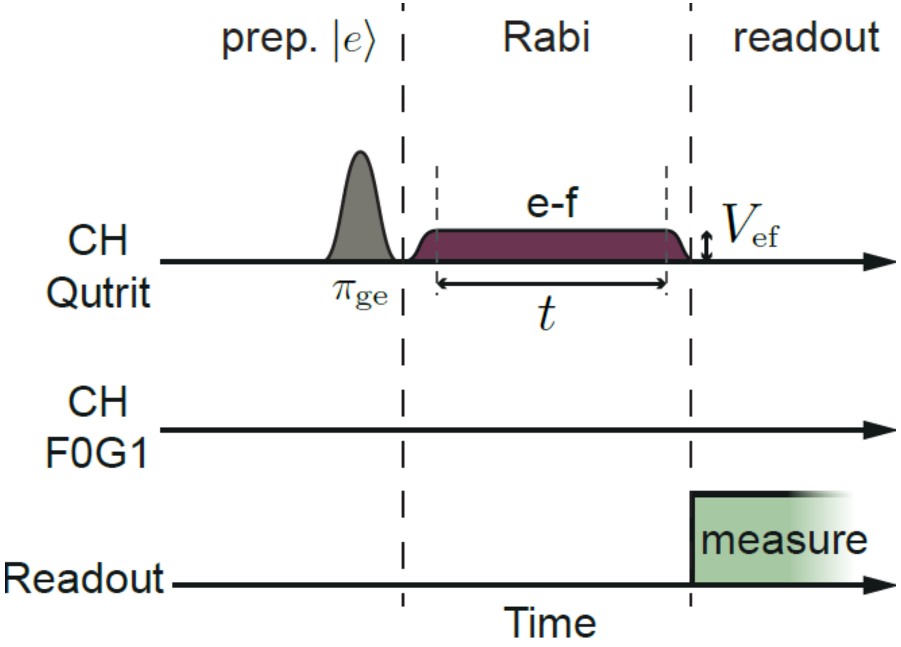

- Drive $|e,0\rangle \leftrightarrow |f,0\rangle$ resonantly while sweeping **duration** of pulse t
- Measure P_f as a function of duration for each amplitude and extract Rate Ω_{ef}
- Repeat for different amplitudes V_{ef} and extract relation between rate and amplitude.

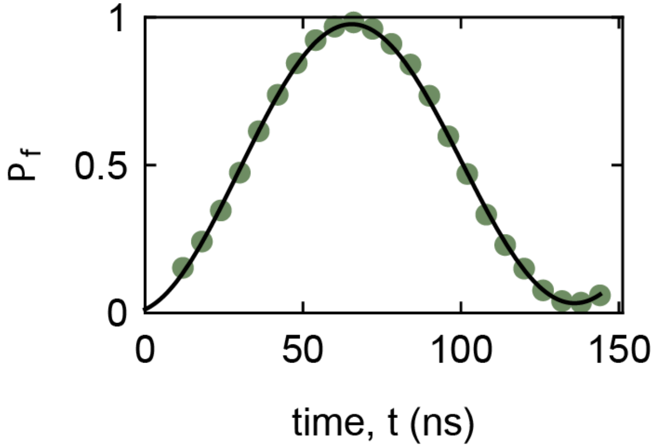

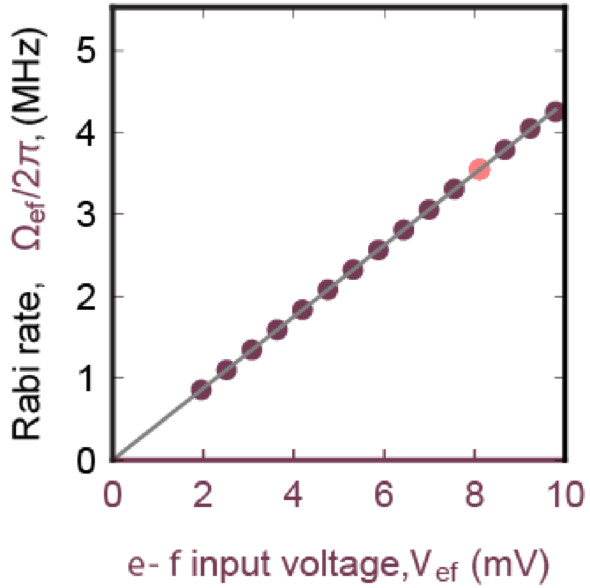

P. Magnard et al. *Phys. Rev. Lett.* **121**, 060502 (2018)

Calibration steps: (3) AC-Stark Shift Calibration for δ_{ef}

- Determine frequency shift of $|e,0\rangle \leftrightarrow |f,0\rangle$ as a function of V_{f0g1} drive strength
- Pulsed for better accuracy of δ_{ef}

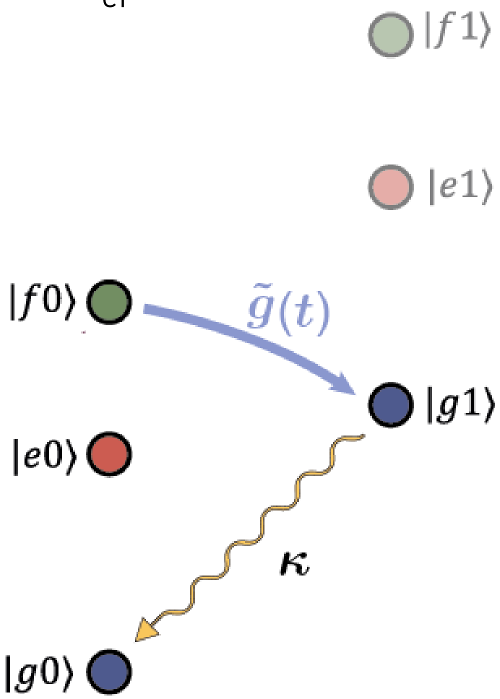

P. Magnard et al.
Phys. Rev. Lett. **121**, 060502 (2018)

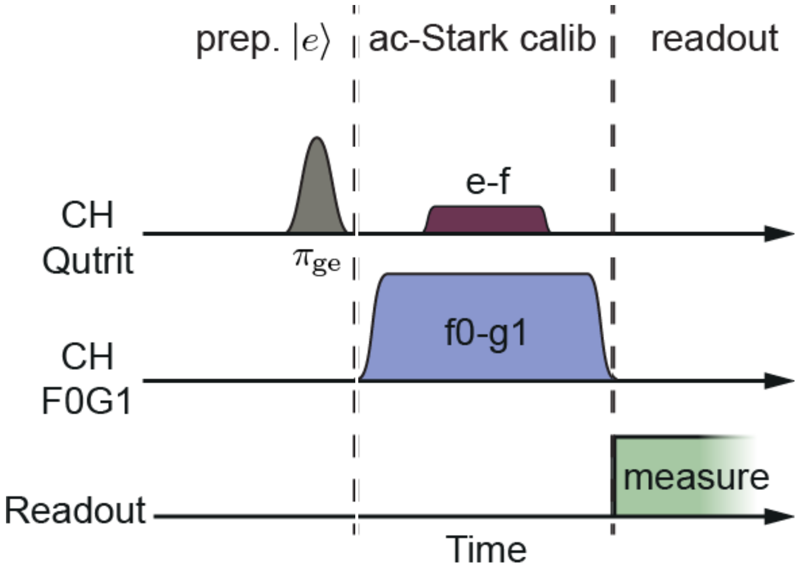

- Prepare qutrit in $|e\rangle$ state
- Start $|f,0\rangle \leftrightarrow |g,1\rangle$ on resonance from calibration step 1
- Apply $|e,0\rangle \leftrightarrow |f,0\rangle$ simultenously
- Sweep frequency of Ω_{ef} drive and measure population in $|e,0\rangle$ to determine resonant frequency
- Repeat for different V_{f0g1}

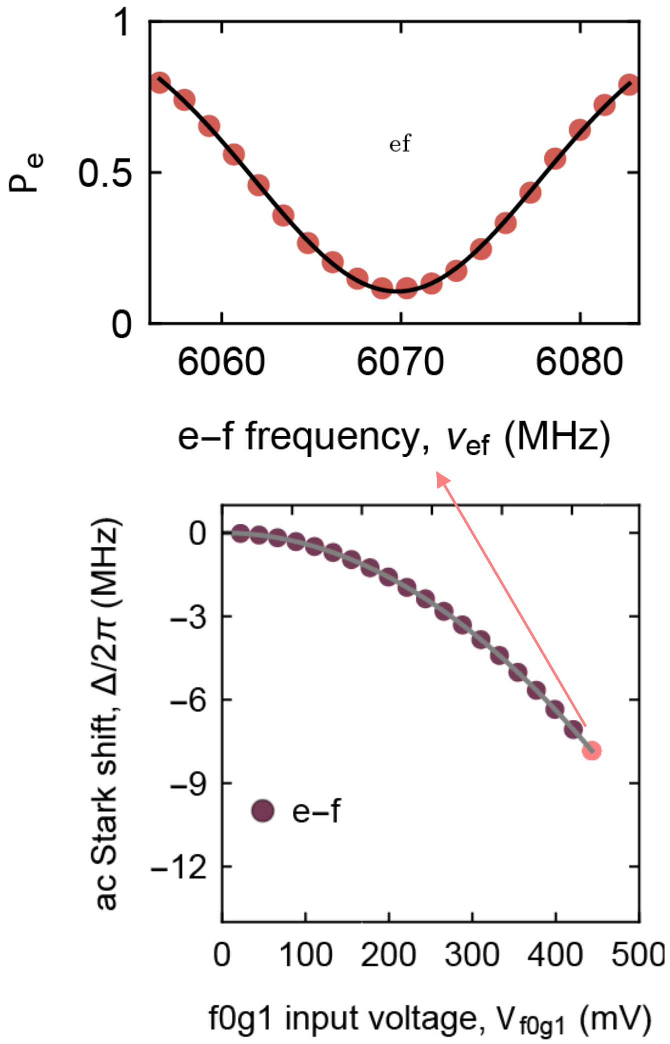

Calibration steps: (4) Calibrate Rabi rate $\tilde{g}$

- Determine Rabi rate as a function of V_{f0g1} drive strength
- Prepare qutrit in $|f\rangle$ state

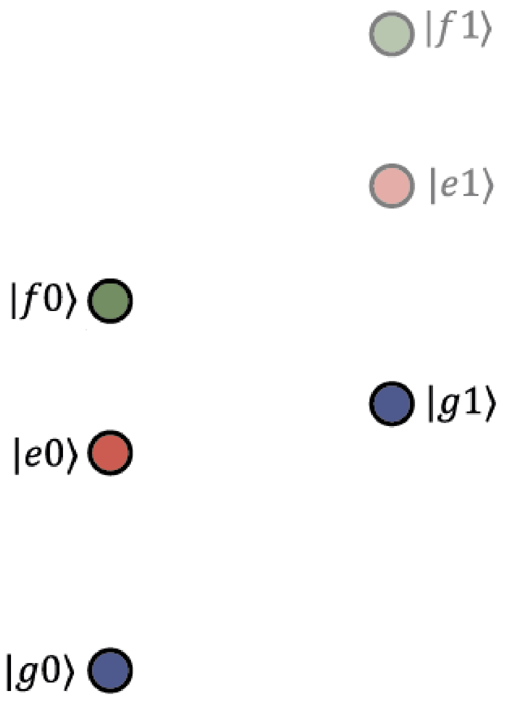

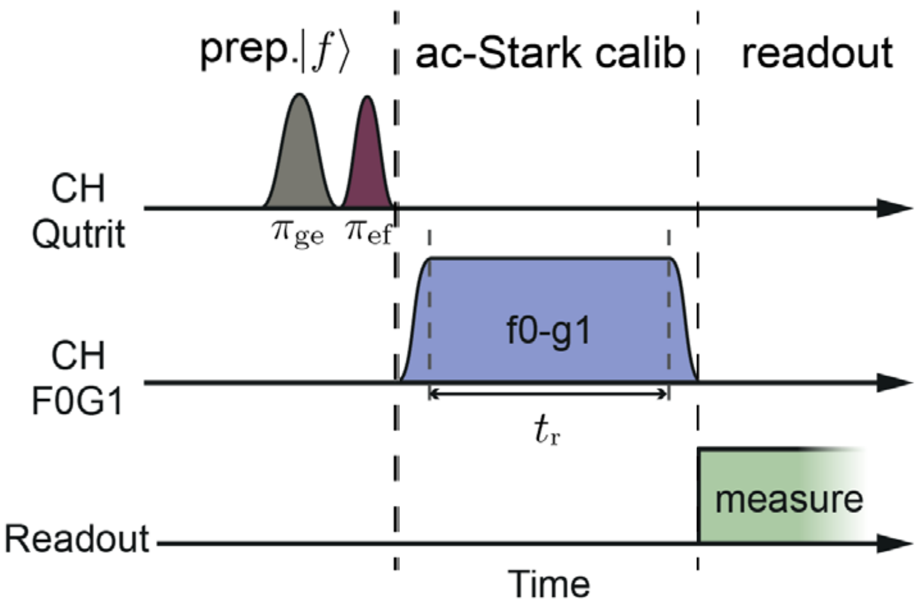

- Keep fixed amplitude V_{f0g1} and frequency ν_{f0g1} based on ac Stark calibration
- Sweep **duration** t_r of $|f,0\rangle \leftrightarrow |g,1\rangle$ pulse
- Measure P_f and extract rate $\tilde{g}$ from fit to two-level Rabi model with loss
- Repeat for different V_{f0g1}

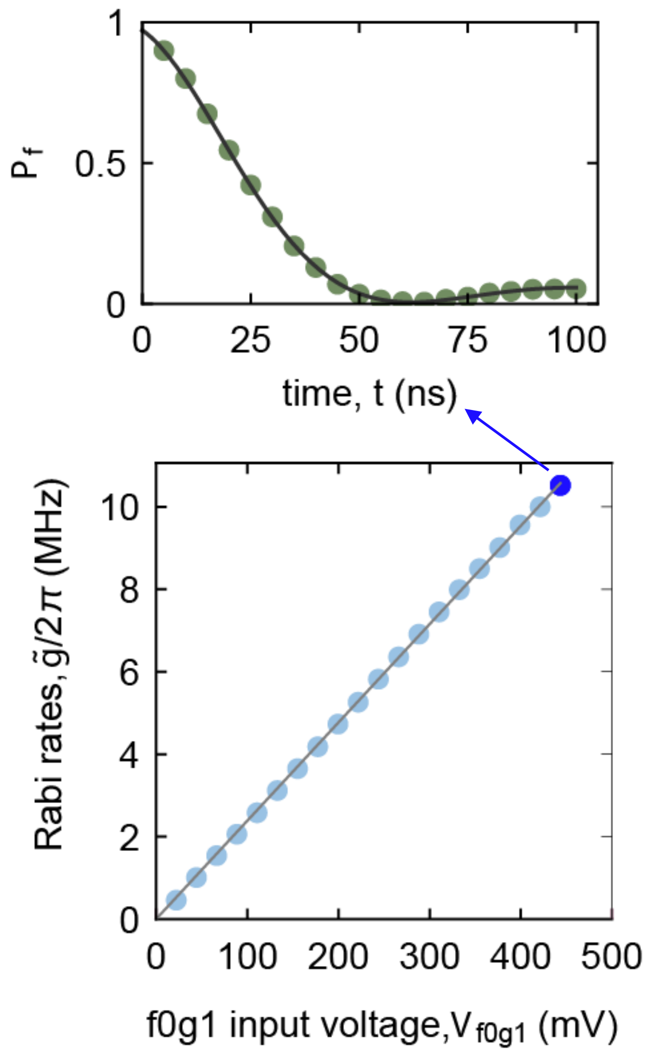

P. Magnard et al.
Phys. Rev. Lett. **121**, 060502 (2018)

Single-Shot Readout for Reset Characterization

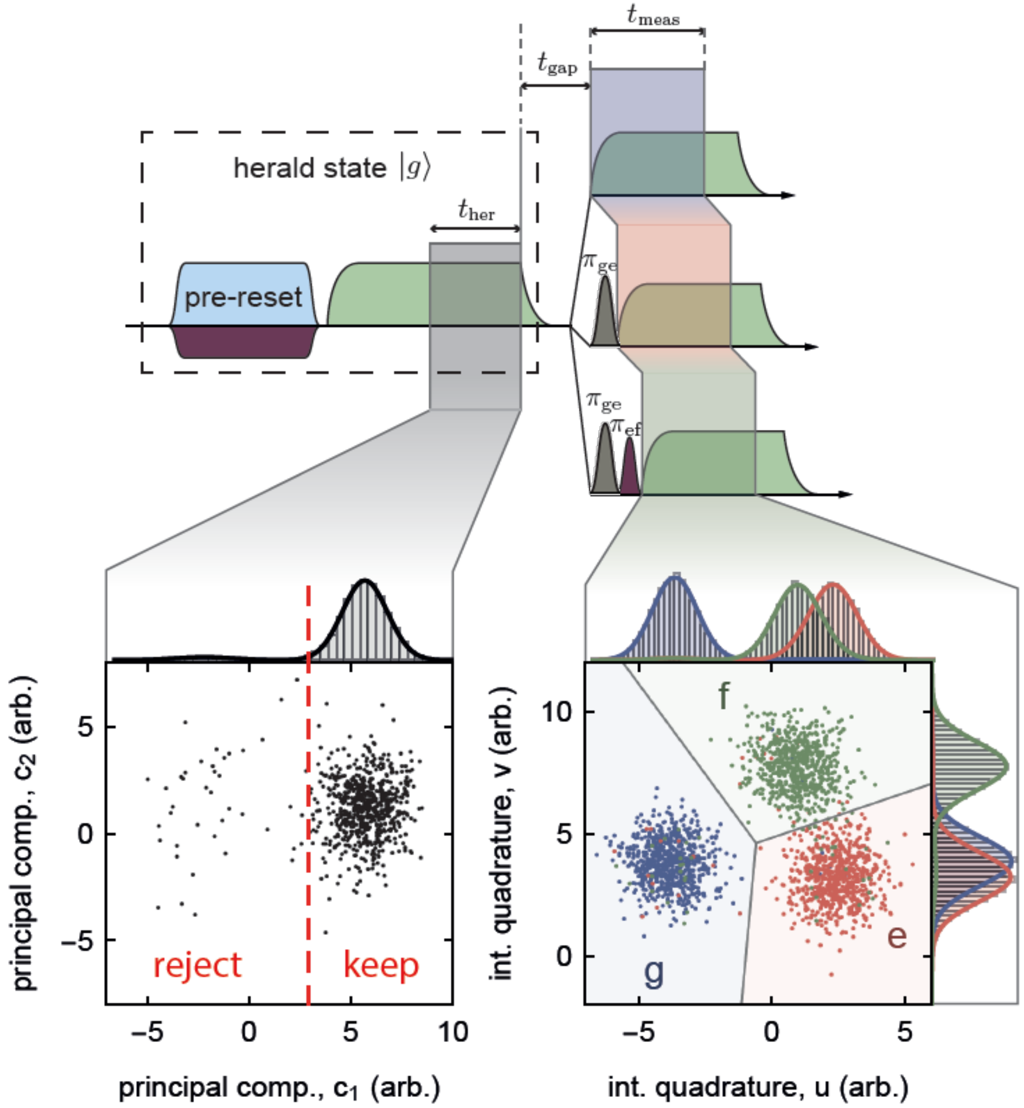

P. Magnard et al. *Phys. Rev. Lett.* **121**, 060502 (2018)

- **reference** by heralding transmon into $|g\rangle$ state
  - perform heralding measurement for $t_{\text{her}} = 72$ ns
  - t_{gap} to wait for resonator field decay
  - Prepare transmon in $|g\rangle$, $|e\rangle$ or $|f\rangle$ state
  - 40'000 single-shot traces for each state
  - obtain reference assignment probability matrix $\boldsymbol{R}$

	$\vert g\rangle$	$\vert e\rangle$	$\vert f\rangle$
g	98.2	2.5	2.4
e	0.9	95.7	4.6
f	0.9	1.8	93.0

- **population** $\boldsymbol{P}$ for reset characterization
  - assignment probability matrix after reset $\boldsymbol{M}$
  - obtain populations by

$$\boldsymbol{P} = \boldsymbol{R}^{-1}\boldsymbol{M}$$

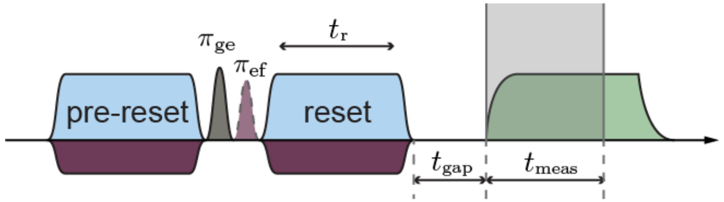

Characterization of Reset Dynamics

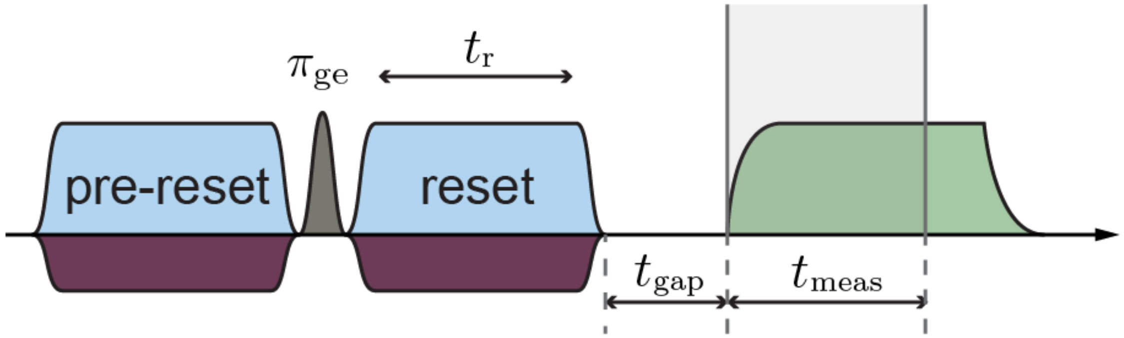

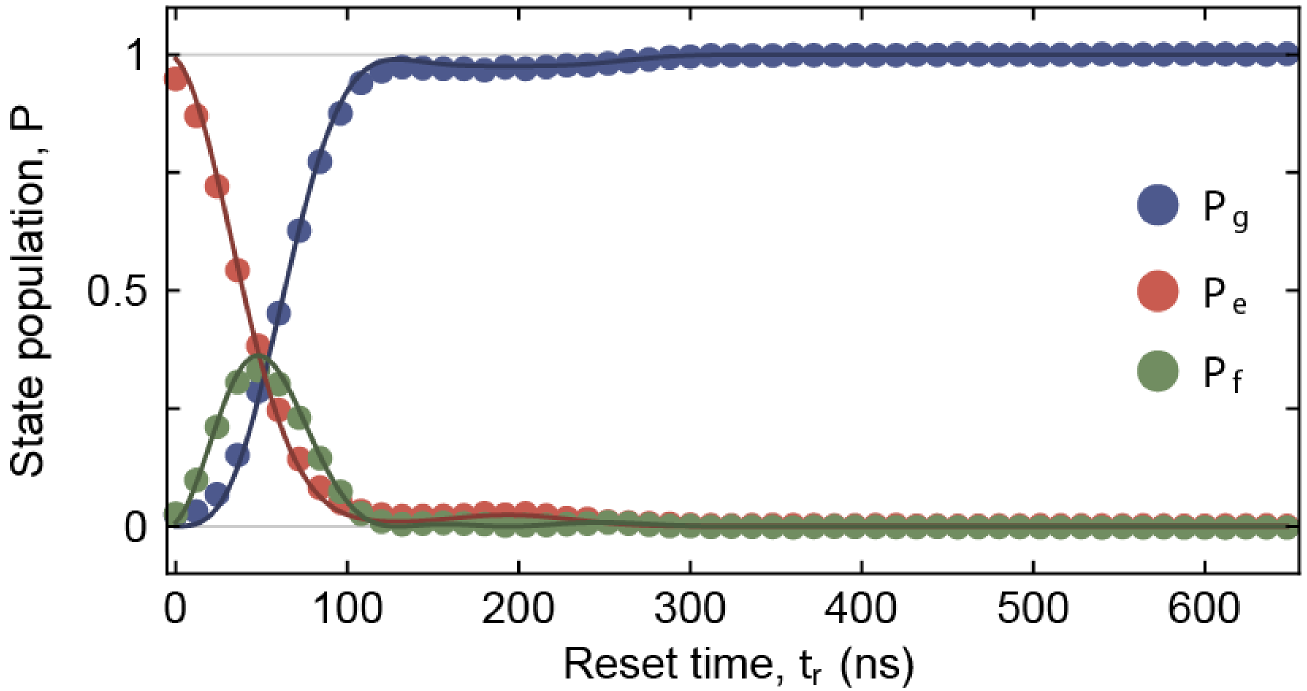

- pre-reset transmon
- prepare $|e\rangle$ state
- sweep reset time t_r
- extract transmon population with single-shot measurement
- $P_{exc} < 1$ % in $t_r < 300$ ns

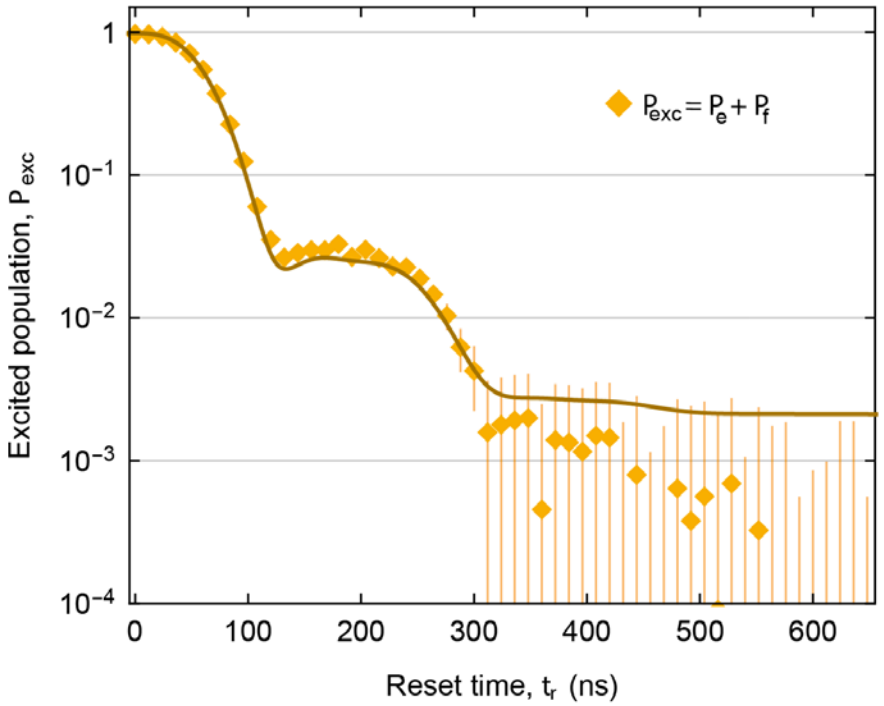

P. Magnard et al. *Phys. Rev. Lett.* **121**, 060502 (2018)

Reset Dynamics for Preparation in $|f\rangle$

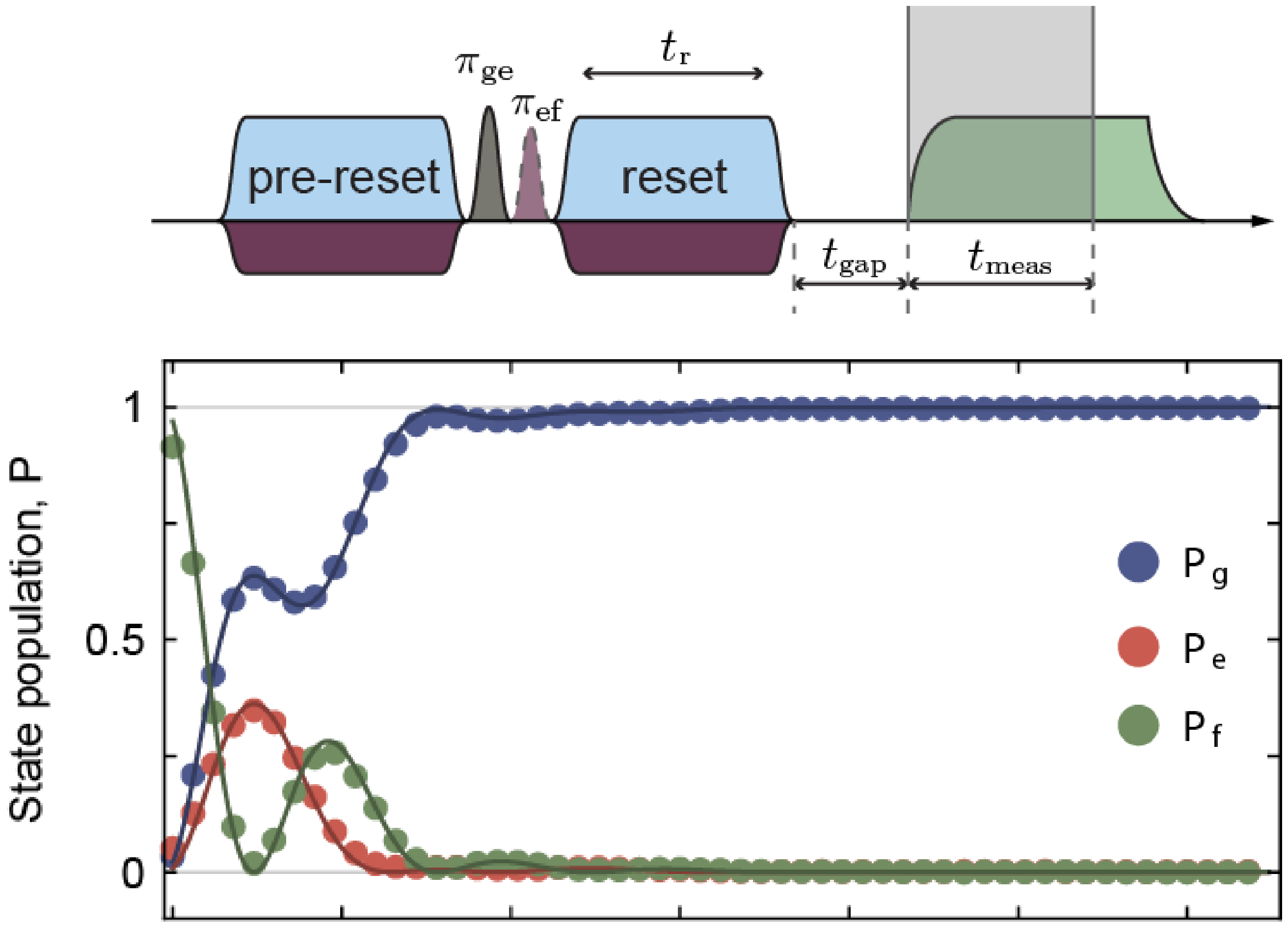

- pre-reset transmon
- prepare $|f\rangle$ state
- sweep reset time t_{r}
- extract transmon population with single-shot measurement
- illustrates reset of $|e\rangle$ & $|f\rangle$ state into the ground state

P. Magnard et al. *Phys. Rev. Lett.* **121**, 060502 (2018)

Excited State Population *vs.* Reset Time for Diff. Parameter Sets

- driven model for $|e,0\rangle$, $|f,0\rangle$ and $|g,1\rangle$ with resonator decay

➡ optimal Ω_{ef} for each $\tilde{g}$

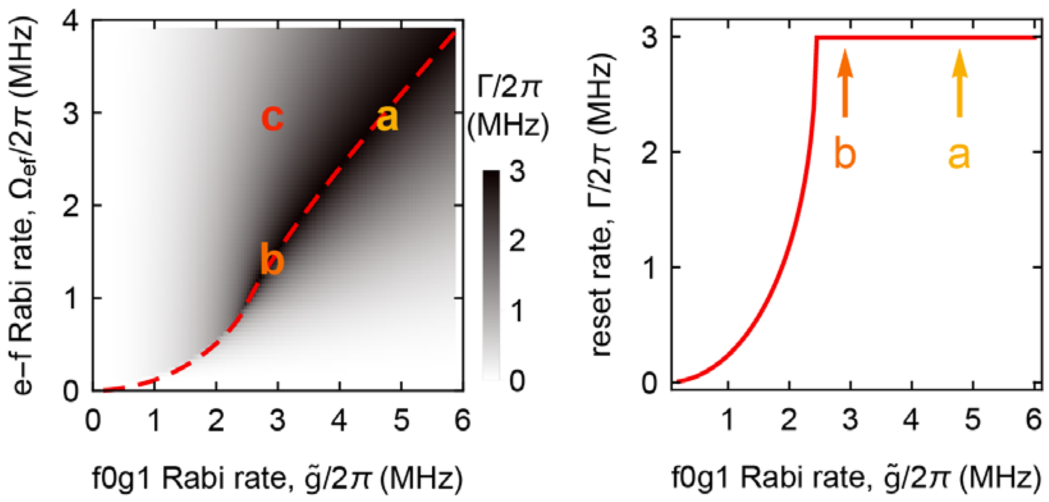

- characterization at ideal parameter sets a and b and at non-ideal configuration c

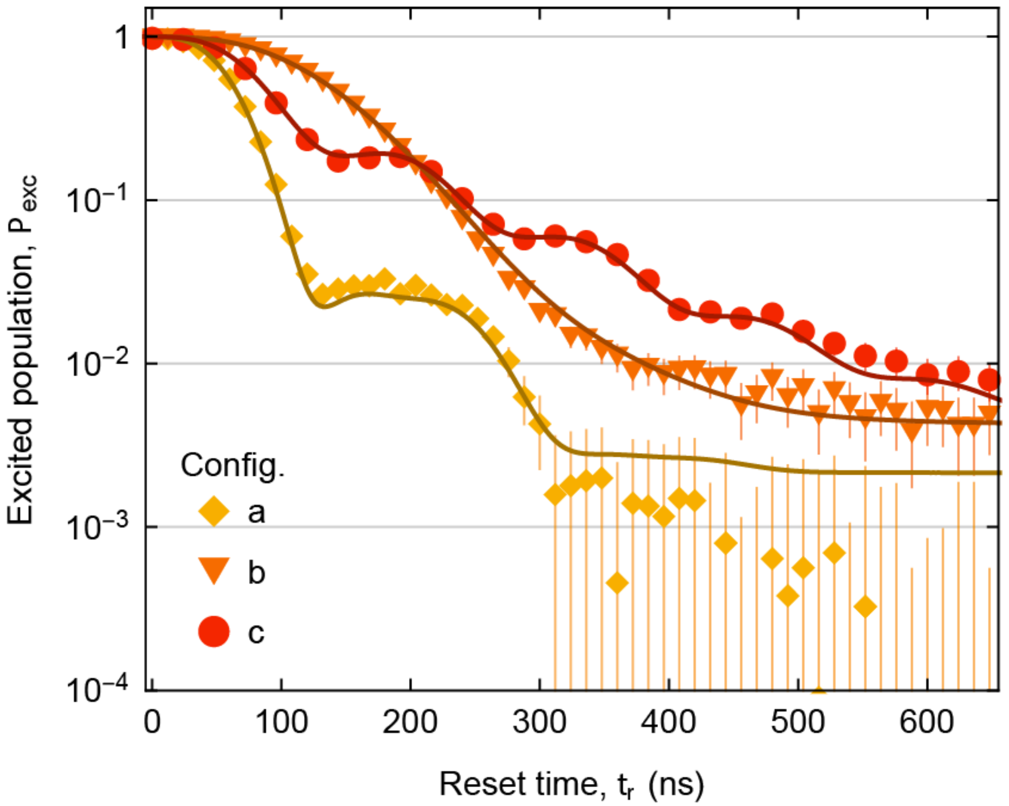

- master equation result in good agreement with data for all configurations

P. Magnard et al. *Phys. Rev. Lett.* **121**, 060502 (2018)

Demonstrated Performance of Reset for Superconducting Qubits

Achieved Goals:

- Reset qubits on-demand on a time scale short compared to T_1 and T_2
- High reset fidelity = small residual excited population

Performance metrics:

- High reset rate Γ
- Low residual excited state population P_{ex}

Reset schemes:

- Projective measurement + feedback (green squares)
- Qubit frequency tuning with flux pulse (yellow triangles)
- Microwave drive-induced dissipation (red circles)

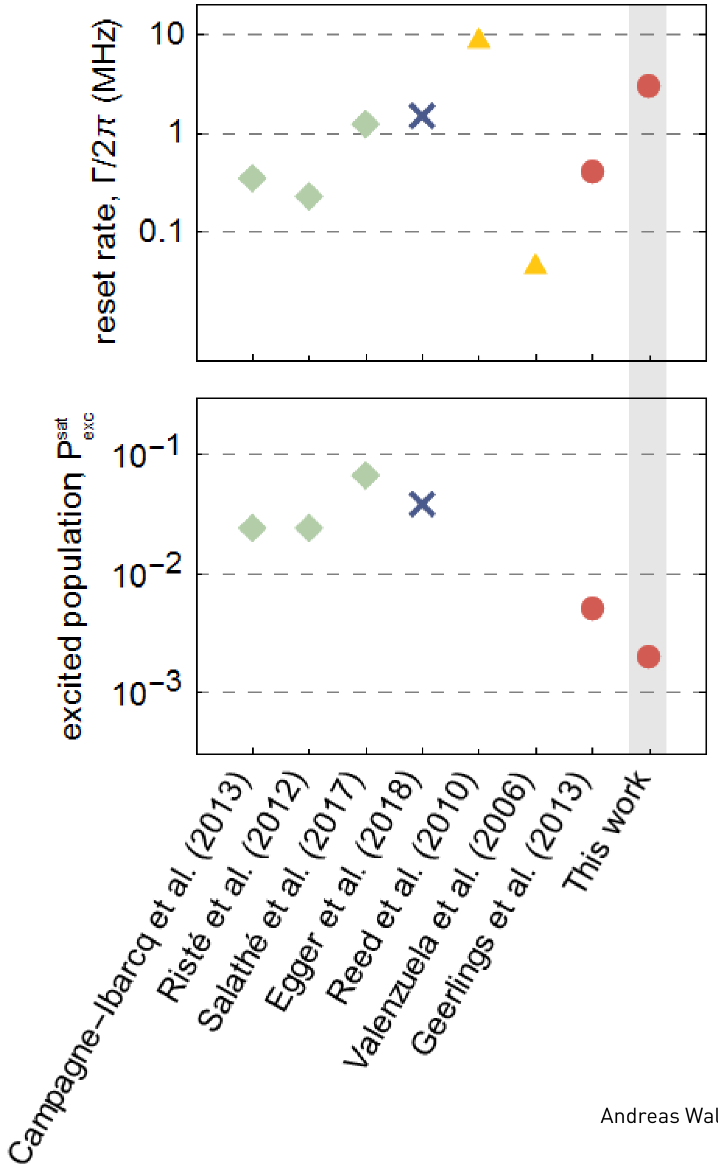

A Single Architecture ...

... for fast, high fidelity single shot readout

F ~ 98.25 (99.2) % at 48 (88) ns integration time and resonator population n ~ 2.2 with

- Optimized sample design
- Low-noise phase-sensitive Josephson parametric amplifier

T. Walter, P. Kurpiers *et al., Phys. Rev. Applied* **7**, 054020 (2017)

... for unconditional reset

- 99% reset fidelity in < 300 ns

P. Magnard *et al., Phys. Rev. Lett.* ***121***, 060502 (2018)

... that is multiplexable

- Single feedline for 8 qubits (nodes)
- Reduced cross-talk using Purcell filters

J. Heinsoo *et al., Phys. Rev. Applied* **10**, 034040 (2018)

Approach for Multiplexed Readout and Reset Architecture

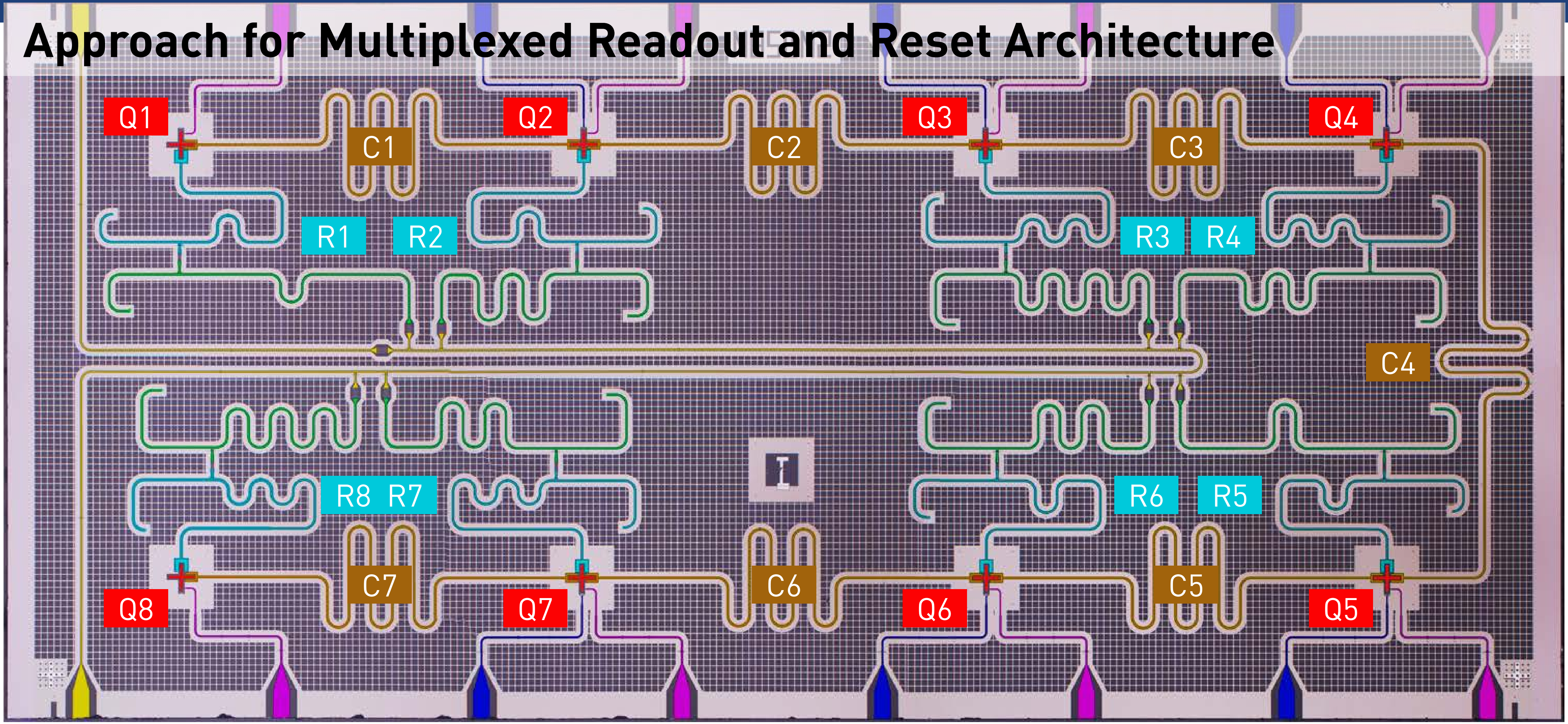

- Qubits
- Readout resonators
- Purcell filters
- Coupling Bus resonators
- Charge lines
- Flux lines
- Feed line

J. Heinsoo *et al.*, *Phys. Rev. Applied* **10**, 034040 (2018)

A Single Architecture …

… for fast, high fidelity single shot readout

F ~ 98.25 (99.2) % at 48 (88) ns integration time and resonator population n ~ 2.2 with

- Optimized sample design
- Low-noise phase-sensitive Josephson parametric amplifier

T. Walter, P. Kurpiers *et al.*, *Phys. Rev. Applied* **7**, 054020 (2017)

… for unconditional reset

- 99% reset fidelity in < 300 ns

P. Magnard *et al.*, *Phys. Rev. Lett.* ***121***, 060502 (2018)

… that is multiplexable

- Single feedline for 8 qubits (nodes)
- Reduced cross-talk using Purcell filters

J. Heinsoo *et al.*, *Phys. Rev. Applied* **10**, 034040 (2018)

… for remote entanglement and state transfer, with time-bin encoding against photon loss

- Deterministic, 50 kHz rate
- ~ 80% transfer and entanglement fidelity

P. Kurpiers, P. Magnard *et al.*, *Nature* **558**, 264 (2018)
P. Kurpiers, M. Pechal *et al.*, *arXiv:*1811.07604 (2018)

Networks for Quantum Communication and Distributed Computing

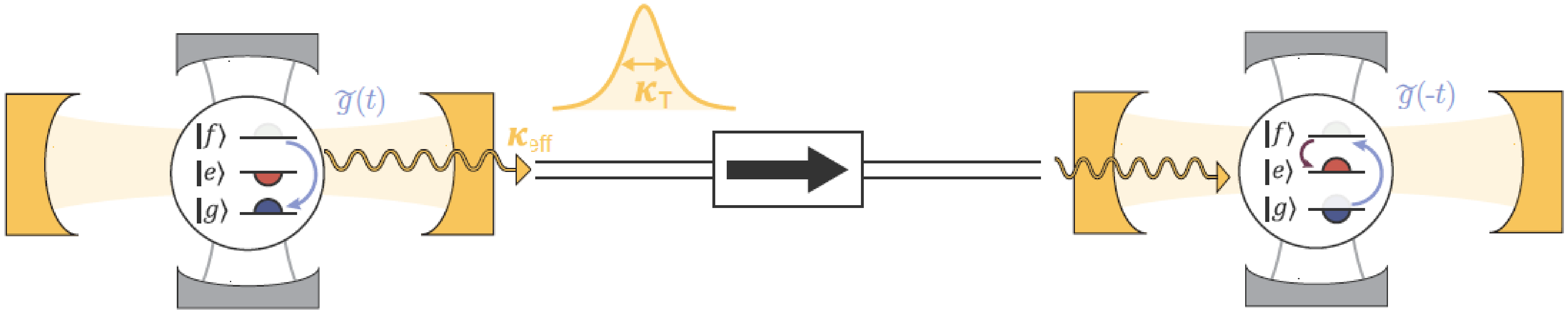

Nodes of quantum network

- Store …
- Process …
- Send …
- Receive …

… quantum information

Applications

- Expanding quantum processors by connecting modules
- Performing error correction across different nodes
- Generating distributed entanglement for communication using repeaters

Desired properties of channel

- Coherent
- Deterministic
- High data rate

A. Fowler et al., Phys. Rev. Lett., 104, 180503 (2010)

L.-M. Duan and C. Monroe, Rev. Mod. Phys. 82, 1209 (2010)

Reiserer and G. Rempe, Rev. Mod. Phys. 87, 1379 (2015)

The Challenge of Achieving Deterministic Remote Entanglement

Over 15 years of experiments:

- **Remote entanglement** realized in a wide variety of quantum systems
- Protocols:
  - Single or two-photon interference + detection
  - Measurement-induced
  - Direct transfer with (shaped) photons
  - Most/all probabilistic or heralded, typically with entanglement generation rates < 100 Hz

2018:

- Four realizations of deterministic protocols with **superconducting circuits**
  - three following the proposal by Cirac *et al.* using shaped photons/radiation fields
  - one using resonant mode

Julsgaard et al. (2001)
Chou et al. (2005)
Matsukevich et al. (2006)
Chou et al. (2007)
Laurat et al. (2007)
Yuan et al. (2008)
Atomic Ensembles

Moehring et al. (2007)
Matsukevich et al. (2008)
Maunz et al. (2009)
Slodicka et al. (2013)
Hucul et al. (2014)
Trapped Ions

Lettner et al. (2011) — Single atom BES
Lee et al. (2011) — Vibrational States of Diamond
Usmani et al. (2012) — rare-earth crystals

Hofmann et al. (2012)
Ritter et al. (2012)
Rosenfeld et al. (2017)
Single atom

Bernien et al. (2013)
Pfaff et al. (2014)
Hensen et al. (2015)
Humphreys et al. (2018)
Nitrogen Vacancy

Roch et al. (2014)
Narla et al. (2016)
Dickel et al. (2018)
Campagne-Ibarcq et al. (2018)
Axline et al. (2018)
Kurpiers et al. (2018)
Leung et al. (2018)
Superconducting Circuits

Delteil et al. (2016)
Stockill et al. (2017)
Quantum Dot

Cirac *et al.*, *Phys. Rev. Lett.* **78**, 3221 (1997)
P. Kurpiers, P. Magnard et al., *Nature* 558, 264 (2018)

Deterministic Remote Entanglement with Microwave Photons

Mediated by **Blue-Sideband**: 3D

P. Campagne-Ibarcq *et al., Phys. Rev. Lett.* **120**, 200501 (2018)

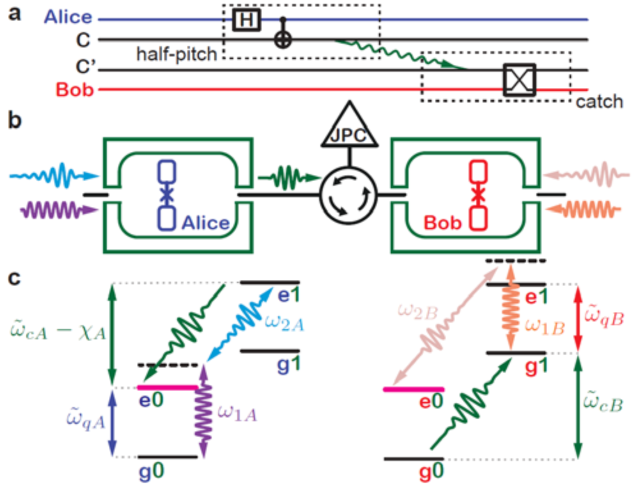

Mediated by **Parametric Conversion**: 3D

C. Axline *et al., Nature Physics* **14**, 705 (2018)

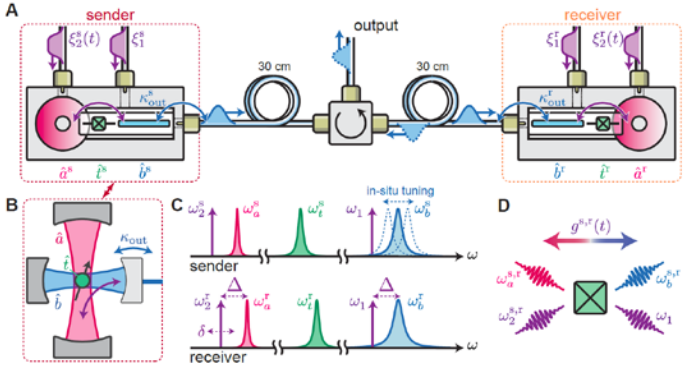

Mediated by **Multimodal Channel with tunable coupling**: 2D

N. Leung *et al., npj Qu. Inf.* **5**, 18 (2019)

Y. Zhong *et al., Nat. Phys.* (2019)

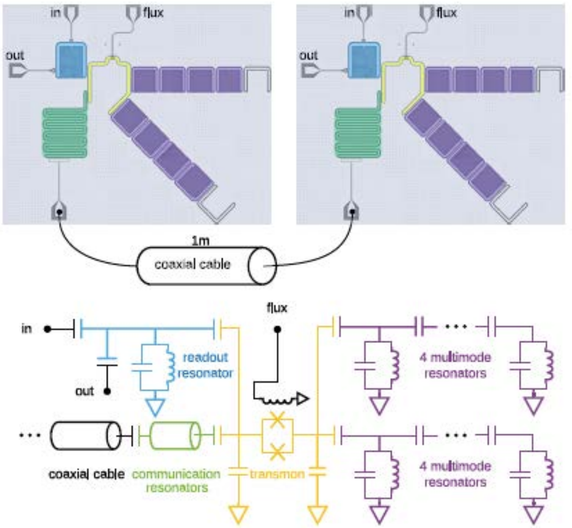

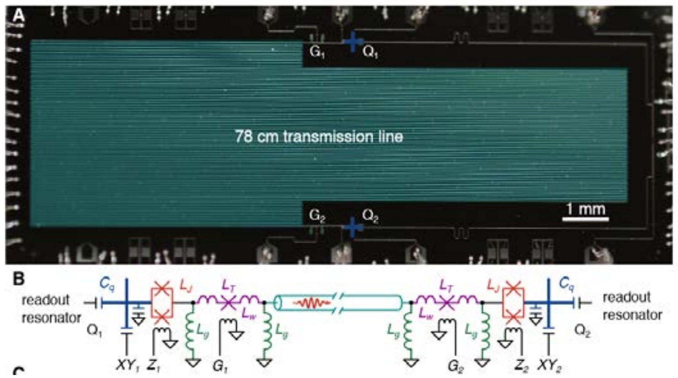

Mediated by **Raman Process**: 2D

P. Kurpiers, P. Magnard *et al., Nature* **558**, 264 (2018)

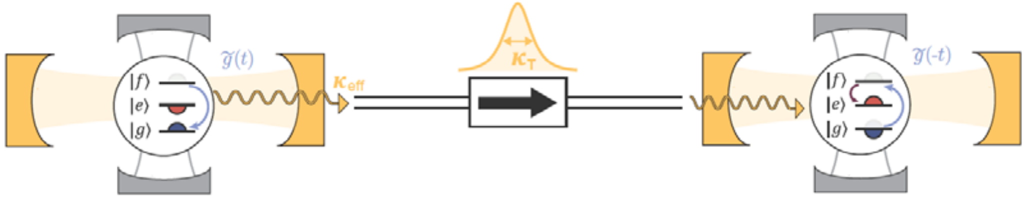

Quantum Networks for Distributed Quantum Computing

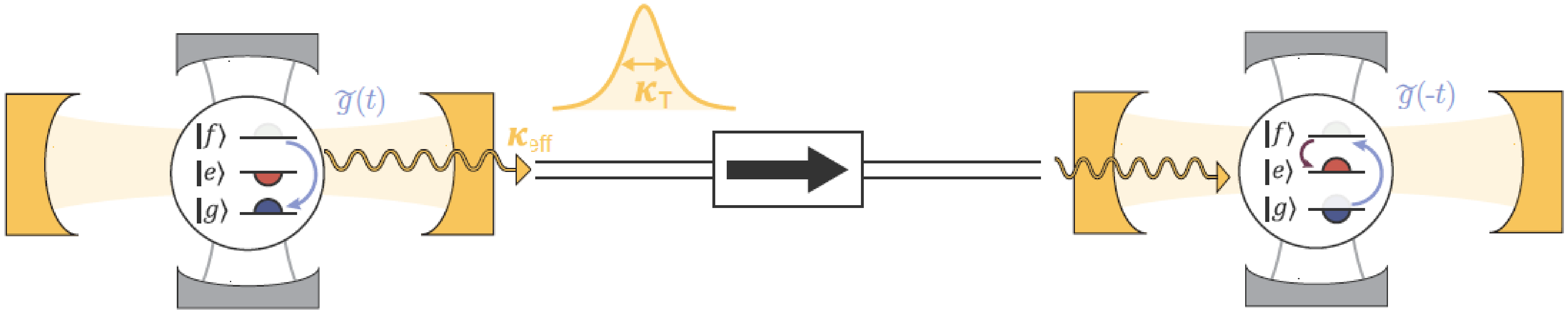

Universal quantum node:
- Send
- Receive
- Store
- Process

Direct quantum channel:
- Coherent link
- Deterministic, ideally

Applications:
- Creating distributed entanglement
- Distributed quantum computing
- Quantum error correction across different nodes using surface code

A. Fowler *et al.*, *Phys. Rev. Lett.* ***104***, 180503 (2010)
L.-M. Duan and C. Monroe, *Rev. Mod. Phys*. **82**, 1209 (2010)
Reiserer and G. Rempe, *Rev. Mod. Phys*. **87**, 1379 (2015)

Circuit QED Realization

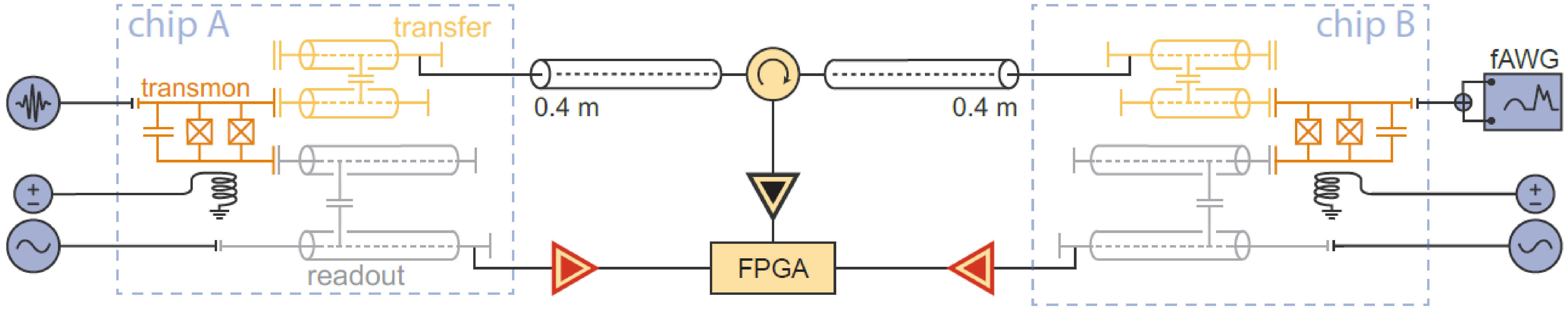

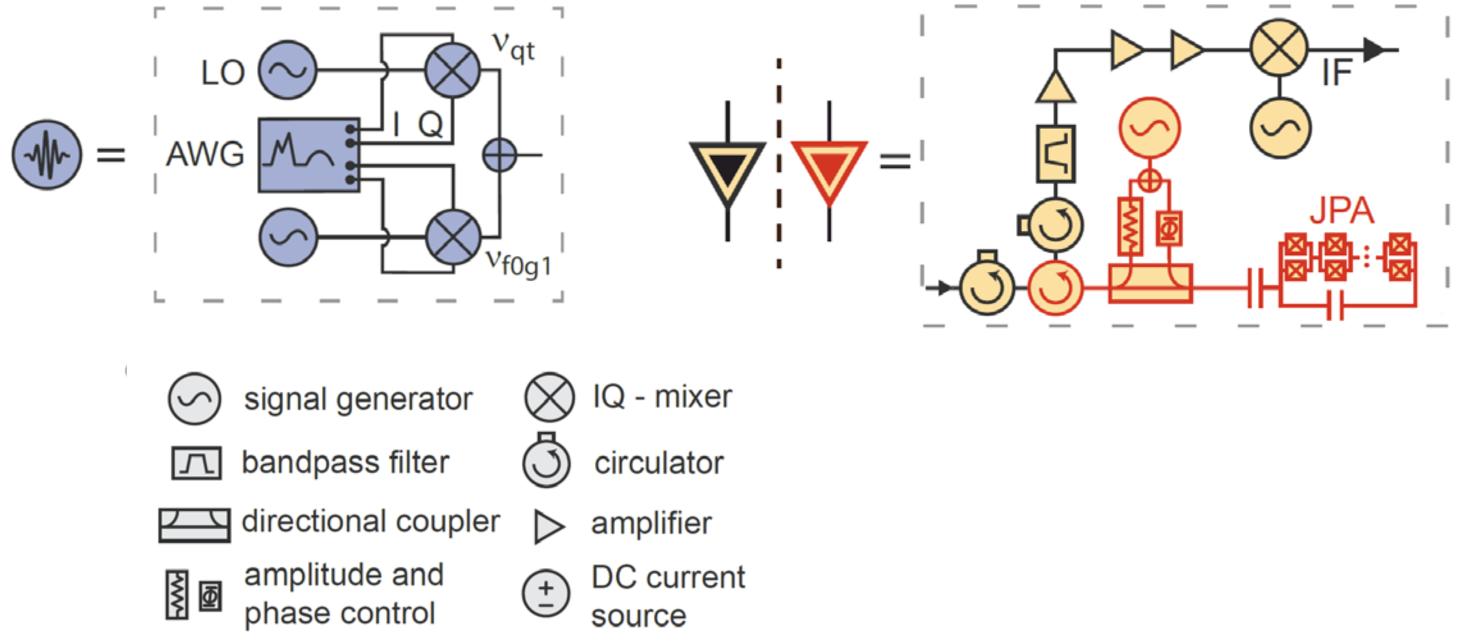

- Two independent chip-based circuit QED systems
- Independent readout and transfer circuits
- dedicated Purcell filters for increased coupling rates
- 0.9 m coaxial link
- Parametric amplifiers
- FPGA real-time processing

Photon Shaping at Microwave Frequencies

- Single photon pulses with controlled amplitude and phase profile

$$= \int \psi(t) a^\dagger(t) |0\rangle \, \mathrm{d}t$$

- Realized with atoms/ions for optical frequency photons ...

e.g. A. Kuhn, M. Hennrich, G. Rempe, PRL 89, 067901 (2002)

- ... and recently with superconducting circuits for microwave photons

Y. Yin, *et al.*, PRL 110, 107001 (2013)
S. J. Srinivasan, *et al.*, PRA 89, 033857 (2014)
M. Pechal, *et al.*, Phys. Rev. X 4, 041010 (2014)

- System capable of emitting shaped photons may also absorb them with high efficiency
  → potential building block for quantum network

J. I. Cirac, P. Zoller, H. J. Kimble and H. Mabuchi, PRL 78, 3221 (1997)

S. Zeytinoglu *et al., PRA* 91, 043846 (2015)
M. Pechal *et al., Phys. Rev. X* 4, 041010 (2014)

Microwave Induced Tunable Coupling

- Raman schemes known from experiments in optical domain
  - Coherent drive stimulates transition between two atomic states, excess energy is radiated as a photon

e.g.: M. Keller *et al.*, Nature 431, 1075 (2004)

- Microwave-driven coupling of 2nd qubit excited state (f) to ground state (g) with one photon in the cavity mode (1)

$$H = \omega_r a^\dagger a + \omega_q b^\dagger b + \frac{1}{2}\alpha b^\dagger b^\dagger b b + \frac{1}{2}(\Omega(t) b^\dagger + \Omega^*(t) b) + g(a^\dagger b + a b^\dagger)$$

$$H_{\text{eff}} = \boxed{\tilde{g}(t)|g1\rangle\langle f0| + \text{h.c.}}$$

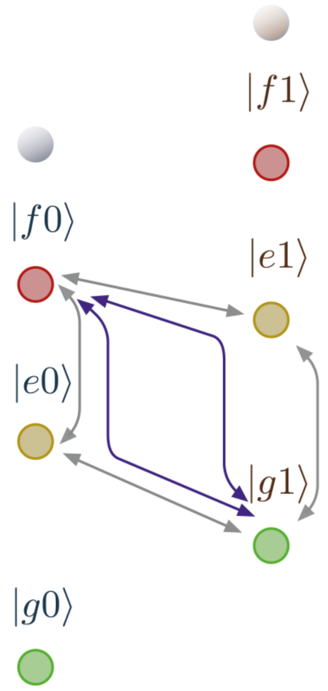

S. Zeytinoglu *et al., PRA* 91, 043846 (2015)

M. Pechal *et al., Phys. Rev. X* 4, 041010 (2014)

Photon Shaping Process

- Amplitude and phase of the effective coupling *g(t)* controllable by drive tone

$$H_{\text{eff}} = \tilde{g}(t)|g1\rangle\langle f0| + \text{h.c.}$$

  - all-microwave control in contrast to approaches based on flux-tuning of transition frequency

Y. Yin *et al.*, PRL 110, 107001 (2013)
S. J. Srinivasan, *et al.*, PRA 89, 033857 (2014)

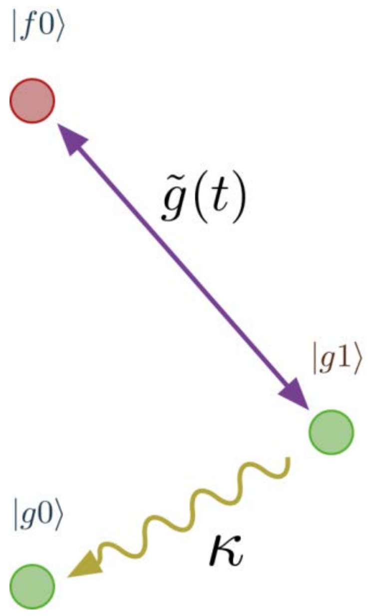

- Control over population of the emitting *g1* state combined with rapid decay to *g0* from cavity at rate κ
  - shaped photon
- Trapping in the ground state
  - only a single photon is emitted

M. Pechal *et al.*, *Phys. Rev. X* 4, 041010 (2014)

Experimental Setup

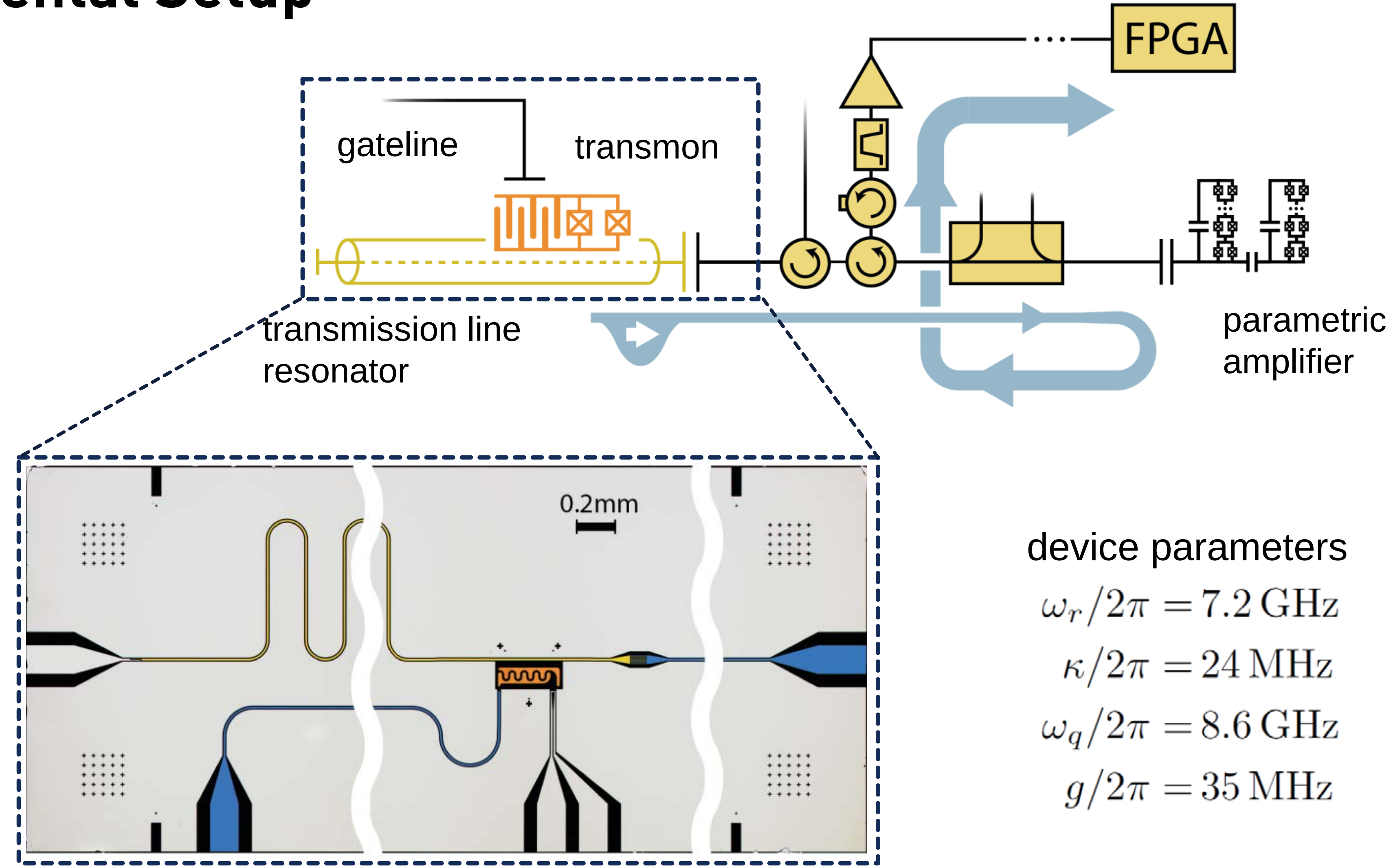

device parameters

$$\omega_r/2\pi = 7.2\,\mathrm{GHz}$$
$$\kappa/2\pi = 24\,\mathrm{MHz}$$
$$\omega_q/2\pi = 8.6\,\mathrm{GHz}$$
$$g/2\pi = 35\,\mathrm{MHz}$$

M. Pechal *et al.*, *Phys. Rev. X* 4, 041010 (2014)

Creating Time-Reversal Symmetric Single Photons

Pulse Scheme:

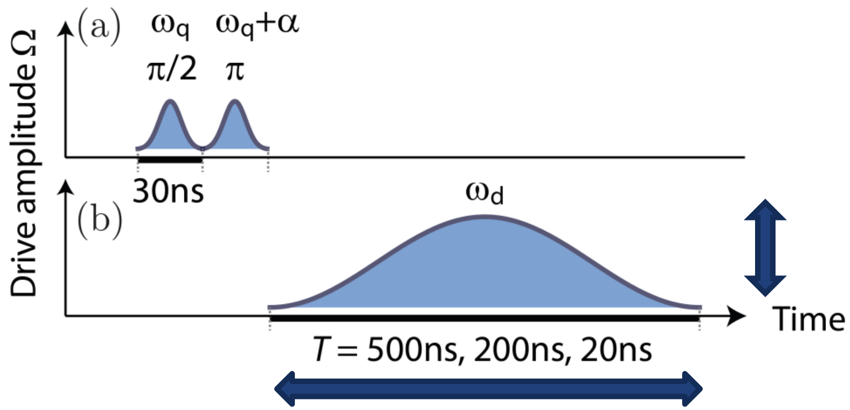

Quadrature Amplitude Measurement:

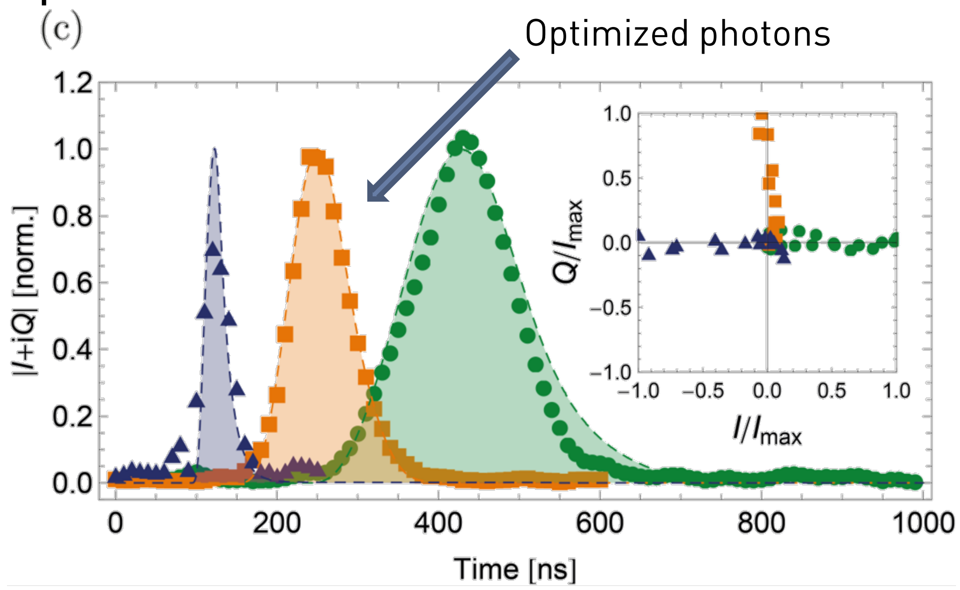

- (a) System prepared in a *fo+go* superposition
- (b) classical coupling pulse *g(t)* induces photon emission → *o+1*
- Adjust duration, amplitude and phase of the pulse to optimize symmetry of the photon

- Symmetry 98 % (overlap with time reversed photon pulse)
- Constant photon pulse phase by compensation of Stark shifts through time dependent variation of drive phase

M. Pechal *et al.*, *Phys. Rev. X* 4, 041010 (2014)

Single Photon Anti-Bunching & Full State Tomography

- Density matrix reconstructed from moments of quadrature amplitude distribution

C. Eichler *et al., PRA* 86, 032106 (2012)

- Single photon state *1*
  - Intensity correlations: $g^{(2)} = 0.06$
  - State fidelity: $F = 0.76$
- Superposition with vacuum *0+1*
  - Intensity correlations: $g^{(2)} = 0.03$
  - State fidelity: $F = 0.86$
- Here: imperfections dominated by qubit decoherence

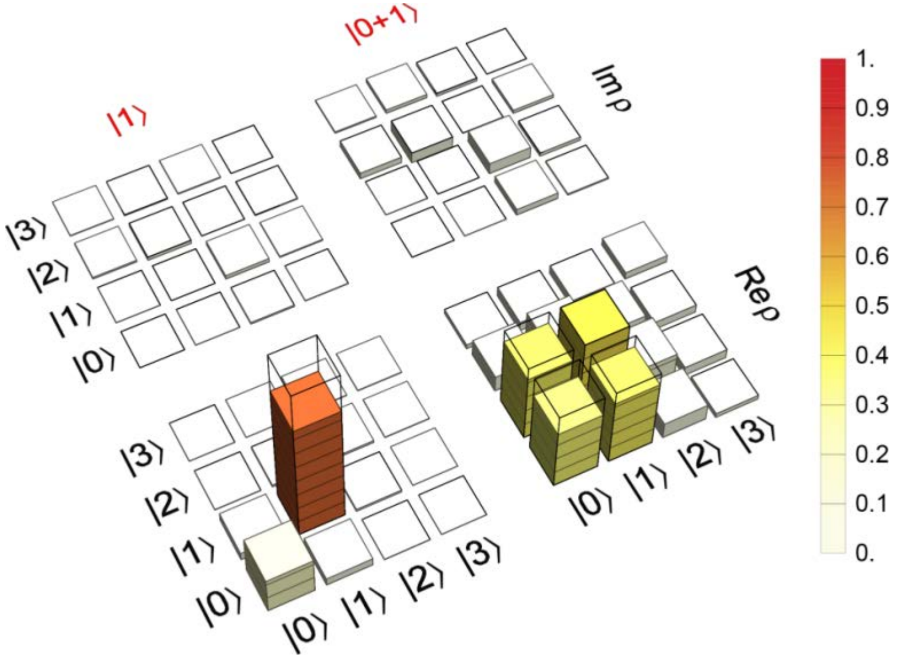

M. Pechal *et al., Phys. Rev. X* 4, 041010 (2014)

Amplitude and Phase Modulated Single Photon Pulses

Single photons with modulated envelopes

- prepared using a train of 6 drive pulses *g(t)*
- relative phase freely adjustable
  - one out of 6 single-photon-pulse components with inverted phase

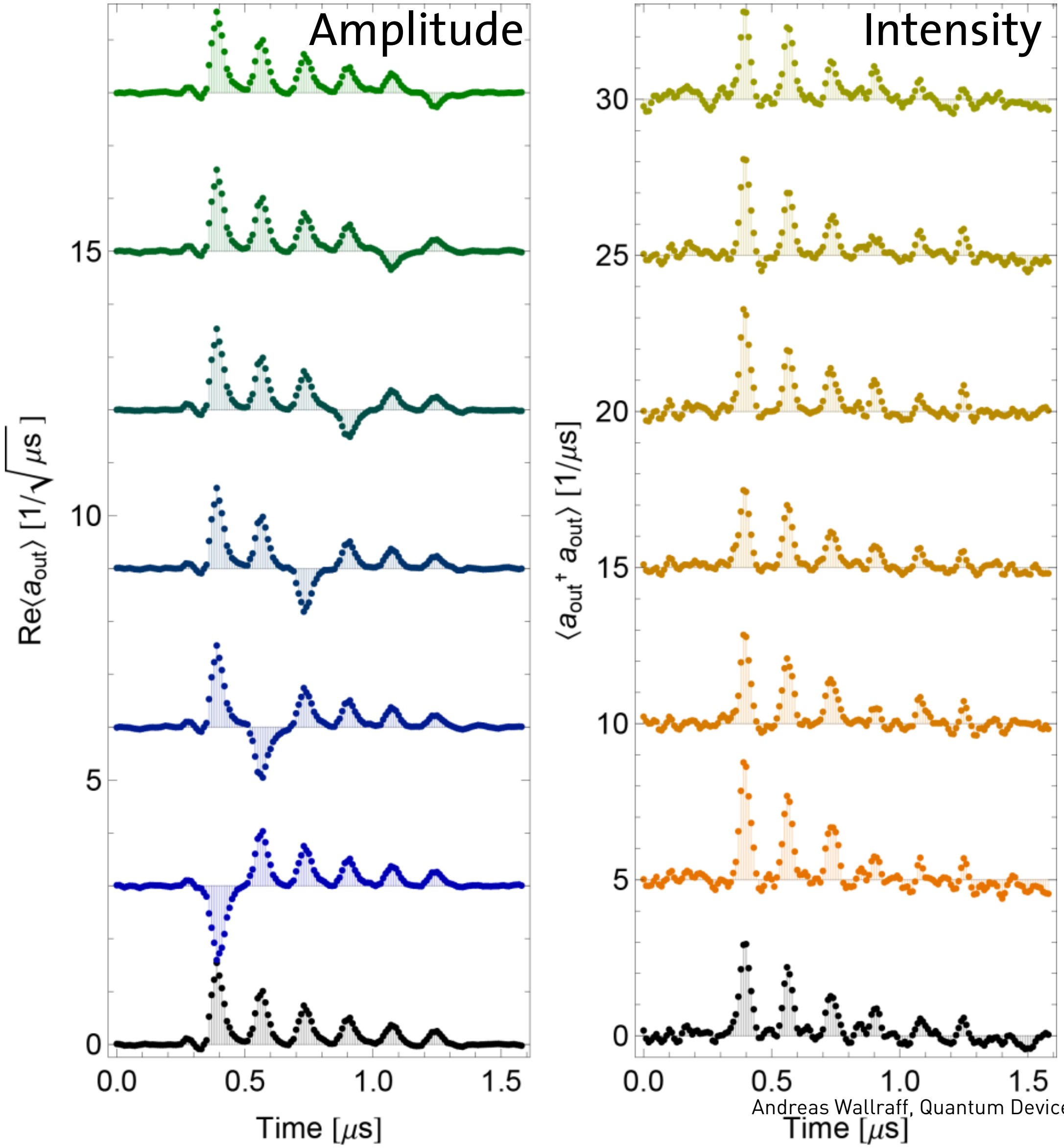

M. Pechal *et al.*, *Phys. Rev. X* 4, 041010 (2014)

Time-Reversal Symmetric Photon Emission

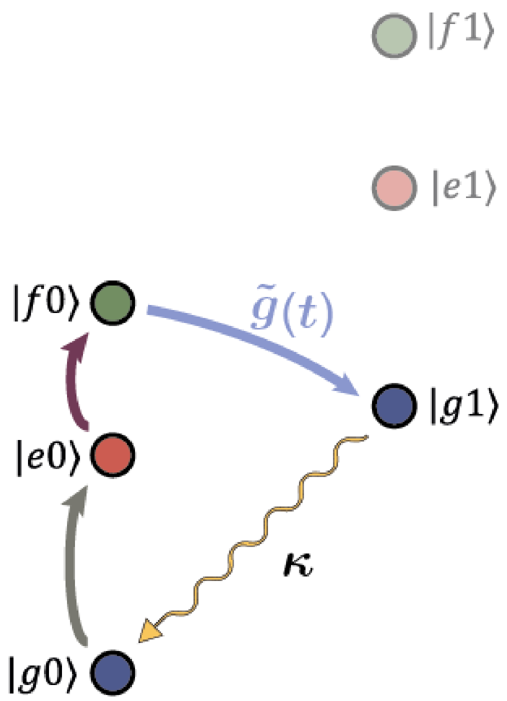

$$H_{\text{eff}} = \tilde{g}(t)|g,1\rangle\langle f,0| + h.c$$
$$\tilde{g}(t) \propto g\Omega(t)\, e^{i\phi}$$

Cavity QED

- Strong coupling
- Detuned dressed state level diagram

$|g,1\rangle$ population ...

- ... controls emission of shaped photon
- Amplitude and phase controled by drive $\tilde{g}(t)$
- All-microwave process
- Single photon emission enforced by trapping in dark state $|g,0\rangle$
- Stark-shift and Rabi-rate calibration is essential

- time-symmetric photon with envelope

$$\frac{\sqrt{\kappa_{\text{eff}}}}{2\cosh(\kappa_{\text{eff}}\, t/2)}$$

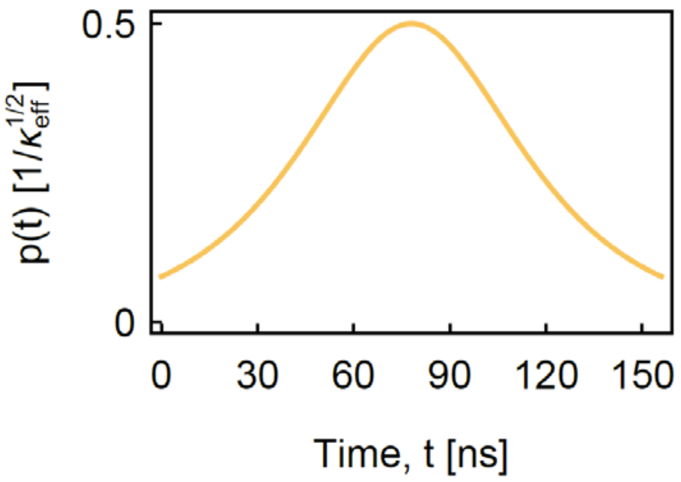

M. Pechal *et al. Phys. Rev. X* **4**, 041010 (2014)
S. Zeytinoglu *et al., Phys. Rev. A* **91**, 043846 (2015)
P. Magnard *et al., Phys. Rev. Lett.* **121**, 060502 (2018)

Shaped Photon Emission from Receiving Node (B)

Measurement of Qutrit Population Dynamics:

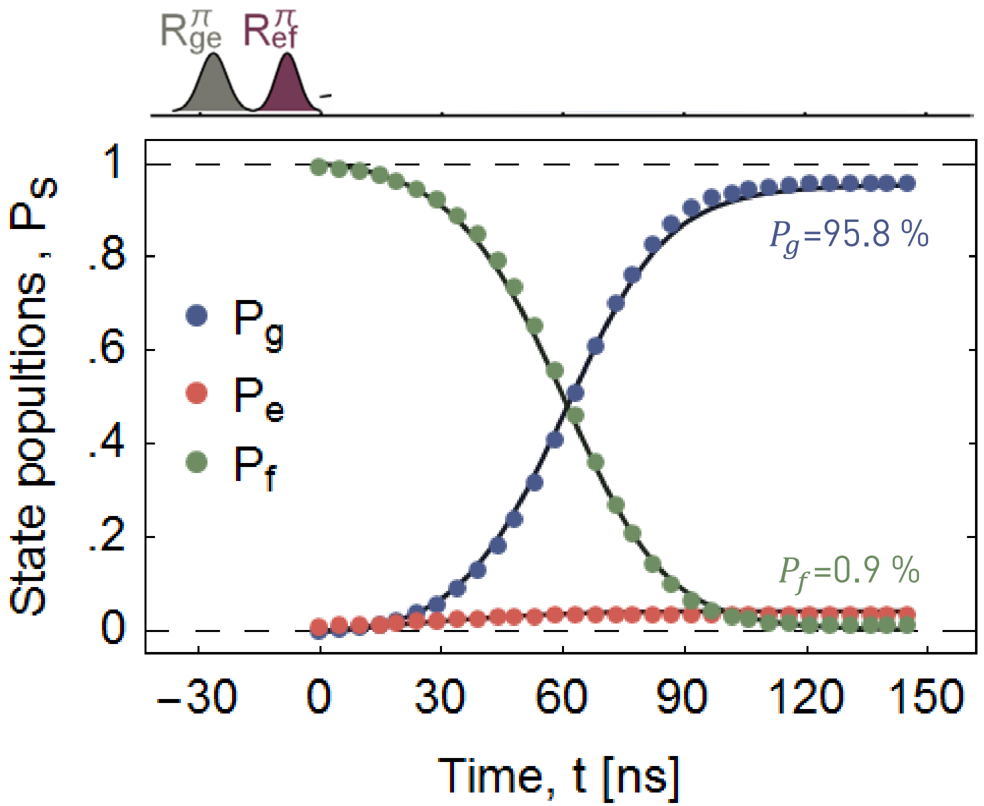

- prepare qutrit in $|f\rangle$ state
- Apply $|f,0\rangle \leftrightarrow |g,1\rangle$ drive
- Truncate at time t
- $|g,e,f\rangle$ populations well described by master-equation-simulation

P. Kurpiers, P. Magnard *et al., Nature* **558**, 264 (2018)

Measurement of Qutrit Population Dynamics upon Photon Emission

Qutrit population at node B:

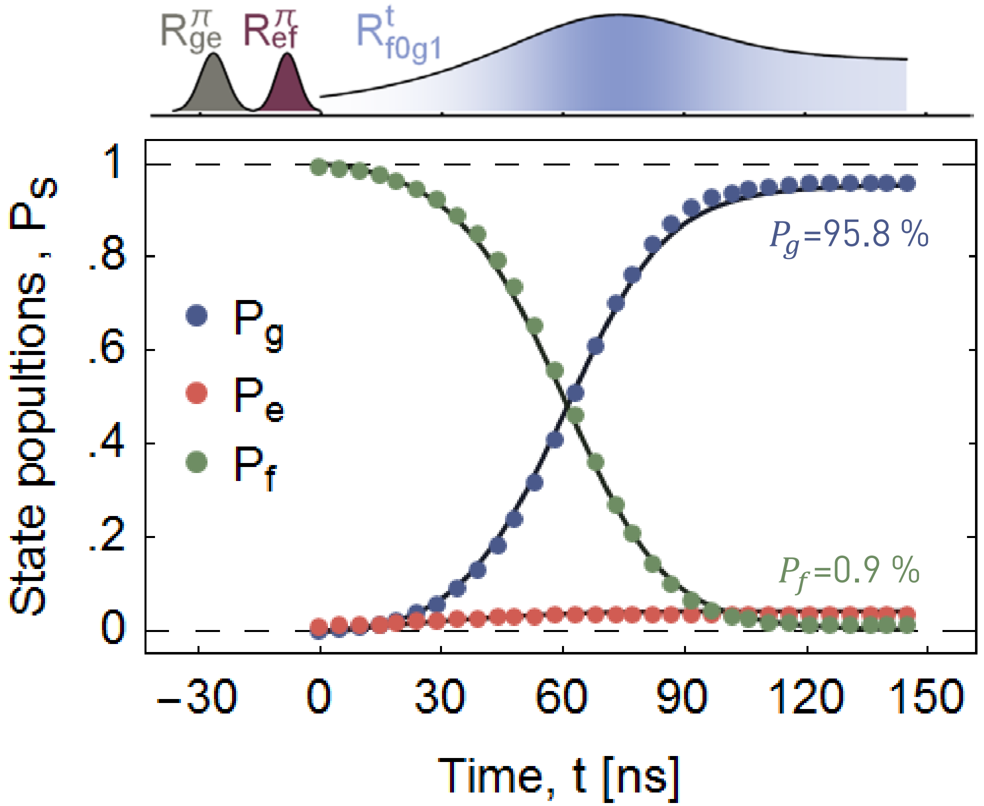

- Excellent agreement with master equation simulation

Envelope of emitted photon:

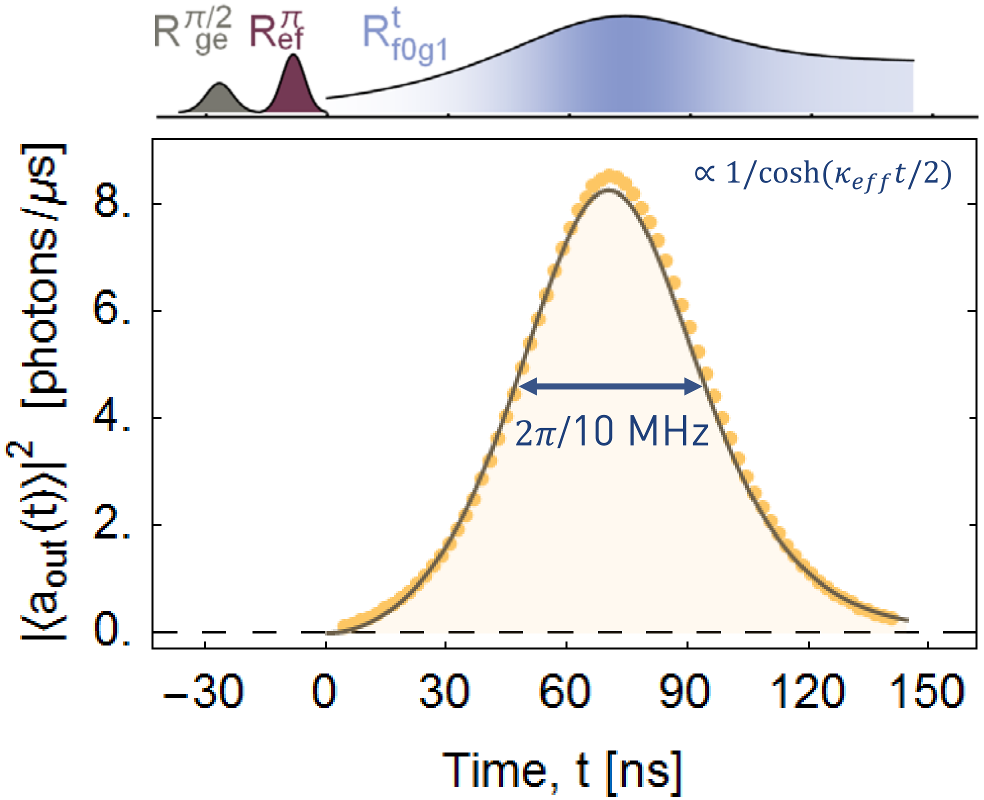

- Similar results at node A
- Allows to measure photon loss between A & B

P. Kurpiers, P. Magnard *et al., Nature* **558**, 264 (2018)

Characterization of Photon Loss

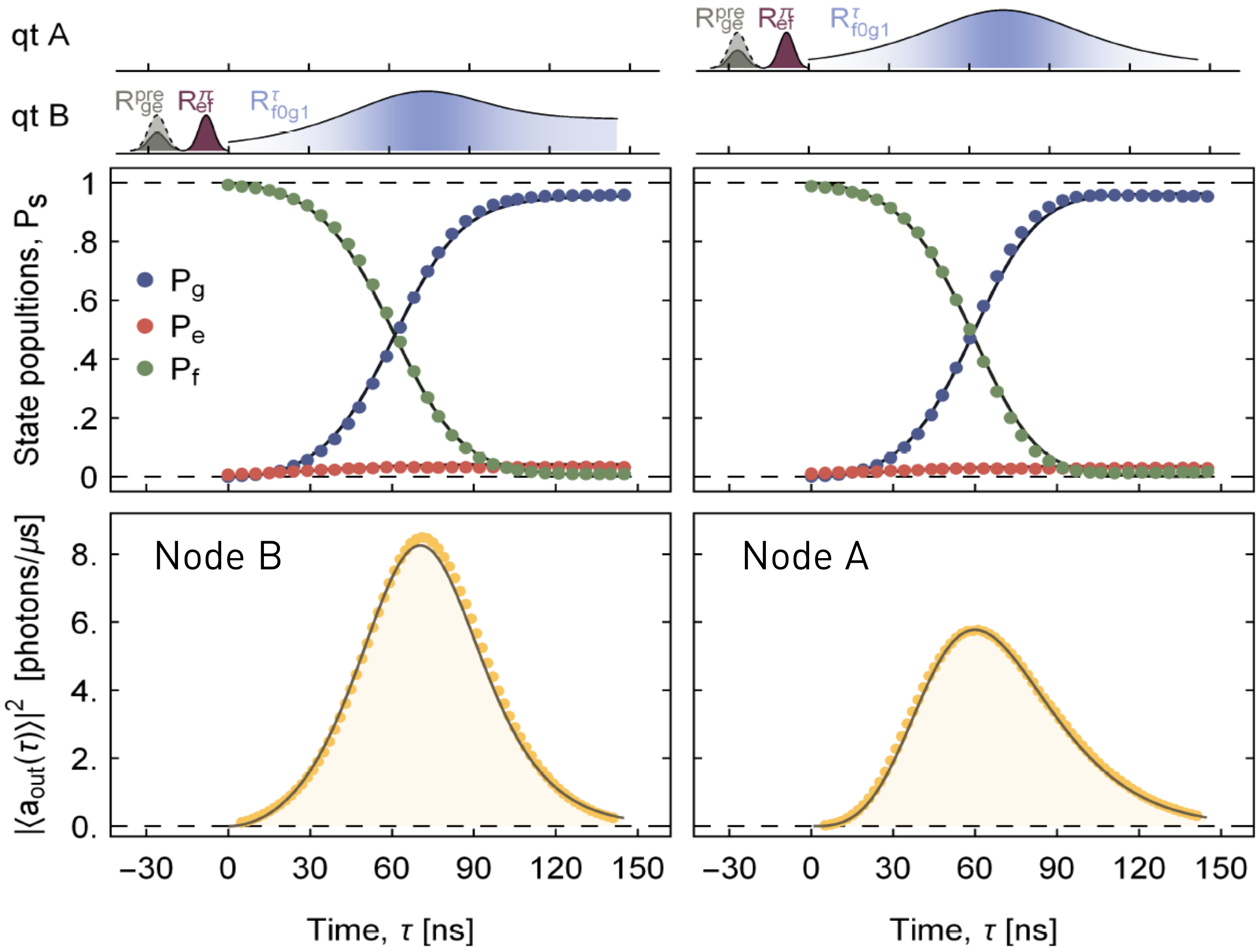

- Similar emission dynamics and performance at node A
- Photon shape disturbed by reflection off of node B
- Compare integrated $|\langle a_{out}(\tau)\rangle|^2$ emitted from node A and B
  - Total photon loss: 23 ± 0.5 %
  - due to
    - Circulator: 13%
    - 0.4 m cable: 4%
    - PCB: 4%
  - extracted from independent measurements & manufacturer data

P. Kurpiers, P. Magnard *et al., Nature* **558**, 264 (2018)

P. Kurpiers et al., EPJ Quantum Technology 4, 8 (2017)

Absorption Dynamics of Qubit State Transfer

Population of receiving qutrit:

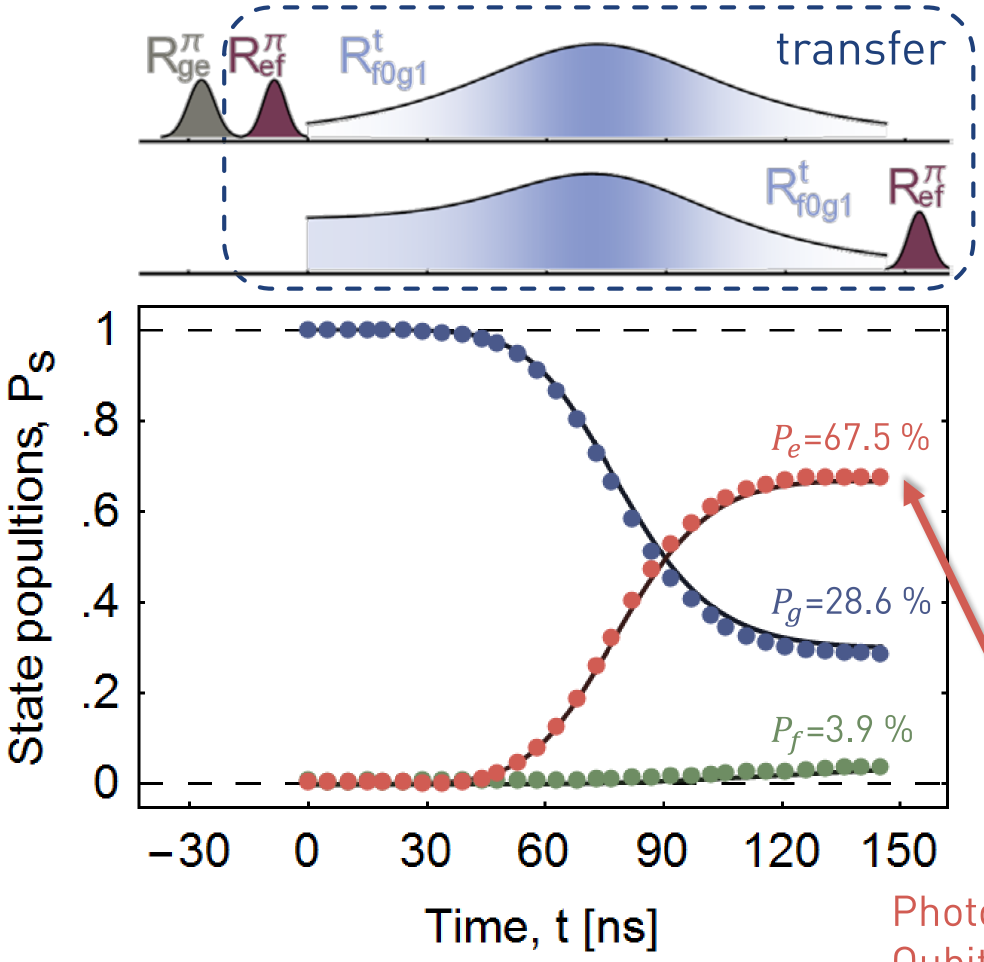

Envelope of reflected photon (superposition with vac.):

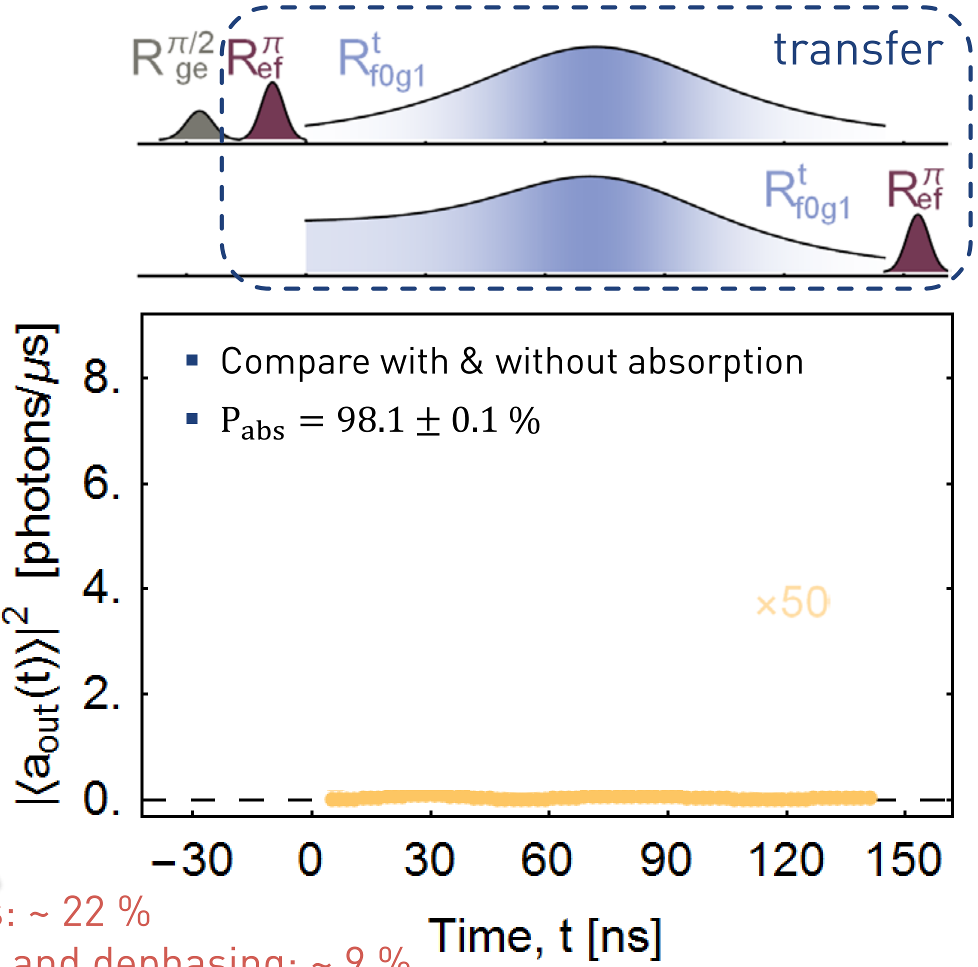

- Compare with & without absorption
- $P_{abs} = 98.1 \pm 0.1$ %

Photon loss: ~ 22 %
Qubit decay and dephasing: ~ 9 %
Pulse truncation: ~ 1.5%

P. Kurpiers, P. Magnard *et al., Nature* **558**, 264 (2018)

Process Tomography of Quantum State Transfer

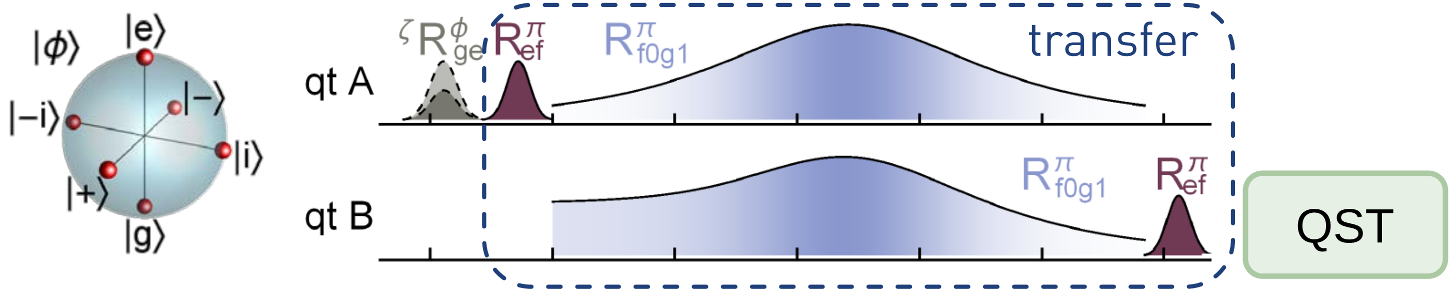

- Prepare qubit A in six mutually unbiased input states $|\phi\rangle$
- Quantum state tomography on qubit B

Input state:

$|\mathrm{i}\rangle = \frac{1}{\sqrt{2}}(|g\rangle + \mathrm{i}|e\rangle)$

$\boxed{\mathcal{F}^{s}_{|\mathrm{i}\rangle} = 87.9 \pm 0.1\ \%}$

$|e\rangle$

$\boxed{\mathcal{F}^{s}_{|\mathrm{e}\rangle} = 66.8 \pm 0.1\ \%}$

Output state:

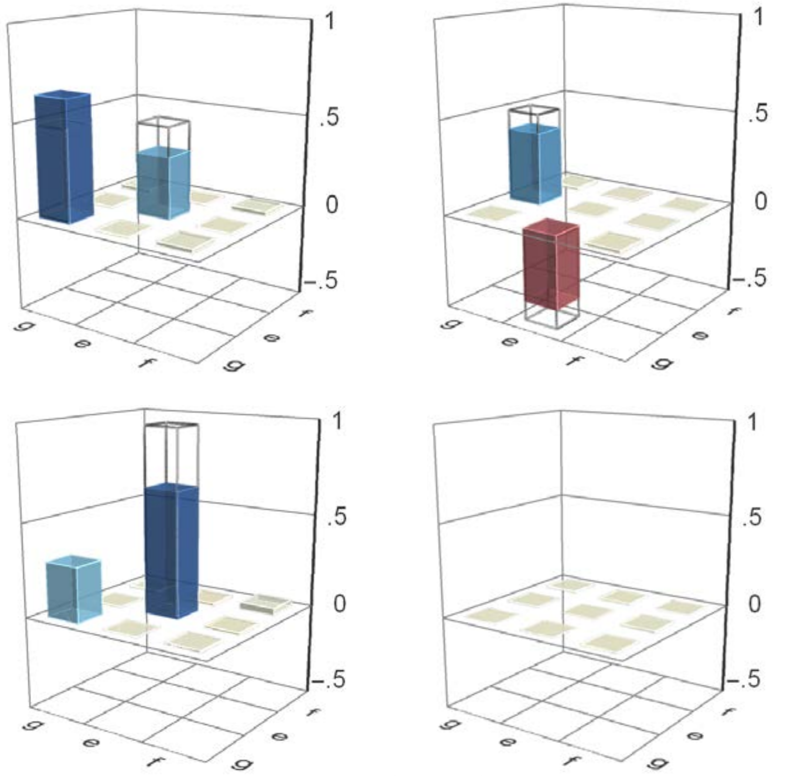

- Average state fidelity
  - $\mathcal{F}^{s}_{\mathrm{avg}} = \frac{1}{6}\sum\langle\phi|\rho_{\mathrm{m}}|\phi\rangle = 86.0 \pm 0.1\ \%$ >2/3

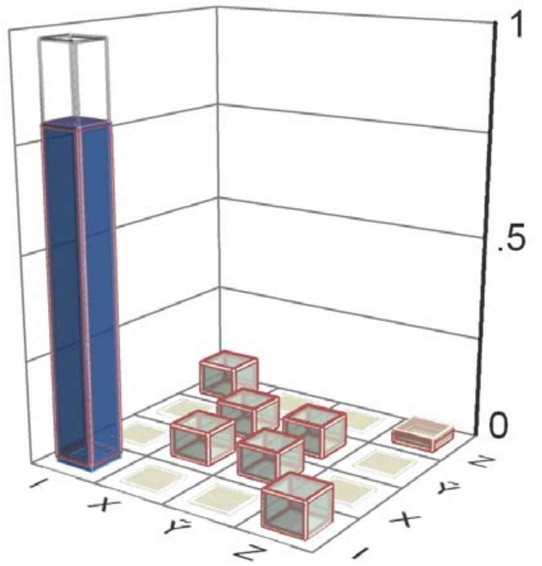

Transfer Process Matrix:

- Process fidelity
  - $\mathcal{F}^{p} = \mathrm{Tr}(\chi\chi_{\mathrm{ideal}}) = 80.02 \pm 0.07\ \%$ >1/2
- trace distance from MES $\sqrt{\mathrm{Tr}[(\chi_{\mathrm{m}} - \chi_{\mathrm{sim}})^2]} = 0.014$

P. Kurpiers, P. Magnard *et al.*, *Nature* **558**, 264 (2018)

Generation of Remote Entanglement

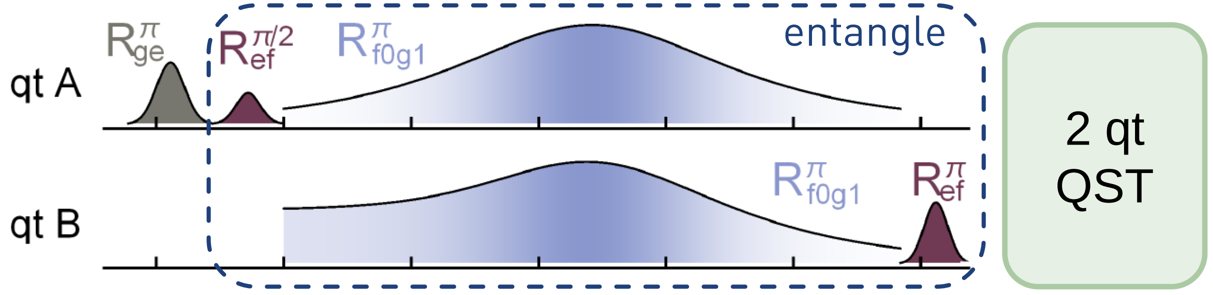

Density matrix of qubit pair:

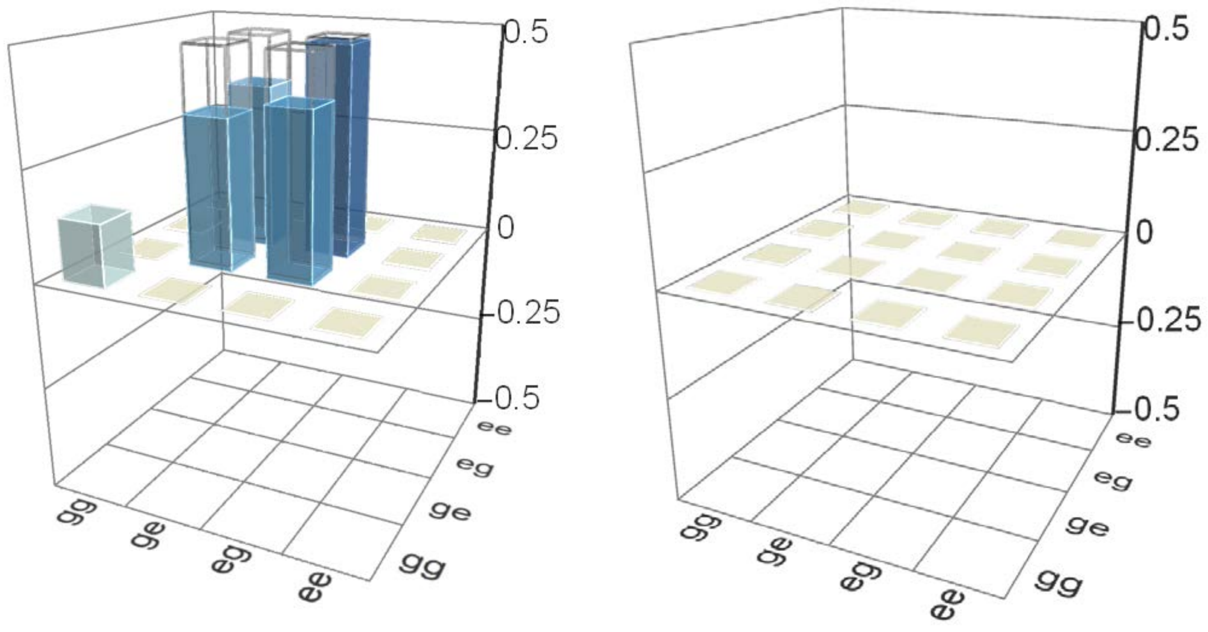

Protocol:

- Use entanglement scheme
- Perform full 2-qutrit state tomography

2-qubit subspace of 2-qutrit system

- Bell-state $|\psi^+\rangle = (|e,g\rangle + |g,e\rangle)/\sqrt{2}$
- Fidelity $\mathcal{F}_{\text{avg}}^{s} = \langle\psi^+|\rho_{\text{m}}|\psi^+\rangle = 78.9 \pm 0.1\ \%$
- Concurrence $\mathcal{C}(\rho_{\text{m}}) = 0.747 \pm 0.004$

Master Equation Simulation:

- Infidelity: $1 - \mathcal{F}_{\text{avg}}^{s} = 21.1\ \%$ from
  - ~ 10.5 % photon loss
  - ~ 9 % finite transmon coherence times
  - ~ 1.5 % imperfect absorption or pulse truncation

P. Kurpiers, P. Magnard *et al., Nature* **558**, 264 (2018)

Performance Metric Summary and Next Steps

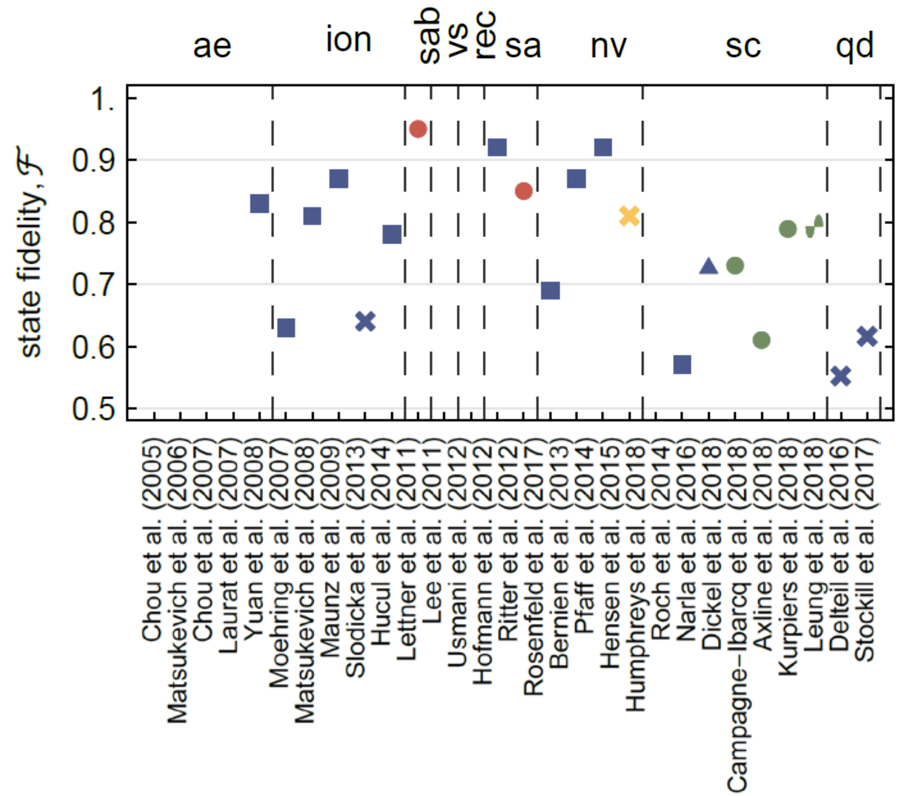

- state transfer rate: Γ = 50kHz
- concurrence of remote entanglement protocol:
  C = 0.75
- deterministic (un-heralded) remote entanglement fidelity: F = 0.80

P. Kurpiers, P. Magnard *et al., Nature* **558**, 264 (2018)

Room for improvements (verified in simulations)

- With reduced photon loss and advances in qutrit coherence:
  - $\frac{\kappa}{2\pi}$ = **18 MHz** , 12% photon loss, $T_1 = T_2 \sim \mathbf{30\ \mu s}$
  - $\mathcal{F}_{sim} = \langle\psi^+|\rho_{sim}|\psi^+\rangle \sim 93\%$

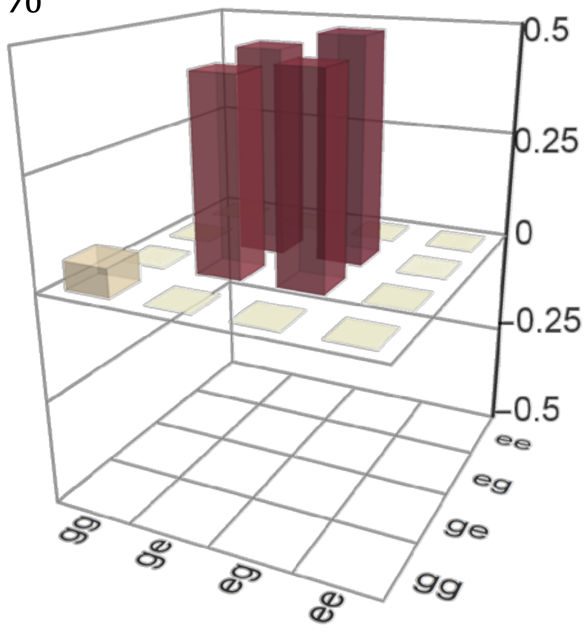

- Further improvements expected by heralding

P. Kurpiers, M. Pechal et al., arXiv:1811.07604 (2018)

Loss Detection in Remote Entanglement Protocol: Time-Bin Encoding

emitter

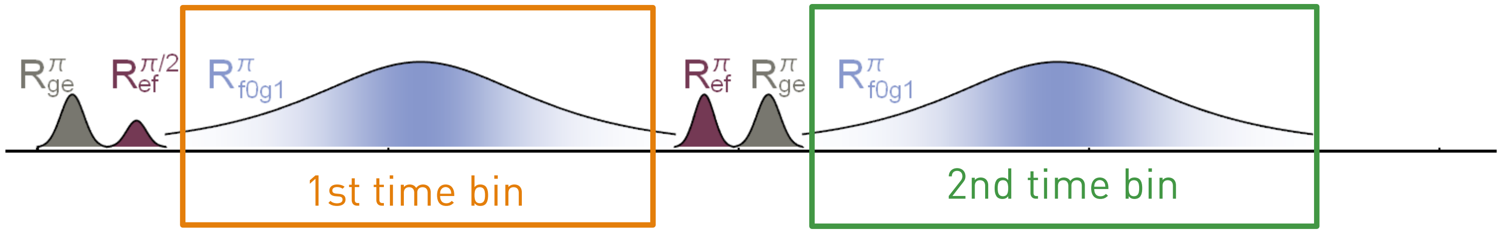

$1/\sqrt{2}\,(|e\rangle + |f\rangle)$

$|e,0,0\rangle$ $\qquad$ $|e,0,0\rangle \rightarrow |f,0,0\rangle \longrightarrow$ $\qquad$ $|g,0,1\rangle$

$|f,0,0\rangle \longrightarrow$ $\qquad$ $|g,1,0\rangle \rightarrow |e,1,0\rangle$ $\qquad$ $|e,1,0\rangle$

$1/\sqrt{2}\,(|g,0,1\rangle + |e,1,0\rangle)$

receiver

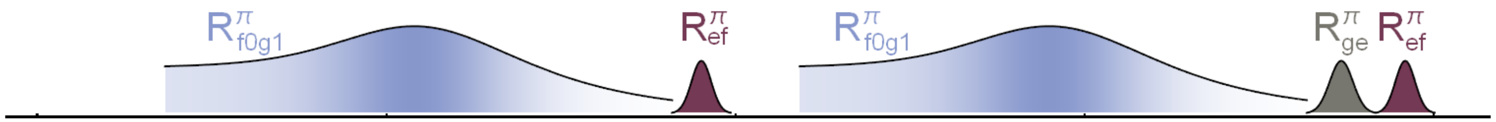

p: loss probability

$1/\sqrt{2}\,(|0,1,g\rangle + |1,0,g\rangle)$

$|0,1,g\rangle$ $\qquad$ $|0,1,g\rangle \rightarrow |0,1,g\rangle \longrightarrow$ $\qquad$ $|0,0,f\rangle \rightarrow |0,0,e\rangle$

$|1,0,g\rangle \longrightarrow$ $\qquad$ $|0,0,f\rangle \rightarrow |0,0,e\rangle$ $\qquad$ $|0,0,e\rangle \rightarrow |0,0,g\rangle$

$|\psi^+\rangle = 1/\sqrt{2}\,(|g,e\rangle + |e,g\rangle)$

photon loss $\qquad$ $|0,0,g\rangle$ $\qquad$ $|0,0,g\rangle$ $\quad$ $|0,0,g\rangle$ $\qquad$ $|0,0,g\rangle \rightarrow |0,0,f\rangle$

$$(1-p)|\psi^+\rangle\langle\psi^+|$$
$$+\,p\,(|\mathrm{gf}\rangle\langle\mathrm{gf}| + |\mathrm{ef}\rangle\langle\mathrm{ef}|)$$

Brendel *et al., Phys. Rev. Lett.* 82, 2594 (1999)
P. Kurpiers, M. Pechal *et al.*, arXiv:1811.07604 (2018)

Time Bin Entanglement

Alice

P. Kurpiers, M. Pechal et al., arXiv:1811.07604 (2018)

Time Bin Entanglement

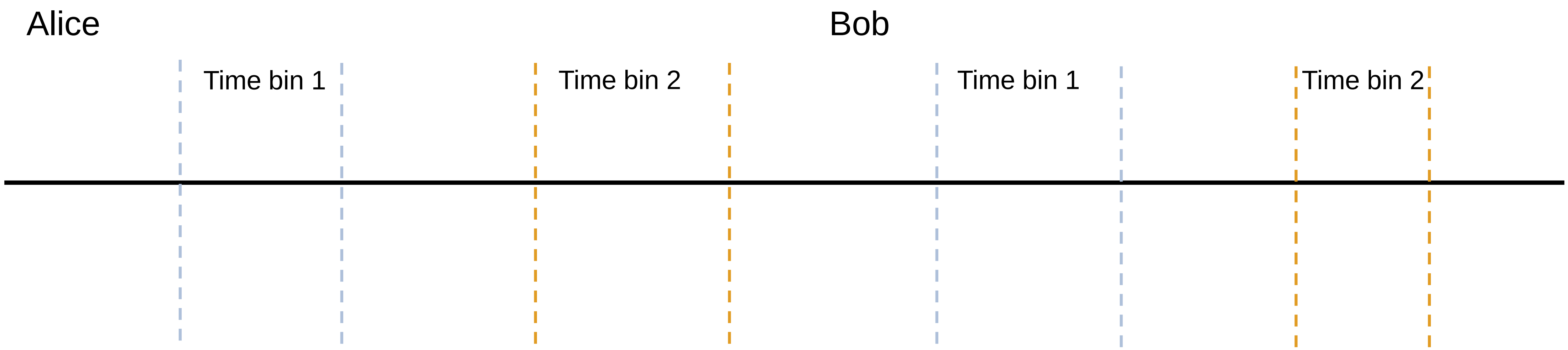

P. Kurpiers, M. Pechal et al., arXiv:1811.07604 (2018)

Time Bin Entanglement

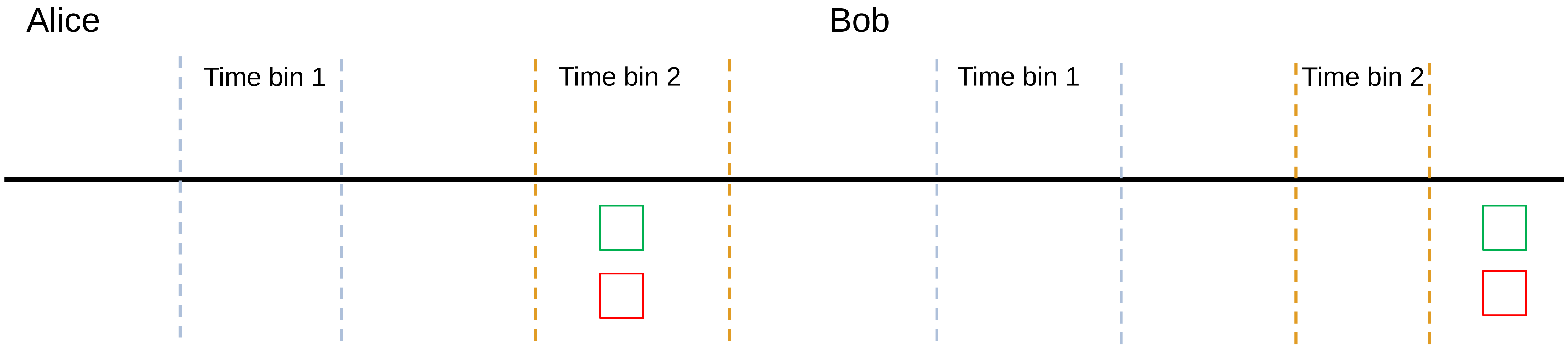

- Generates the Bell state $\Psi^{+} = \frac{1}{\sqrt{2}} \left(|e\rangle_A \otimes |g\rangle_B + |g\rangle_A \otimes |e\rangle_B \right)$

P. Kurpiers, M. Pechal et al., arXiv:1811.07604 (2018)

Time Bin Entanglement

Alice Bob

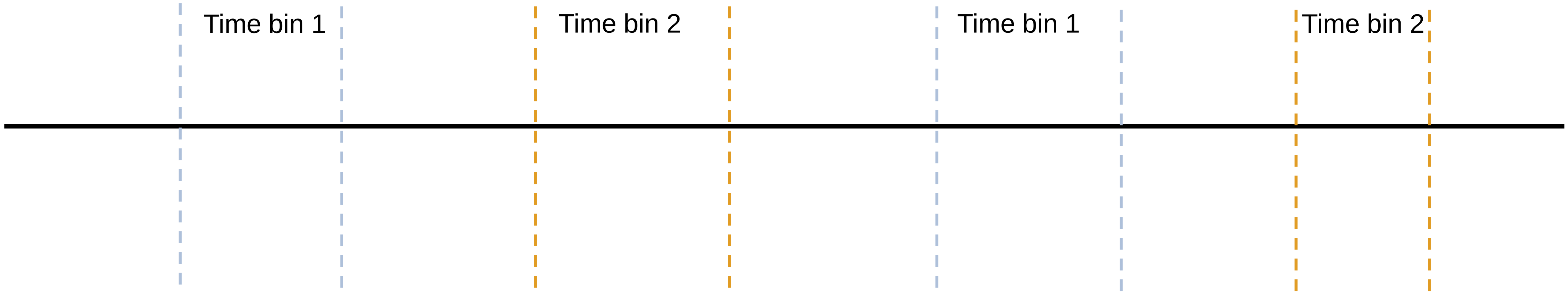

- Generates the Bell state $\Psi^+ = \frac{1}{\sqrt{2}}\left(|e\rangle_A \otimes |g\rangle_B + |g\rangle_A \otimes |e\rangle_B\right)$
- If photon is lost or not absorbed then Bob's qubit ends in $|f\rangle$ state

P. Kurpiers,M. Pechal et al., arXiv:1811.07604 (2018)

M. Jerger et al.,Phys. Rev. Applied, 6, 014014 (2016)

Benchmarking Loss Detection: Remote Entanglement

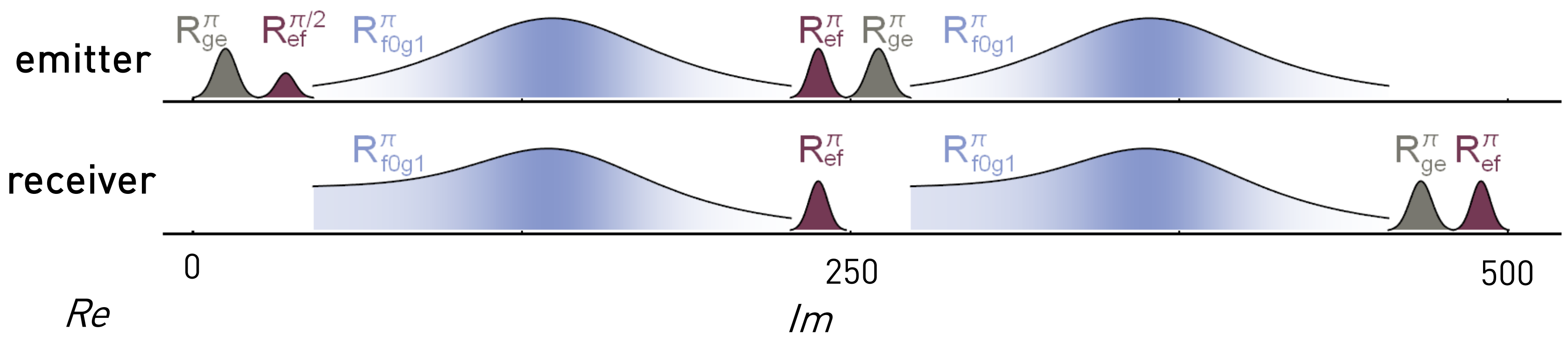

2 qutrit QST

$|\psi^+\rangle = 1/\sqrt{2}(|ge\rangle + |eg\rangle)$

p: loss probability

$$(1-p)|\psi^+\rangle\langle\psi^+| + p(|\mathrm{gf}\rangle\langle\mathrm{gf}| + |\mathrm{ef}\rangle\langle\mathrm{ef}|)$$

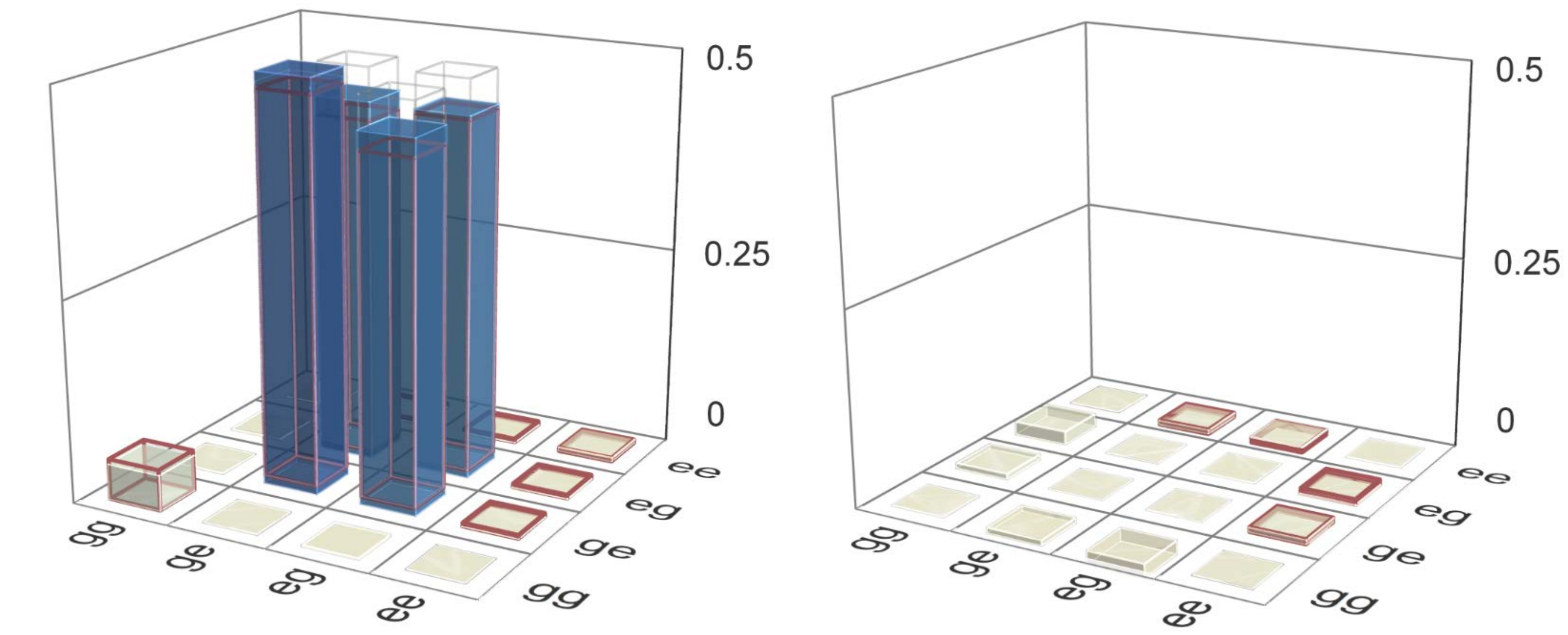

2-qutrit density matrix

- Bell state fidelity (2-qubit subspace)

  $\mathcal{F}^s = \langle\psi^+|\rho_m|\psi^+\rangle = 55.3 \pm 0.3\ \%$

With **ideal loss detection**

- Bell state fidelity

  $\mathcal{F}^s_{ld} = \langle\psi^+|\rho_{cor}|\psi^+\rangle = 92.4 \pm 0.4\ \%$

- improvement > 10 %

P. Kurpiers, M. Pechal *et al.*, arXiv:1811.07604 (2018)

Post-selected remote entangled state

$|\psi^+\rangle = 1/\sqrt{2}(|ge\rangle + |eg\rangle)$

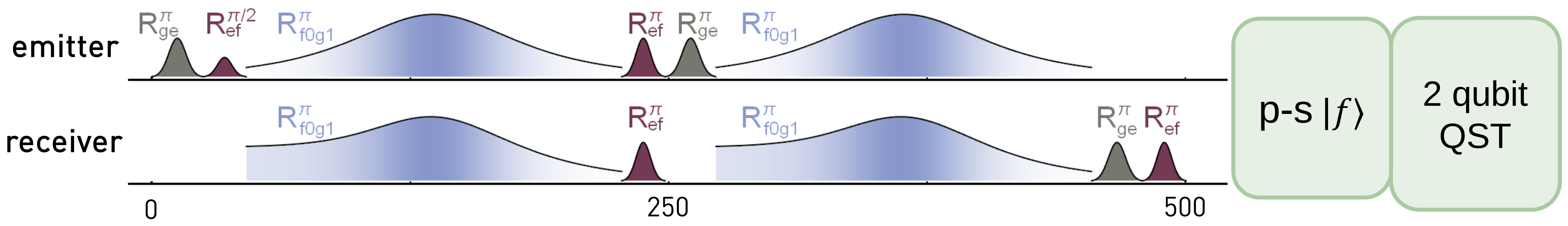

$|\psi^+\rangle\langle\psi^+|$

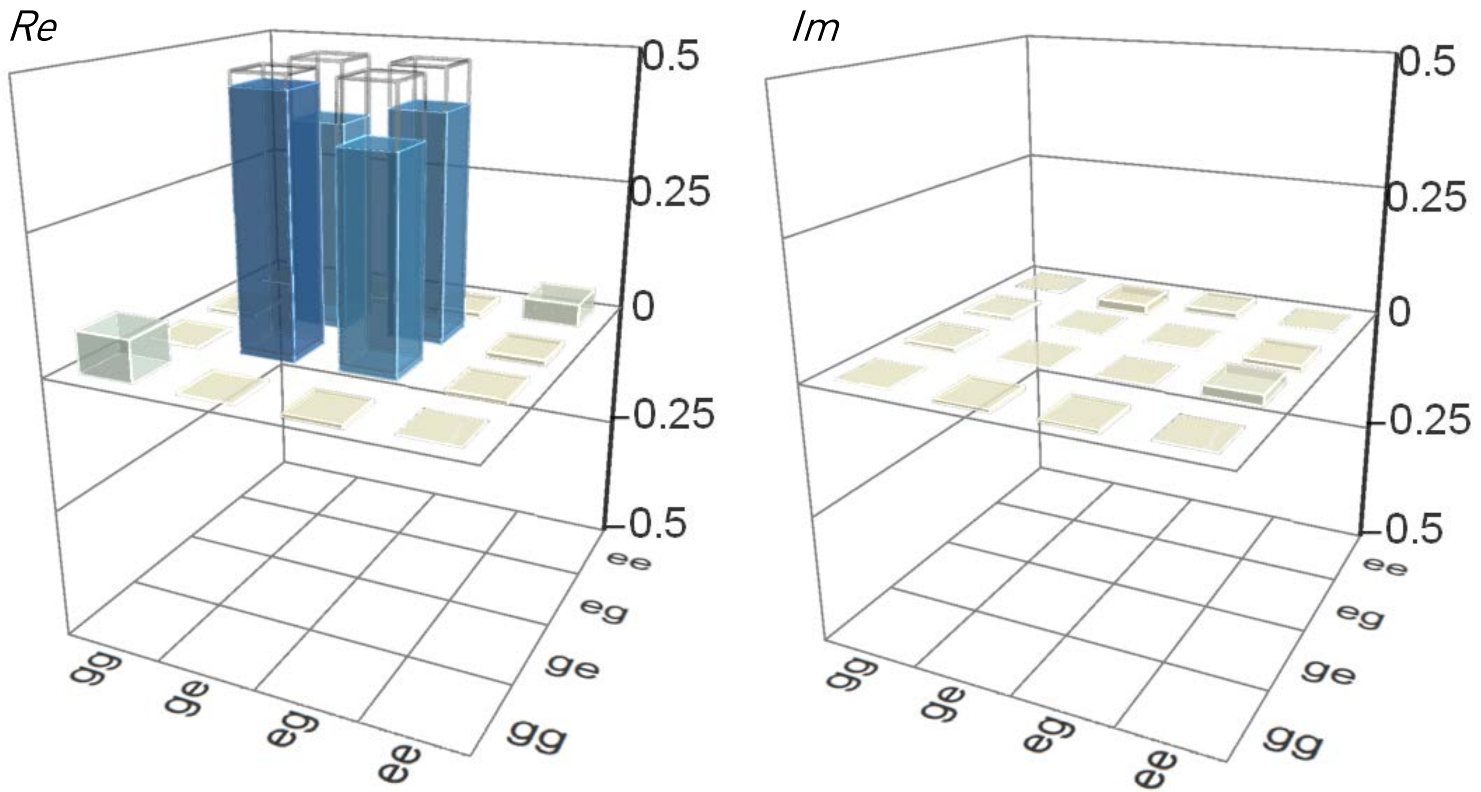

Post-selection on no loss detected

- 61.5 % of data retained
- Bell state fidelity

  $\mathcal{F}^{s}_{ps} = \langle\psi^+|\rho_{ps}|\psi^+\rangle = 82.3 \pm 0.4\ \%$
- improvement ~ 5 %

P. Kurpiers, M. Pechal *et al.*, arXiv:1811.07604 (2018)

Benchmarking Loss Detection: Qubit State Transfer

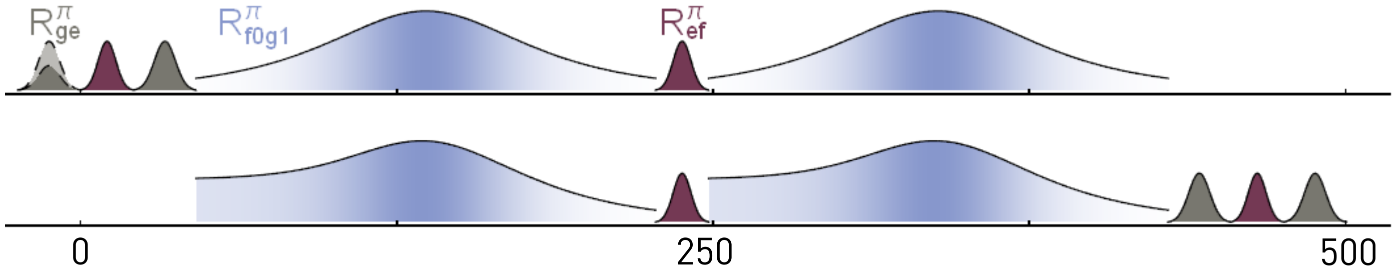

- direct transfer

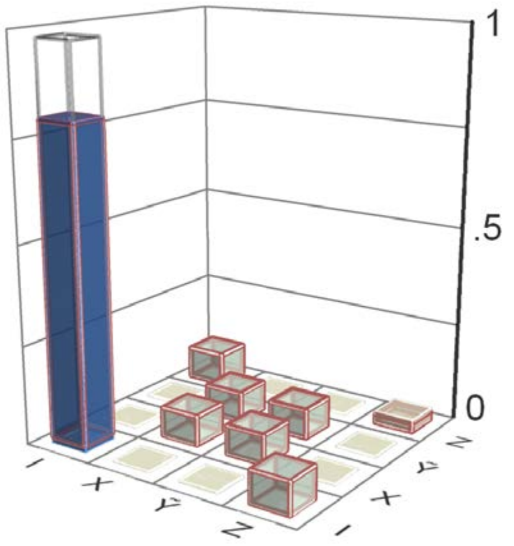

$$\mathcal{F}^p = \mathrm{Tr}(\chi\chi_{\mathrm{ideal}})$$
$$= 80.02 \pm 0.07\ \%$$

P. Kurpiers, P. Magnard *et al., Nature* **558**, 264 (2018)

- time-bin encoding with loss detection

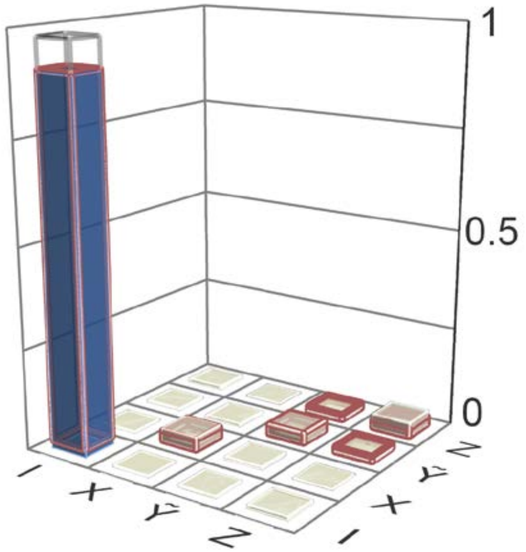

$$\mathcal{F}^p_{tb} = \mathrm{Tr}(\chi\chi_{\mathrm{ideal}})$$
$$= 90.3 \pm 0.2\ \%$$

P. Kurpiers, M. Pechal *et al.,* arXiv:1811.07604 (2018)

A Single Architecture ...

... for fast, high fidelity single shot readout

F ~ 98.25 (99.2) % at 48 (88) ns integration time and resonator population n ~ 2.2 with

- Optimized sample design
- Low-noise phase-sensitive Josephson parametric amplifier

T. Walter, P. Kurpiers *et al., Phys. Rev. Applied* **7**, 054020 (2017)

... for unconditional reset

- 99% reset fidelity in < 300 ns

P. Magnard *et al., Phys. Rev. Lett.* ***121***, 060502 (2018)

... that is multiplexable

- Single feedline for 8 qubits (nodes)
- Reduced cross-talk using Purcell filters

J. Heinsoo *et al., Phys. Rev. Applied* **10**, 034040 (2018)

... for remote entanglement and state transfer, with time-bin encoding against photon loss

- Deterministic, 50 kHz rate
- ~ 80% transfer and entanglement fidelity

P. Kurpiers, P. Magnard *et al., Nature* **558**, 264 (2018)
P. Kurpiers, M. Pechal *et al., arXiv:*1811.07604 (2018)

... for single-shot parity and single photon detection

- 13% dark count probability, 16% detection inefficiency
- Wigner tomography, propagating cat states

J.-C. Besse *et al., Phys. Rev. X* **8**, 021003 (2018)

J.-C. Besse *et al., Quamtum Device Lab* (2019)

Summary

- Single-Shot itinerant **single photon detection**
- **Parity detection** of itinerant, multi-photon states
- **Direct Wigner tomography** of itinerant fields
- Heralded **generation of cat states**

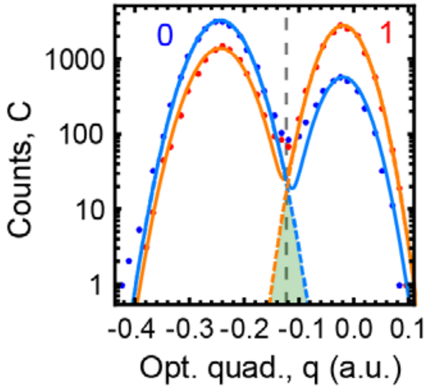

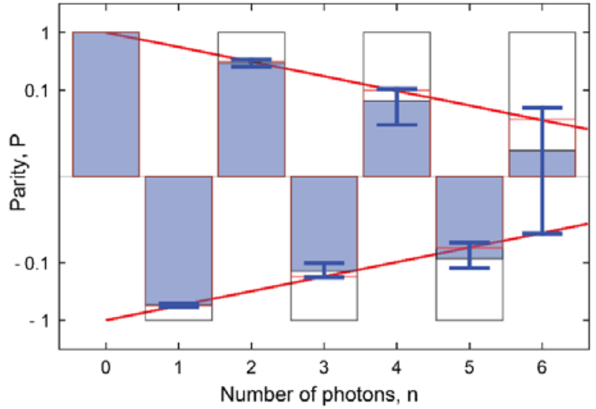

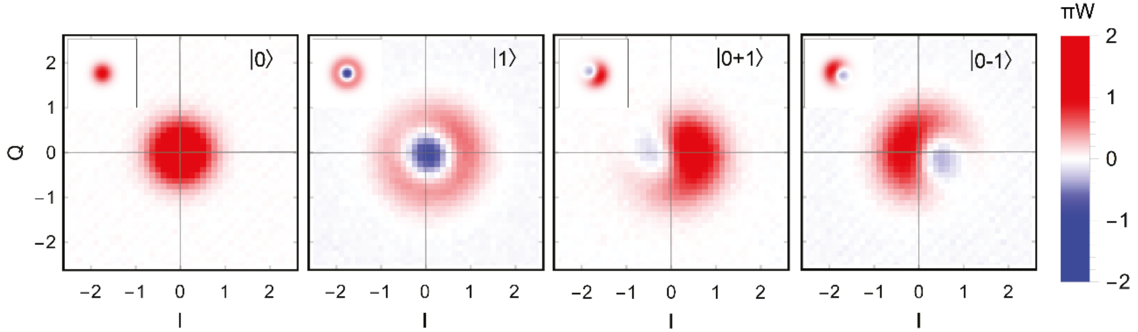

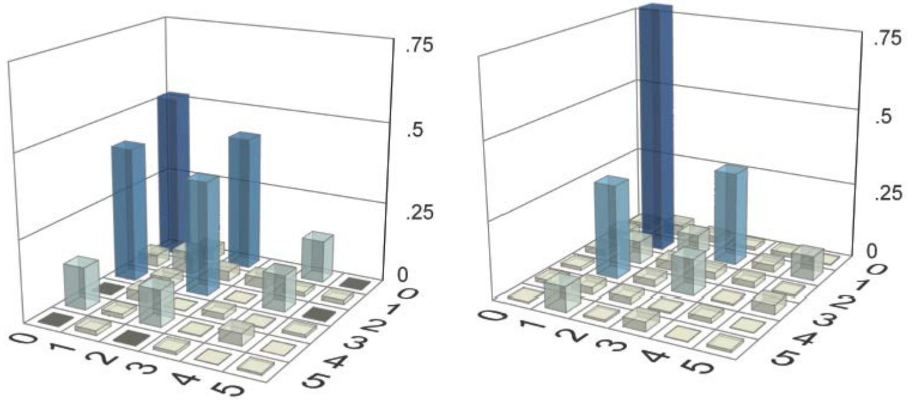

A Single Architecture ...

... for fast, high fidelity single shot readout

F ~ 98.25 (99.2) % at 48 (88) ns integration time and resonator population n ~ 2.2 with

- Optimized sample design
- Low-noise phase-sensitive Josephson parametric amplifier

T. Walter, P. Kurpiers *et al., Phys. Rev. Applied* **7**, 054020 (2017)

... for unconditional reset

- 99% reset fidelity in < 300 ns

P. Magnard *et al., Phys. Rev. Lett.* ***121***, 060502 (2018)

... that is multiplexable

- Single feedline for 8 qubits (nodes)
- Reduced cross-talk using Purcell filters

J. Heinsoo *et al., Phys. Rev. Applied* **10**, 034040 (2018)

... for remote entanglement and state transfer, with time-bin encoding against photon loss

- Deterministic, 50 kHz rate
- ~ 80% transfer and entanglement fidelity

P. Kurpiers, P. Magnard *et al., Nature* **558**, 264 (2018)
P. Kurpiers, M. Pechal *et al., arXiv:*1811.07604 (2018)

... for single-shot parity and single photon detection

- 13% dark count probability, 16% detection inefficiency
- Wigner tomography, propagating cat states

J.-C. Besse *et al., Phys. Rev. X* **8**, 021003 (2018)

J.-C. Besse *et al., Quamtum Device Lab* (2019)

... for parity check with feedback and reset

C. Andersen, A. Remm, S. Balasiu *et al., arXiv:*1902.06946 (2019)

Entanglement Stabilization with Parity Measurements and Feedback

Results

- Demonstrated weight-2 parity measurement of ZZ and XX.
- Bell state stabilized for 12 rounds of ZZ- & XX- parity stabilization with 74% fidelity.
- Realizes important element for future quantum error correction schemes.
- performance currently limited by feedback latency in relation to T_1 and T_2

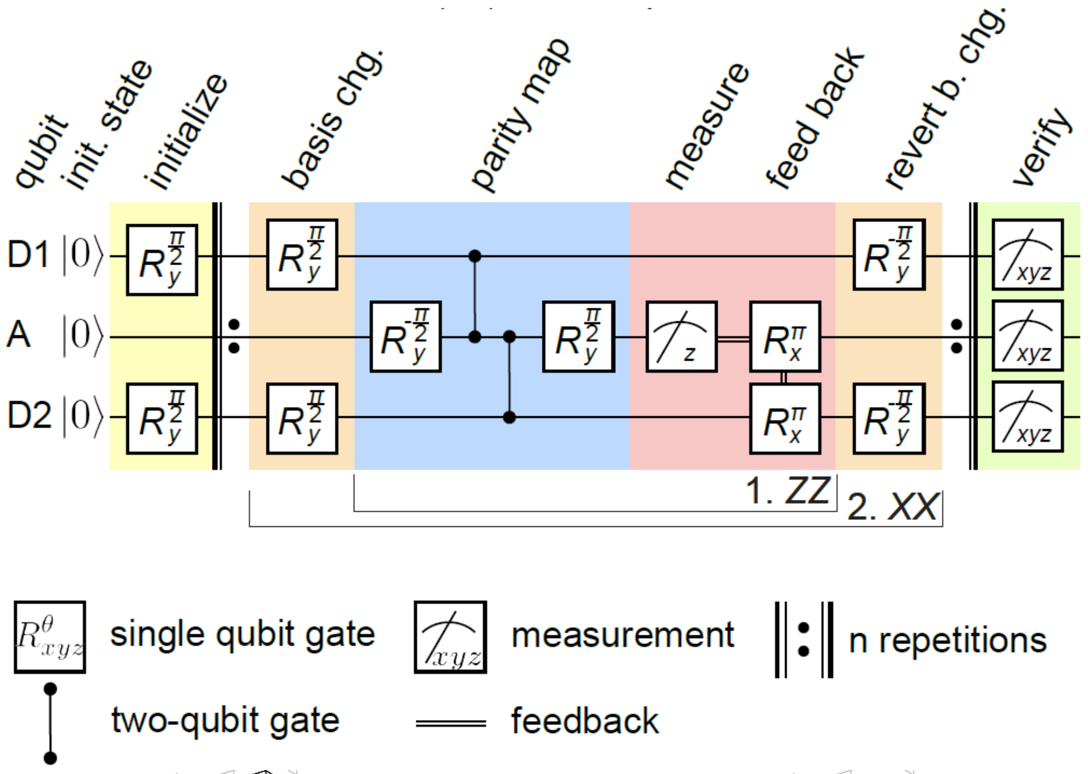

Outlook

- Extend toward surface code
- Next step: weight-4 parity checks with feedback
- Surface 7 and Surface 17 codes

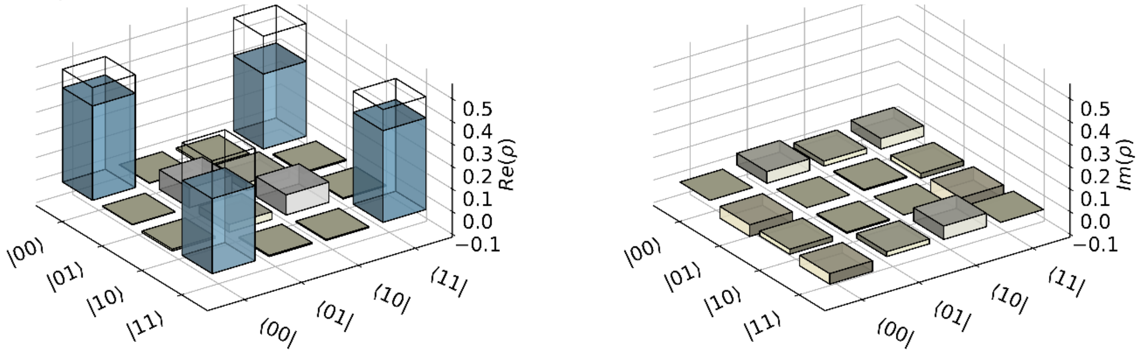

C. Andersen, A. Remm, S. Balasiu *et al., arXiv:*1902.06946 (2019)

A Single Architecture …

… for fast, high fidelity single shot readout

F ~ 98.25 (99.2) % at 48 (88) ns integration time and resonator population n ~ 2.2 with

- Optimized sample design
- Low-noise phase-sensitive Josephson parametric amplifier

T. Walter, P. Kurpiers *et al.*, *Phys. Rev. Applied* **7**, 054020 (2017)

… for unconditional reset

- 99% reset fidelity in < 300 ns

P. Magnard *et al.*, *Phys. Rev. Lett.* ***121***, 060502 (2018)

… that is multiplexable

- Single feedline for 8 qubits (nodes)
- Reduced cross-talk using Purcell filters

J. Heinsoo *et al.*, *Phys. Rev. Applied* **10**, 034040 (2018)

… for remote entanglement and state transfer, with time-bin encoding against photon loss

- Deterministic, 50 kHz rate
- ~ 80% transfer and entanglement fidelity

P. Kurpiers, P. Magnard *et al.*, *Nature* **558**, 264 (2018)
P. Kurpiers, M. Pechal *et al.*, *arXiv:*1811.07604 (2018)

… for single-shot parity and single photon detection

- 13% dark count probability, 16% detection inefficiency
- Wigner tomography, propagating cat states

J.-C. Besse *et al.*, *Phys. Rev. X* **8**, 021003 (2018)

J.-C. Besse *et al.*, *Quamtum Device Lab* (2019)

… for parity check with feedback and reset

C. Andersen, A. Remm, S. Balasiu *et al.*, *arXiv:*1902.06946 (2019)

The ETH Zurich Quantum Device Lab

incl. undergrad and summer students

Eidgenössische Technische Hochschule Zürich
Swiss Federal Institute of Technology Zurich

QSIT Quantum Science and Technology
National Centre of Competence in Research

FNSNF Swiss National Science Foundation

QuSurf

IARPA BE THE FUTURE

erc

ETH zürich

Want to work with us?
Looking for Grad Students, PostDocs and Technical Staff.